Evaluation and Mitigation of Alkali Silica Reaction (ASR) in Cementitious Materials

A Thesis

Presented in Partial Fulfillment of the Requirements for the

Degree of Master of Science

with a

Major in Civil Engineering

in the

College of Graduate Studies

University of Idaho

by

Ebenezer Fanijo

Major Professor: Emad Kassem, Ph.D., P.E.

Committee Members: Ahmed Ibrahim Ph.D., P.E.; Nielsen, Richard, Ph.D., P.E.

Department Chair: Patricia J. S. Colberg, Ph.D., P.E.

December 2019

Authorization to Submit Thesis

This thesis of Ebenezer Fanijo, submitted for the degree of Master of Science with a Major in Civil Engineering and titled "Evaluation and Mitigation of Alkali Silica Reaction (ASR) in Cementitious Materials," has been reviewed in final form. Permission, as indicated by the signatures and dates below, is now granted to submit final copies to the College of Graduate Studies for approval.

Major Professor:	_____ Emad Kassem, Ph.D., P.E.	Date: _____
Committee Members:	_____ Ahmed Ibrahim, Ph.D., P.E.	Date: _____
	_____ Richard Nielsen, Ph.D., P.E.	Date: _____
Department Administrator:	_____ Patricia J. S. Colberg, Ph.D., P.E.	Date: _____

ABSTRACT

Alkali Silica Reaction (ASR) is recognized as a major distress in concrete for over a century. In United States, ASR is a major cause in deterioration of highway concrete structures (i.e., bridges and pavements). Current methods such as the 14-day Accelerated Mortar Bar Test (AMBT) and 1-year Concrete Prism Test (CPT) used to evaluate ASR potential have limitations. Limited research was conducted on new proposed methods such as the 56-day Miniature Concrete Prism Test (MCPT) and 6-month Accelerated Concrete Prism Test (ACPT) proposed to overcome the limitations of existing methods. In addition, there is a need to reduce or mitigate ASR especially in Idaho where 80% of aggregates are reported reactive.

This study conducted comprehensive laboratory evaluation of ASR susceptibility of various aggregates using different test methods. There were strong correlations between the 56-day MCPT method and both the 14-day AMBT and the 1-year CPT methods. Also, the expansion results of the 14-day AMBT method correlated well with the 1-year CPT method. Furthermore, the 6-month ACPT method provided comparable results to the 1-year CPT. these results show the validity of various test methods to evaluate ASR potential. Recommendations were provided to revise the expansion threshold of MCPT to identify reactive aggregates.

The use of Supplementary Cementitious Materials (SCMs) along with glass powder was found to reduce ASR expansion substantially. Binary or ternary blends of 20% replacement of slag, glass powder or silica fume can be used for ASR mitigation without compromising other concrete properties. These results were also supported by the findings of the microstructure and chemical analysis where SCMs were found to reduce the cracks formed in concrete due to ASR expansion.

Acknowledgements

First, I would like to express my sincere appreciation to my supervisor Dr. Emad Kassem for showing me the limitless support and patience and believing on me. I am grateful to my supervisor who dedicated his time and effort to achieve my research goals, and who promptly responded to my difficulties and queries. Working under his supervision paved my way to achieve my goals. Needless to say, none of this would have been possible without his help and direction.

I would like to thank Dr. Ahmed Ibrahim, and Dr. Richard Nielsen for being my committee members and guiding me towards the MS degree. Also, I would like to extend my gratitude to Dr. Debakanta Mishra of Boise State University. My sincere thanks to Mr. Don Parks for being there always in the lab with his helping attitude. Additional thanks go to all of my awesome lab mates Assi, Hamza, Robin, Simpson, Kevin, Charles and Md. Shajalal (Boise State University) for all your supports. My appreciation also goes to Mr. Niyi Arowojolu, for being there with me as my friend and consulting with him in my research work.

This study is part of a research project (RP 271) funded by the Idaho Transportation Department (ITD). I greatly appreciate all the support provided by the ITD personnel in collecting materials and related information essential for this research. I am also grateful to the Department of Civil and Environmental Engineering and the National Institute for Advanced Transportation Technology (NIATT) at the University of Idaho for providing all the necessary resources for completing this research.

Dedication

In the memory of my father, my loving mother (Pastor Comfort F. Fanijo) and my beloved brother Dr. Cornelius Adewale who always supported me and inspired me to be a good person. Additional dedication goes to Omobolanle Ogunseiju and my two other brothers (Olaniyi and Olawale Fanijo).

Table of Contents

List of Tables

List of Figures

CHAPTER ONE: INTRODUCTION

1.1 Background and Problem Statement

Alkali Silica Reaction (ASR) has been recognized as a major distress in concrete for over a century. It is considered the second main concern after corrosion facing highway concrete structures (i.e., bridges and pavements) (Stantion, 1941). In the United States, ASR is a major cause in deterioration of highway concrete structures (Fournier et al., 1994). ASR is a chemical reaction between silica in aggregates and alkalis in cement in the presence of moisture. This reactivity causes an undue expansion and cracks in hardened concrete which over time results in demolition. Deformation due to ASR is a phenomenon that was first recognized during 1940's in America and since then has being observed in many other countries (Stantion, 1941). Despite several published articles investigating both the fundamental and practical aspects of ASR (Diamond, 1992), the mechanism is not easily understood due to the complex chemical reaction between the cement alkali content and aggregate's silica minerals. However, the alkalis contained in the pore solution, the reactive amorphous silica present in aggregates, and the presence of moisture are identified as major factors affecting ASR.

The majority of aggregates used in Idaho are very reactive with high silica content. About 80% of aggregates used in the state are reported reactive or highly reactive (ITD, 2012). ITD research project (RP) 212 indicated that many aggregate sources in Idaho have high ASR potential especially in the presence of moisture; therefore, appropriate test methods are needed to evaluate concrete expansion due to ASR and to adequately determine the mitigation strategies for them. There are two prominent test methods used to evaluate aggregate susceptibility to ASR: ASTM C 1293 and ASTM C 1260. The ASTM C 1293 test method is found to provide strong correlation with field performance; however, it takes up to one full year to complete one test. On the other hand, ASTM C 1260 is a rapid test that takes only 14 days to complete. However, ASTM C 1260 may not provide reliable results in all cases due to the harsh testing conditions. The current test methods used in Idaho to evaluate ASR have shown conflicting results depending on the length and type of test even on the same aggregate source. According to ITD research project RP 212, it was found that some aggregate sources that passed ASTM C 1293 failed in ASTM C 1260. The current test methods used in Idaho

were either found too long (i.e., ASTM C1293 that takes one full year) or too harsh (i.e., ASTM C1260) which makes it difficult to conduct an accurate assessment of ASR.

Due to the shortcomings of both test methods (i.e., ASTM C 1293 failing in ASTM C 1260), an alternative test method called AASHTO TP 110 was recently proposed. This new test method takes 56 days with an additional 28 days in case of slow reacting aggregates. This test is conducted at 60^{o}C which is less harsh compared to ASTM C 1260 that is conducted at 80^{o}C. Also, the new test method (i.e., AASHTO TP 110) takes much less time (maximum of 84 days) compared to ASTM C1293 that takes one full year. The preliminary results of AASHTO TP 110 showed that it provides a strong correlation with field performance as well as to the results of ASTM C 1293. Further research is needed for selecting accurate test methods to evaluate ASR as well as strategies to prevent or mitigate the ASR reactivity in aggregates used in Idaho. This study evaluated aggregate susceptibility to ASR using the new test method AASHTO TP 110. The results of AASHTO TP 110 were compared and correlated with both 14-day ASTM C 1260 and 1-year ASTM C 1293 test procedures. In addition, a new method that was recently proposed to evaluate ASR potential, was also examined. This method is an Accelerated ASTM C1293 that is conducted for only 6 months instead of one year as in the conventional ASTM C1293. Furthermore, a mitigation procedure was proposed using binary and ternary blends containing Supplementary Cementitious Materials (SCMs). The microstructural analysis, pozzolanic activity effect and chemical composition of mixtures containing SCMs were performed using the Thermogravimetric Analysis (TGA), Scanning Electron Microscopy (SEM) and Energy-Dispersive X-Ray Spectral Analysis (EDS). Such methods can be used to optimize the mix design to produce a mix that has better resistance to ASR. ITD is moving towards adopting performance-based specifications, therefore, such methods would be very helpful.

1.2 Research Goal and Objectives

The main goal of this research study is to evaluate alternative test methods to overcome the shortcomings of current test methods used to assess ASR susceptibility. The new test methods include AASTHO TP 110 and the Accelerated Concrete Prism Test (ACPT) 6-month test protocols. Furthermore, this study examined the applicability of using Supplementary

Cementitious Materials (SCMs) to mitigate the detrimental effects of ASR. In order to meet the goals of this study, the following main objectives were achieved.

- Evaluate ASR potential of various aggregates (both fine and coarse) using different test methods including ASHTO TP 110 (maximum of 84 days), ASTM C 1260 (14 days), ASTM C1293 (one year), and accelerated ASTM C1293 (six months).
- Select suitable test method(s) to assess the susceptibility of aggregates to ASR.
- Develop and propose strategies to prevent or mitigate ASR in highway concrete structures. Such strategies use SCMs such as silica fume, blast furnace slag and waste glass.
- Assess the effectiveness of mitigation strategies through advanced chemical and microstructural analysis using Thermogravimetric Analysis (TGA), Scanning Electron Microscopy (SEM) and Energy-Dispersive X-Ray Spectral Analysis (EDS).

1.3 Research Tasks

In order to achieve the objectives of this research study, the following tasks were completed.

Task 1: Review of Published Literature

This task involved extensive review of published literature on various aspects of Alkali-Silica Reaction (ASR). The main subjects of the literature review were as follows;

1) An extensive overview and mechanism of ASR.
2) Effects of ASR on concrete structures.
3) Factors that affect ASR in concrete structures.
4) Test protocols used to assess ASR with correlation among them.
5) ASR mitigation using SCMs and waste glass.
6) Microstructural characterization and chemical analysis of ASR.

Task 2: Identify Different Aggregates Sources across Idaho

Under this task, several aggregate types and sources were identified and selected across Idaho. The selected aggregates have different ASR potential and mineralogy. The database that was developed in ITD RP 212 was used in selecting the aggregate sources.

Task 3: Evaluate the ASR potential using Various Test Methods

Under this task, the selected aggregates under Task 2 were tested for ASR potential using various test methods including

1) AASTHO TP 110 Test method which is also known as Miniature Concrete Prism Test (MCPT). Both coarse and fine aggregate sizes were tested in accordance with the requirements of each test methods. The AASTHO TP 110 test is conducted for 84 days. Although most reactive aggregates can be identified in 56 days, the test was conducted over 84 days to evaluate the slow-reacting aggregates.
2) ASTM C 1260 test method which is also known as Accelerated Mortar Bar Test (AMBT). This test is conducted for 16 days to evaluate the susceptibility of fine aggregates to ASR.
3) ASTM C 1293 test method which is also known as Concrete Prism Test (CPT) (CPT). This test was found to provide good correlation with field performance in terms of ASR potential. This test was conducted for one full year. In addition to the CPT, a new testing protocol called "Accelerated Concrete Prism Test (ACPT)" was also conducted. In the ACPT, the test aggregates are tested for six months. Both CPT and ACPT were conducted on selected number of test aggregates.

Task 4: Examine the Correlation between Various Testing Protocols

Under this task, the author analyzed the results of Task 3 and examined the correlation among between various different test protocols. This includes a comparison between AASTHO TP 110, ASTM C 1260, and ASTM C1293 (both 1-year and 6-month duration) test methods for both fine as well as coarse aggregates. Based on the results of this task, the author recommended suitable test method(s) to assess the susceptibility of aggregates to ASR.

Task 5: Develop and Propose Mitigation Strategies for Reactive Aggregates

Under this task, various ASR mitigation strategies were examined through binary and ternary blend containing Supplementary Cementitious Materials (SCMs) including silica fume, blast furnace slag and waste glass powder to suppress the adverse effects of ASR. In addition, the author examined the effects of most effective blend on workability and strength of concrete.

Task 6: Microstructural Characterization and Chemical Analysis of ASR

Under Task 6, the author examined the chemical composition and microstructure of test samples prepared with and without the use of ASR mitigation additives. This task used advanced characterization methods including Thermogravimetric Analysis (TGA), Energy-Dispersive X-Ray Spectral Analysis (EDX), and Scanning Electron Microscopy (SCM). This task provides a fundamental understanding of the effect of ASR mitigation on the chemical composition as well as the microstructure of concrete samples.

Task 7: Provide recommendation and guidelines for ASR evaluation and mitigation

Based on the results of this study, the author developed recommendation and guidelines for ASR evaluation and mitigation. The author also developed and recommended a job mix for effective ASR mitigation in concrete using AASTHO TP 110.

1.4 Thesis Organization

This thesis consists of eight chapters. Chapter 1 provides background and problem statement, research goal and objectives, research tasks, and thesis organization. Chapter 2 presents a full research background information or literature review on Alkali Silica Reaction (ASR); the factor affecting ASR and its effects on concrete structures; the test method used for ASR identification, and mitigation procedures from past studies.

Chapter 3 discusses the test aggregate selection, various testing protocols used to asses ASR potential, experimental design and test mixtures. Chapter 4 includes the test results of the comprehensive laboratory testing program. In addition, it provides detailed discussion of the results and findings of various testing protocols including ASTM C1260 (14-day AMBT method), ASTM C 2393 (1-year CPT method), AASTHO TP 110 (56-days MCPT), and the new approach 6-month CPT approach used to evaluate the susceptibility of test aggregates to ASR. In addition, the author discussed the correlation between various test methods.

Chapter 5 examines the feasibility of using supplementary cementitious materials (SCMs) for ASR mitigation. This chapter covers the laboratory testing program including testing matrix and protocols. The results and discussion of ASR mitigation strategies are provided in Chapter 6.

Chapter 7 discusses the microstructural characterization and chemical analysis conducted to understand the effect of ASR mitigation on the chemical composition as well as the

microstructure of concrete samples. Finally, the author summarized the main findings of this research and provided recommendations in Chapter 8.

CHAPTER TWO: LITERATURE REVIEW

2.1 Introduction

Portland cement concrete (PCC) consists of 60% to 75% aggregates, 10% to 15% of Portland cement and/or other cementitious materials (admixture) and water has been recognized as the most widely used construction material in the world (Naik, 2008). The presence of reactive amorphous or poor crystalized silica of many natural aggregates reacts with the alkalis (i.e., sodium [Na] and potassium [K]) in cement or admixtures which produces a deleterious chemical reaction over time. This interaction is widely known as the alkali-aggregate reactivity (AAR). This reactivity is a prominent concrete durability and serviceability problem in highway concrete structures such as pavements, bridges, and other structures, resulting in definite reduction in its serviceability and life span (Thomas et al., 2008; ACI, 2008). AAR is sub-divided into two kinds of reactions; 1) Alkali-Silica Reaction (ASR) developed due to reactive silica minerals in aggregate and 2) Alkali-Carbonate Reaction (ACR) generated by aggregates composing carbonate and dolomite (Diamond, 2006).

The prominent form of AAR is the ASR which was initially observed by Stanton (1941). ASR is a destructive chemical reaction that occurs between the active silica constituents (reactive minerals) of aggregate and alkalis in the cement and other pozzolanic materials. Such reaction causes a definite expansion in the presence of moisture or a pore solution of concrete (Farny and Kerkhoff, 2007). Most structures built with concrete in America during 1940's developed ASR and eventually failed and collapsed over this period of time. ASR causes deformation which is manifested into an extensive expansion, cracking and map-related cracking, pop-out, gel exudation and white deposits on concrete on concrete (Fournier et al., 1994). Much research has been conducted on ASR over the last 80 years beginning from the pioneering work of Stanton in 1941 (Figure 2.1). According to Diamond (1992), numerous published articles on ASR have grown extensively over the five decades from 1970 to 2010 making the subject of ASR in concrete an intense awareness of concrete durability problem.

Figure 2.1: A typical ASR in concrete and Mr. Stanton (Stanton, 1941)

According to Diamond (1992), the deterioration of concrete caused by ASR is continual, expensive and generally slow. The ASR reaction produces an alkali-silica gel over time which leads to progressive deformation of concrete internal forces triggering loss in serviceability and longevity (Stanton, 1941; Diamond, 1992). The ASR-induced distress, in turn, leads to major damage in concrete structures and eventually causes collapse or demolition of the structure (Grattan-Bellew & Mitchell, 2002; Islam, 2010; Bach et al., 1993; Wang et al., 2010). This section provides an overview of the ASR mechanism, its effect on concrete structures, test procedures used to assess aggregate susceptibility to ASR, in addition to ASR mitigation procedures.

2.2 Mechanism of Alkali-Silica Reaction (ASR)

ASR is a deleterious chemical reaction with multi-stage process. This reaction product (gel) is hygroscopic having a greater ability to absorb water. In the presence of water or pore solution, this gel causes an expansion or swelling leading to cracks (Diamond, 2006; Farny and Kerkhoff, 2007). The absence of appropriate amount of active silica in aggregates, adequate alkali concentration from Portland cement, or sufficient moisture inhibits gel formation. Figure 2.2 shows a schematic of ASR mechanism in concrete.

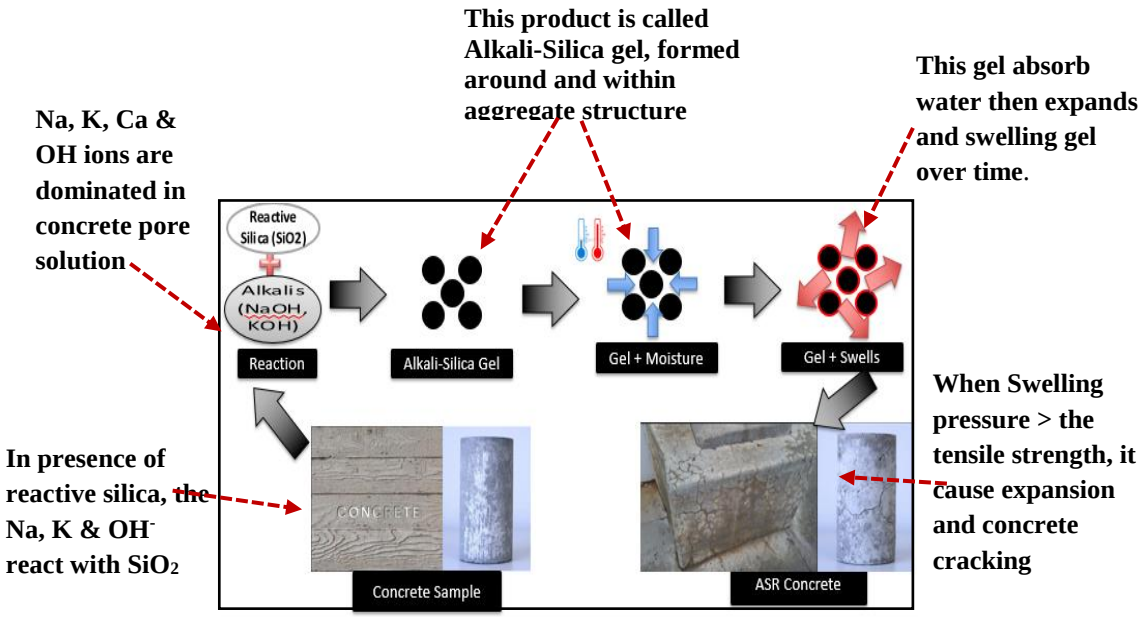

Figure 2.2: A Schematic of ASR mechanism

The chemical reaction occurs between reactive silica in aggregates and alkali hydroxide in pore solution of concrete. The present state of silica (SiO_2) in aggregates is chemically passive (in the form of quartz) and mainly structured as siloxane groups (≡Si-O-Si≡). However, the disorderliness of crystalline silica at the surface causes them to have the affinity to attract water and produces amorphous hydrous silica (silanol group [≡Si-OH]) (Glasser, 1992). Thereafter, the silica(s) inclines towards dissolution in the presence of high concentrated hydroxyl ions by first neutralizing silanol groups (≡Si-OH) and then attacking siloxane groups ((≡Si-O-Si≡) as illustrated in Equation 1.1 and 1.2 (Thomas et al., 2013).

$$\equiv Si\text{-}OH + OH^- \rightarrow Si\text{-}O^- + H_2O \qquad \textbf{Eq. 2.1.}$$

$$\equiv Si\text{-}O\text{-}Si\equiv + 2OH^- \rightarrow 2Si\text{-}O^- + H_2O \qquad \textbf{Eq. 2.2.}$$

The structure gradually breaks down and attracts the soluble alkalis hydroxides generated from alkali metal ions. This alkalis are present abundantly in concrete pore solution (in cement, aggregates and environment) as Na^+ or K^+ (Godart, 2013). The calcium hydroxide, $Ca(OH)_2$ and Calcium Silicate Hydrate (C-S-H) produced from cement and water also added to the OH^- in pore solution. Alkali-silicate solution/silicic acid (Si-OH) and gel (depending on the level of moisture) are the preliminary products of reaction between this siloxane groups (≡Si-O-Si≡) and hydroxyl ions (Equation 1.3). Thereafter, the Si-OH reacts with more

OH- and alkali metals forming alkali silicate hydrate and water as presented in Equations 1.4 and 1.5 (Godart, 2013; Swamy, 2002; Ichikawa & Miura, 2007; Bazant & Steffens, 2000). The gel product expands and causes cracks in the aggregates particles and cement paste leading to deterioration of concrete structures (Dron, 1993; Thaulow et al., 1996; Diamond, 2006).

$$\equiv Si\text{-}O\text{-}Si\equiv + OH^- + R^+(Na) \rightarrow \equiv Si\text{-}O\text{-}Na + H\text{-}O\text{-}Si\equiv \quad \textbf{Eq. 2.3}$$

$$\equiv Si\text{-}OH + OH^- + Na^+ \rightarrow \equiv Si\text{-}O\text{-}Na + H_2O \quad \textbf{Eq. 2.4}$$

$$\equiv Si\text{-}O\text{-}Na + nH_2O \rightarrow \equiv Si\text{-}O^- - (H_2O)_n + Na^+ \quad \textbf{Eq. 2.5}$$

.3 Factors Affecting Alkali-Silica Reactivity (ASR)

The swelling gel of ASR does not directly cause concrete distress but as the swelling gel absorbs moisture, it expands and induces stresses. Such stresses can exceed the tensile strength of concrete causing progressive cracking and associated deterioration. The three main components widely accepted as important for ASR in concrete materials are:

- presence of reactive siliceous components in aggregates (both coarse and fine)
- adequate alkali content from cementitious materials, and
- Presence of moisture along with other factors (e.g., temperature, relative humidity, additives).

2.3.1 Reactive Aggregate

The durability and chemical stability of any major concrete structure is determine by the quality of aggregates used in such structure. About 65% to 75% of most concrete volume is made up of aggregates. As a result, aggregates (coarse and fine sizes) have a significant influence on concrete properties affected by ASR. According to FHWA and Engineering and Geology, Inc. (IEG), many aggregate sources are reported reactive (containing high silica content) and exhibited high ASR potential when exposed to poor-solution of high alkaline (FHWA, 2011). The chemical composition, crystallinity and amorphous level of aggregate, and the degree of solubility of the amorphous silicate in alkaline concrete pore solution affect the aggregate reactivity to ASR (Leger, 1996). The porosity of aggregate increases the rate of ASR susceptibility. Fine aggregates are generally more susceptible to ASR (Farny, 2007) since they have higher surface area compared to coarse aggregates of the same type (Hobbs,

1988; Wood, 1968). In general, the expansion increases as the particle size decreases (Hobbs, 1988; Staton, 1941; Baronio et al., 1987). Table 2.1 reports ASR expansion as a function of aggregate size using both mortal bar and concrete prism test.

Table 2.1: Mortar Bar/Concrete Prism ASR Expansion as a Function of Aggregate Size

Type of Materials / Test	Aggregates Size Ranges for ASR	Insignificant ASR with Size	Reference
Siliceous magnesium limestone containing opal & chalcedony (Mortar/concrete prism)	0.17 – 0.6mm		Stanton, 1941
Opaline aggregate particles in mortar bar	0.07 - 0.85mm		Wood, 1968
Mortar bars made of siliceous aggregates	0.15mm		Zhang et al., 1999
0.48mm Mortar bars made of only reactive aggregates	0.48mm		Kuroda et al., 2004
Mortal Bar expansion	-	>0.02mm <0.05-0.15mm	Hobbs & Gutteridge, 1979 Han and Tan, 1999 Shayan, 2008
Mortal Bar	-	Up to 0.1mm	Shao et al., 2000 Moisson et al., 2004

2.3.2 Alkalinity of Cementitious materials

Portland cement is known to be the primary source of alkalis in ASR in concrete structures. Aggregates, supplementary cementing materials, SCM (e.g., silica fume, natural pozzolans, slag cement, fly ash and many others), external sources (e.g., seawater and deicing salts), and chemical admixtures also contribute to the additional alkali in concrete leading to ASR (Berube et al. 2002, Diamond 2006). Though aggregates, cement or other cementitious materials contain a numerous alkali metals the presence of sodium, Na and potassium, K ions contribute significantly to ASR concrete damage.

The conventional North American Portland cement contains 0.2% to 1.2% sodium oxide (Na_2Oeq) while the total alkali content contains in cement is approx.. 1.65% of Na_2Oeq (Diamond, 2006). Despite the low percent of alkalis, their high solubility plays an important role in ASR. Furthermore, the total alkali content in concrete mixtures increases with the use

of seawater, ground water, and water from industries with sodium and potassium solution. In addition, the use of retarders, plasticizers, water reducers and air-entraining, admixtures may contain Na and K ions that increase the alkali content.

2.3.3 Roles of Environmental Factors

There are environmental factors that increase the susceptibility of concrete to ASR. These factors include moisture content, temperature and associated concrete alkali redistribution due to seasonal climatic variations (temperature and wetting/drying cycles), and penetration of alkalis through seawater and deicers. The optimum combination of silica from aggregates source and alkalis from cement is essential to initiate ASR, whereas the environmental factors are essential to ASR deleterious expansion. Water is require to initiate or begin ASR in concrete, in which it acts as a transporter of the alkali ions from Portland cement. The pressure in concrete is induced when the gel absorbs water leading to greater expansion and aggregate cracking in surrounding paste over a long period of time. Therefore, high ASR expansion in concrete mixture is developed generally by highly reactive aggregates with high alkali cement content when expose to substantial amount of moisture. A highly reactive aggregates with high alkali cement content without sufficient presence of water show no or little expansion (Diamond et al. 1981). In addition, the rate of ASR expansion increases as temperature increases (Diamond et al. 1981). The relative humidity (RH) was found also to affect the ASR expansion. A relative humidity of 80 percent or more have shown to be increase ASR expansion (Pedneault, 1996). In that the swelling gel (called the alkali-calcium-silicate-hydrate) take place at a RH of 80% and above.

2.4. Effect of ASR on Concrete Structures

The effect of ASR is immediate but research shows that the effect continues over a period of time that leads at the end to concrete damage. ASR affects the structural compressive, tensile and flexural strengths, modulus elasticity of concrete over time. In addition, it causes excessive expansion, cracking, surface pop outs, joint sealant extrusion, surface deposits and discolorations. Figure 2.3 shows some of these distresses.

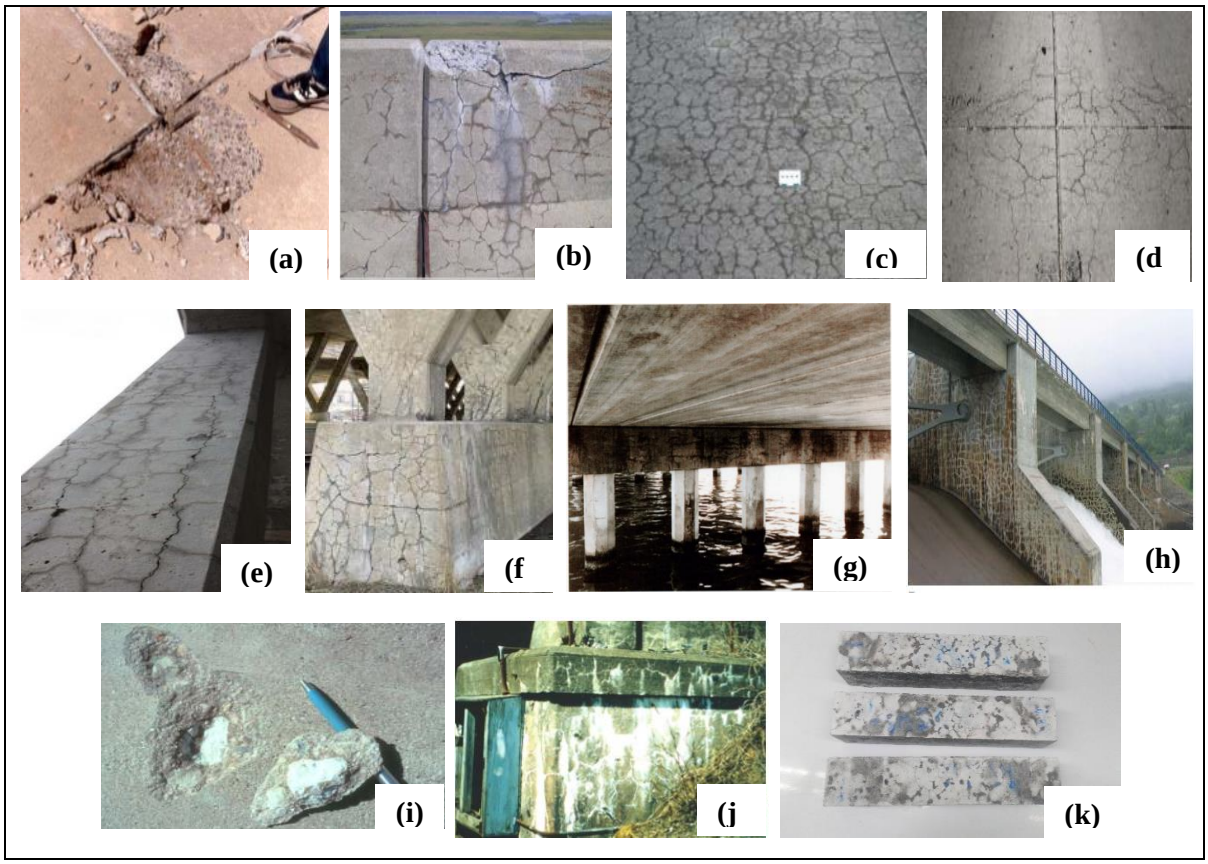

Figure 2.3: (a) Concrete spalling joint induced by ASR; (b) Parapet wall of bridges movement; (c) A well-developed cracks associated with ASR; (d) D-cracking associated with ASR; (e) Longitudinal cracking related to ASR in column bridges; (f) Verticals cracks shown in parapet walls; (g) Horizontal Cracking on pier cap of bridge; (h) Map cracking in bridge wing walls cause by ASR; (i) Pop outs distress; (j) Surface discoloration and exudation; (k) Expansion & Cracks seen in testing

2.4.1 Concrete Expansion in Pavement and Bridges

Concrete expansion is one of the major effects caused by ASR. The expansion of pavement is generally increases as a result of the swelling gel of ASR. Though the deterioration expansion in concrete is fairly slow, it was found to be progressive over a period of time (Diamond 1992). The expansion leads to loss in durability and serviceability, and service life of concrete structures. This expansion can be represented in a form of random map cracking, longitudinal cracks and joint spalling of concrete pavements (Figure 2.3a) (Stanton, 1941). In bridges, the ASR expansion varies from one member to another. This causes distresses such as joint closure, deflections with associated squeezing of sealing materials and eventually leading to concrete spalling joints. Also, it leads to adjacent concrete structure movement as shown Figure 2.3b (Thomas et al., 2012).

2.4.2 Cracking in Pavement and Bridges

Concrete cracking is one of the major distresses seen in concrete pavements and bridge decks. In concrete pavements, at the initial development, cracking is shown on pavement surface as randomly oriented cracks (showing no or little indication of serve cracks). These cracks can be more early seen in smooth surface than on grooved or textured surface and is more pronounced in wetted surfaces. In addition well-defined longitudinal cracks in the form of map cracking or pattern cracking (developed across the pavement width) can be the result of concrete ASR growth. The cracks increase with traffic especially with the jointed and continuous reinforced pavement. Additionally, D-Cracking in concrete pavements can be caused by ASR. The ASR D-cracks progress normally away from the transverse joints and pavement slab edge (Figure 2.3d) (Stark D, 1991; BCA, 1992). ASR associated cracks are observed in bridge decks and bridge columns. These cracks are in form of longitudinal cracks and are interconnected by tight short mini cracks that expand transversely between these longitudinal cracks. Also, white deposits on bridge columns are also observed. Most vertical cracks seen in bridge decks are caused by ASR deformation. The white deposit at the base is a sign of ASR swelling gel and $CaCO_3$ (ACI, 1998; Stark, 1991). Another crack associated with ASR is the horizontal crack in pier cap of bridge over water. The curb section also shows distress due to ASR in form of longitudinal and fine random cracks. These cracks tend to increase in the presence of moisture or in frost areas (Thomas et al 2012).

2.4.3 Pop-outs in Pavement and Bridges

Concrete pop outs occur as a result of poor bonding between cement paste and aggregate particles. ASR causes pop outs in concrete pavements and bridge decks when the surface reactive aggregates undergo expansion damage leading to detachment and separation from the bottom aggregates that have not undergone ASR expansion yet. This effect is more pronounced when the concrete surface aggregates are susceptible to frost action (Diamond, 1992). The gel formed beneath the pop outs indicates that such distress is caused by ASR. The pop outs range from 1in to 2in wide depending on the site location (Figure 2.3i). The durability and serviceability of concrete are not generally affected by pop outs; however, it can lead to roughness of the concrete surface.

2.4.4 Surface Deposits and Color Changes

Surface deposits due to gel exudation and efflorescence occur along cracks in concrete. These surface deposits are white to dark gray in color. The ASR gel excluding from the concrete surface can also be colorless fluid, viscous yellowish or rubber-like or hard (Poole, 1992). The presence of gel on the crack surface is an indication of ASR and it can increase in the presence of moisture, frost, and the use of frost susceptible aggregates. Surface discoloration areas are seen as bleached brown or pinkish in color and extending several inches from cracks (Figure 2.3j) Poole (1992).

2.5 Evaluation of Alkali-Silica Reaction (ASR)

Various test methods are developed and proposed to evaluate aggregates or concrete susceptibility to ASR. Efforts are continued to develop effective test methods to address some limitations of existing test methods. Figure 2.4 shows various test methods used to assess ASR potential. The most used test methods to evaluate reactive aggregates including aggregate petrographic examination, Accelerated Mortal Bar Test (AMBT), Concrete Prism Test (CPT), Miniature Concrete Prism Test (MCPT) in accordance to ASTM C 295, ASTM C1260, ASTM C1293, and AASTHO TP 110 respectively.

2.5.1 Aggregate Petrographic Examination

This method was first developed in 1954 by Mather (Mather et al., 1950) and later modified in 2008 and has become a standard test method (ASTM C295). This test is a reliable and fast method to identify reactive aggregate susceptible to Alkali-Silica Reaction (ASR). Visual and macroscopic examinations are performed on prepared aggregate samples using optical microscope where a thin aggregate section is carefully examined. In another case, the petrographic examination can be achieved by using X-ray diffractions, Scanning Electron Microscopy (SEM) or Infrared Spectroscopy (IR). However, these test methods have some limitations. They cannot be used to evaluate slow reactive aggregates and determine the level of reactivity. In addition, the visual and macroscopic examinations require an expert and skillful petrographic examiner. It consumes a lot of time and resources to identify reactive aggregates. The results of ASTM C295 also depend on the findings of other test methods (AMBT or CPT) to evaluate aggregates susceptibility to ASR and the level of their reactivity (Nixon & Sims, 1996; Touma et al.' 2001; Technical Services Center, 2009).

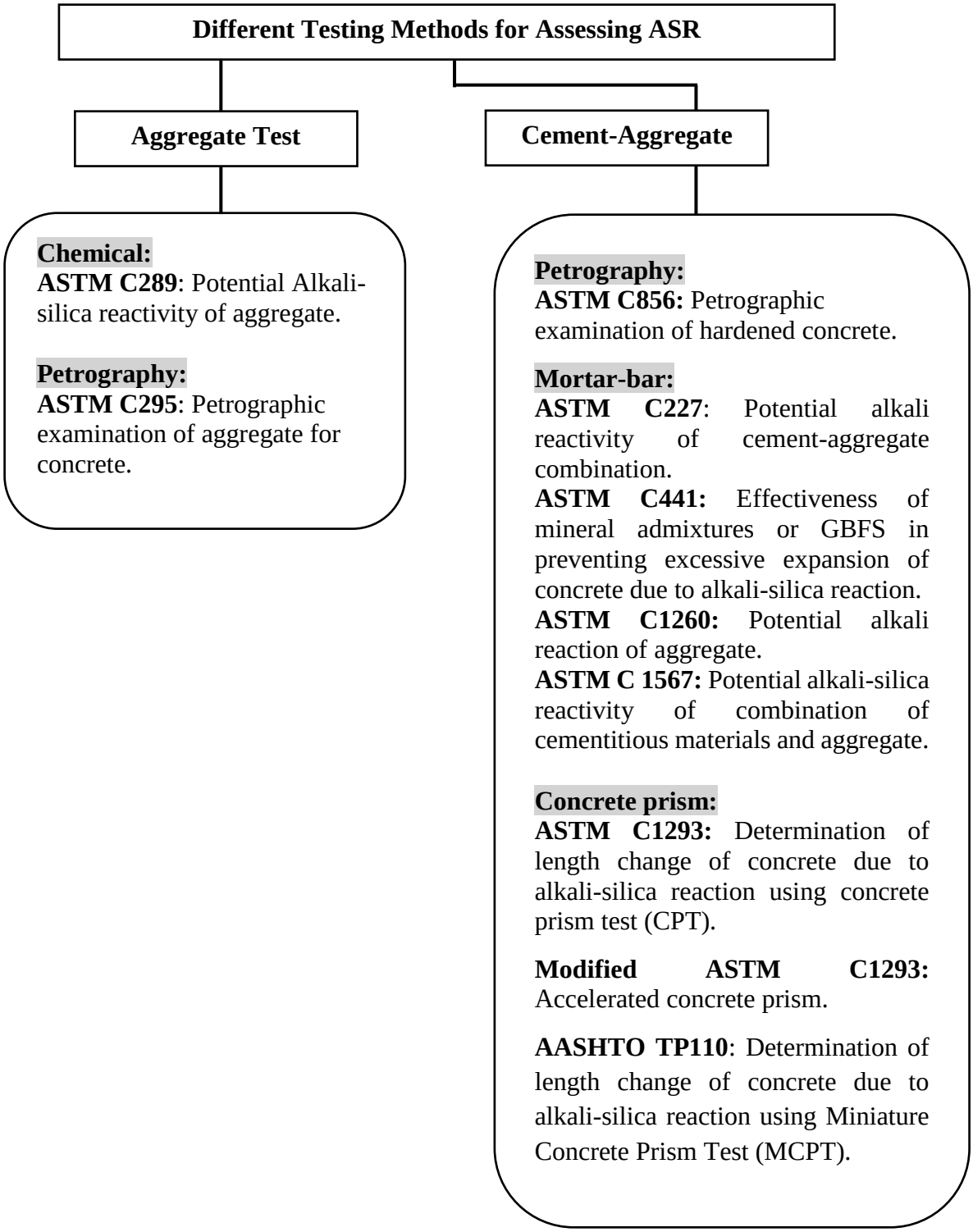

Figure 2.4: Various test methods used to evaluate ASR

2.5.2 Accelerated Mortal Bar Test (AMBT)

The Accelerated Mortal Bar Test (AMBT) is conducted in accordance with ASTM C 1260. This method was developed by Oberholseter and Davies (1986) at the National Building Research Institute (NBRT) in South Africa. In this test, the samples are immersed in sodium hydroxide (NaOH) at 80^{o}C (176^{o}F) for 14 days. Percent expansion, due to ASR, is measured with time.

An expansion less than 0.10% indicate non-reactive aggregates. If the expansion is in between 0.10% and 0.20%, the aggregates are considered slow reactive. An expansion greater than 0.2% indicates reactive aggregates. Some researchers (e.g., Jin, 1998; Malvar and Lenke, 2006; Folliard et al., 2006) indicates that the expansion threshold of 0.10% may be inadequate to evaluate the reactivity of some aggregates. Hooton (1991) proposed the extension of the testing time to 28 and 56 days with an expansion limit of 0.28% and 0.48%, respectively to evaluate low reactive aggregates (Hooton, 1991).

The shortcomings of this test include the fact that a harsh and aggressive environment (high test temperature and curing medium) could alter the expansion result (Berube et al., 1992). Ideker et al. found that the AMBT expansion results of many aggregates are consistent with the field performance (Ideker et al., 2012). It can provide false negative and false positive results. False positive test results indicate that the aggregate is deleterious (reactive) while field performance showed nonreactive and the opposite for false negative test results (Follard et al., 2006; Hooton, 1991). Follard et al. (2006) reported that four aggregates passing ASTM C 1260 failed using the 1-year ASTM C 1293 test. Likewise, false negative cases were reported by ITD RP 212 (2014). Another shortcomings of the ASTM C 1260 test methods is the duration or the test (Berube et al., 1993; Fournier & Berube, 2000 and Folliard et al., 2006). Although some researchers reported that the testing time (14 days) is sufficient to evaluate slow reactive aggregates (Shi et al., 2015; Fernandez-Jimenez et al., 20007), others proposed that the test method should be extended beyond the 14-day period (Palacious et al., 2006). However, Duyou et al. established a good correlation and a valid relationship between AMBT and CPT method when only reactive aggregates were considered (R-value of 0.81) (Duyou et el., 2008).

2.5.3 Concrete Prism Test (CPT)

2.5.3.1 One-Year CPT

This is a standard test method to evaluate the ASR expansion on concrete samples. This method was developed to overcome the limitations of other test methods used to assess susceptibility of aggregates to ASR. This methods evaluates concrete samples instead of aggregates or mortar bars. The expansion is determined based on the length change of the test samples. This test was developed by Swenson and Gillott during the 1950's in Canada (Swenson and Gillott, 1964).

The test procedure involves the use of high-alkali cement with alkali content of 0.90% ± 0.10% of 420 kg/m^3 and sodium hydroxide that is added to the mix water in order to raise cement alkalis to 1.25%. Concrete prisms measuring 75mm x 75mm x 285mm are cured in water for one full year at 100^{o}F. A concrete prism expansion less than 0.04% after one year is considered acceptable and above this value (i.e., 0.04%) is considered reactive. For mitigation, a concrete prism expansion less than 0.04% over a span of 2-year is considered acceptable. This test method is used to assess the reactivity of both fine and coarse aggregates using the concrete prism without excessive crushing unlike the AMBT method. This method (i.e., ASTM C1293) was found to be the most consistent and dependable compared to other test methods [Lu et al., 2008; Ideker et al., 2010].The two major limitations of this test method including long test duration, in which the concrete prisms are subjected to harsh conditions of alkali for one full year which is impractical for specific projects. The other limitation is alkali leaching. Researchers showed that approximately 35% of the alkalis leach out into the water storage after one year, and 20% of the alkalis leach out after only 90 days (Rivard et al., 2003, 2007; Thomas et al., 2012).

2.5.3.2 Six-month ACPT

As a result of the first limitation found in ASTM C 1293 (CPT). In 1992, Ranc and Debray proposed accelerating the rate of expansion in the concrete prism test called Accelerated Concrete Prism Test (ACPT), focusing on shortening its duration by increasing the exposure temperature to 60°C (140 °F). The Accelerated Concrete Prism Test (ACPT) is a revised protocol of the CPT method to overcome the limitations of the latter. This method was introduced by Ranc and Debray (Ranc and Debray, 1992). In this test, the testing time was

reduced from one year to six months by subjecting the test samples to a more aggressive environment. The test uses high-alkali cement meaning an alkali content of 0.90% ± 0.10% of 420 kg/m^3 and by adding sodium hydroxide to the mix water in order to raise cement alkalis to 1.25%. A 75mm x 75mm x 285mm test sample is prepared and cured in water for six months at 140^{o}F (60^{o}C). Different expansion limits were proposed; however, an expansion limit of 0.04% after 26 weeks was adopted (Latifee and Rangaraju, 2014). (Thomas et al., 2006) found that the 3-month expansion results of the accelerated concrete prism tests showed good correlation (R^2 = 0.9808) with results from the 1-year long standard concrete prism test (Thomas et al. 2006).

2.5.4 Miniature Concrete Prism Test, MCPT

2.5.4.1 Development of MCPT

The Miniature Concrete Prism Test (MCPT) is conducted in accordance with AASHTO TP 110. This test method was developed by Latifee and Rangaraju in in 2014. This MCPT is a new test procedure that was proposed to overcome the challenges encountered when using ASTM 1260 (14-day test) and ASTM 1293 (1-year test) test methods. The AASHTO TP 110 test takes about 56 days to complete, with an additional 28 days needed to test slow-reacting aggregates. This testing method was found to provide good correlations with ASTM C 1293 (1-year test) results as well as field performance. Also, it was found to provide reliable and dependable results of aggregate susceptibility to ASR (Latifee and Rangaraju, 2014).

The MCPT uses concrete prisms of 50mm x 50mm x 285mm (2-in x 2-in x 11.25-in). A concrete prism expansion less than 0.04% after 56 days is considered acceptable while an expansion above this value is considered reactive. The test specimens are placed in NaOH solution to accelerate ASR. This method uses a cement content of 1.25% similar to CPT method. It also uses 25mm (½-in) maximum coarse aggregate size rather than 19mm (¾-in) maximum size (used in CPT) without crushing aggregates (as used in the AMBT). Table 2.2 summarizes the main features of the AASTHO TP 110 (Latifee and Rangarajuin 2014).

Table 2.2: MCPT's Mixture proportions (some data extracted from Latifee and Rangaraju, 2014)

Item Mix	**Proportion**
Specimen Size	2-in x 2-in x 11.25-in
Test Duration	56 days – 84days
Storage Temperature	60°C (140°F)
Storage Environment	IN NaOH solution (Soak)
Initial Length (Zero)	24hrs in H_20 at 60°C (140°F)
Cement Type	420kg/m^3
Cement Alkali Content	0.9% +/- 0.1 Na_2O_{eq}
Alkali Boost (Total alkali content)	1.25% Na_2Oeq
Coarse Aggregate (dry Volume Fraction)	0.65
Coarse Aggregate	Maximum size of: 12.5 mm (1/2 in.)
Coarse Aggregate Proportion (% by weight)	1) 12.5 mm – 9.5 mm 2) 9.5 mm – 4.75mm
12.5 mm – 9.5 mm:	57.5%
9.5 mm – 4.75mm	42.5%
Fine Aggregate	Determined based on ACI 211; Absolute Volume Method: ($1 - V_{H2O}$ + Vcg + Vcem)
Water-to-Cement ratio:	0.45

2.5.4.2 Implementation of MCPT in USA

Latifee and Rangaraju (2014) evaluated the susceptibility of 19 fine and coarse aggregates to ASR expansion. These aggregates were from various sources. They correlated the results with both the 14-day AMBT and 1-year CPT test methods. The results showed that this method produced a strong correlation (R-squared = 0.99) with CPT and a weak correlation with the AMBT method (R-squared = 0.5) (Latifee and Rangaraju, 2014; Latifee et al., 2015).A research study conducted in Wyoming evaluated the ASR expansion using various test methods including MCPT, AMBT, CPT, and CAMBT and they correlated the results with field performance (Fertig et al, 2013). The CAMPT test method used in Wyoming is very similar to the MCPT test method except the specimens were cured for 28 days instead of 56 days.

Expansion limits were specified at 0.040% for both CPT and MCPT methods and 0.10% at 14 days for the AMBT method. The results showed that the CPT is generally considered the most accurate testing methods compared to other methods. There was no appreciable correlation between the CPT and MCPT test methods (Fertig et al, 2013).

In Pennsylvania, several test methods were used to study the ASR of different aggregates including Hydrocure LWA, Oley, Union Furnace, Tyrone, Jobe, and Spratt. The results showed poor correlation between MCPT and 1-year CPT (Salwocki, 2016) similar to the study conducted in Wyoming (Fertig et al., 2013). Other expansion data were acquired from other states using the AMBT, CPT and MCPT methods. A recent study by Prasada Rangaraju at Clemson University showed that the expansion of MCPT correlates with the expansion of the AMBT testing while it deviates from the 1-year CPT expansion data. There was a good correlation between MCPT and AMBT expansion values (Rangaraju, 2018).

2.6 Correlation between MCPT and both CPT and AMBT

Table 2.3 summarizes the level of aggregate reactivity or aggregate reactivity classifications for the three test methods (i.e., MCPT, AMBT, and CPT) (AASHTO PP 65; Fertig et al., 2016). Latifee and Rangaraju (2014) tested 12 aggregates from different sources using the three test methods mentioned. The results showed a little discrepancy in expansion results for three aggregates. For instance, QP aggregates which were found to be non-reactive (0.080%, less than the ASTM threshold of 0.10%) using the 14-day AMBT method, were found to be reactive using the 56-day MCPT and 1-year methods. Conversely, SLC and MSP aggregates showed an opposite outcome. The MCPT and CPT methods showed these aggregates to be non-reactive with an expansion of 0.03% and 0.031%, respectively for SLC and 0.023% and 0.03%, , respectively for MSP. While, the 14-day AMBT method reported the same aggregates to be reactive with an expansion of 0.19% and 0.11% for SLC and MSP, respectively.

Figure 2.5 depicts the correlation between the 56-day MCPT and 1-year CPT as well as between 56-day MCPT and 14-day AMBT. To distinguish the aggregate prone to ASR from non-reactive aggregate in the 56-days and 1-year testing method, the expansion bench mark is specified at 0.04% which is based on the accepted criterion of ASTM C1293 standard

method. The R-squared value of the correlation between the 56-day MCPT results and the 1-year CPT was very high (0.99). Meanwhile, using the expansion limits of 0.04% for the 56-day MCPT and 0.10% for the 14-day AMBT to distinguish reactive aggregate from non-reactive aggregates, the correlation was fair (R-squared = 0.49). However, other States show a different correlation among the test methods (Rangaraju, 2018). These results suggested that more studies should be conducted on aggregates with different characteristics to determine the validity of different test methods.

Table 2.3: Classification of Aggregate Reactivity

Reactivity	**1-Year Expansion in CPT,%**	**14-Day Expansion In AMBT, %**	**56-day Expansion in MCPT, %**
R0 Non-reactive	≤ 0.04	≤ 0.10	**≤ 0.03**
R00 Slow/Low Reactive			**> 0.031, ≤ 0.040**
R1 Moderately reactive	> 0.04, ≤ 0.12	> 0.10, ≤ 0.30	**> 0.041, ≤ 0.012**
R2 Highly reactive	> 0.12, ≤ 0.24	> 0.30, ≤ 0.45	**> 0.121, ≤ 0.240**
R3 Very highly reactive	> 0.24	> 0.45	**> 0.241**

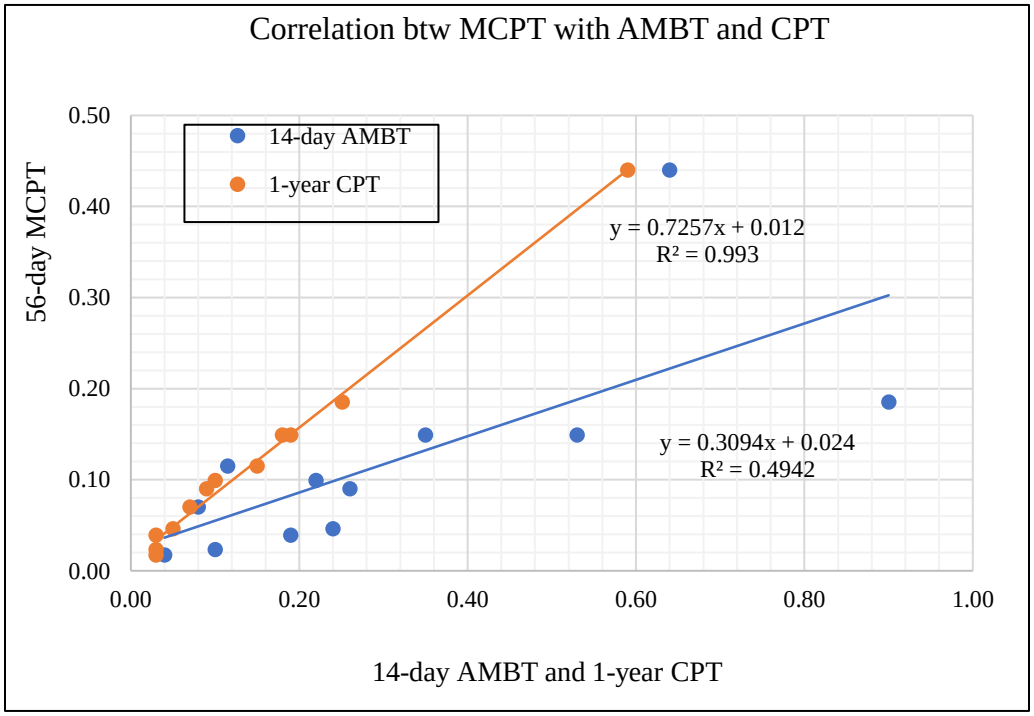

Figure 2.5*:* Correlation between MCPT with CPT and AMBT (Latifee and Rangaraju, 2014)

2.7 ASR Mitigation measures using Waste Glass Powder and other SCMs

One of the most common solid waste materials around the world today is glass. Waste glass poses a huge environmental problem and thereby need urgent solution (Du and Tan, 2013). Waste glass is a non-biodegradable material and is found in massive quantities in landfills (Figure 2.6). However, due to limited space in new landfills, this waste glass is now being found to be more available in densely populated cities in various countries. Recycling or reclaiming of waste glass is the best solution to overcome its environmental impact on society. The recycling of waste glass is important due to the huge amount of resources and processes involved during the production of glass (Saito and Shukuya, 1996; Ruth and Dell'Anno, 1997; Du and Tan, 2013). Such processes also generate large amounts of CO_2 and other greenhouse gases that have detrimental effects on human wellbeing, environmental conditions and climate change (Schmitz et al., 2011; Saito and Shukuya, 1996). Although many countries are reusing waste glass, the rate of cycling is still very low (Du and Tan, 2013). In the United States, only 27% of waste glass is being recycled out of 12 million tons of waste glass generated in 2010 (U.S. EPA., 2012) while only 50% of waste glass is being recycled in European countries out of about 4.2 million tons generated waste glass (European Commission, 2010). Therefore, it is essential to find alternative solutions to utilize the waste glass to reduce energy consumed, landfill space, to improve cost effectiveness and most importantly to conserve natural resources.

The construction industry (especially the cement and concrete industry) is found to be one of the most appealing fields where waste glass can be utilized. Table 2.4 presents the similarity in the chemical composition and mechanical properties of waste glass with the conventional cement and sand. Waste glass can be used as partial replacement for cement or sand in concrete (Shayan, 2002; Taha and Nounu, 2008; Nassar and Soroushian, 2012). Therefore, using waste glass as an alternative construction material in cement and concrete sector can help reduce the cost of materials, energy consumed, reduce CO_2 and other greenhouse emissions, and environment hazards.

Numerous research studies were conducted to evaluate the use of waste glass in highway concrete structures. Some research studies considered the use of crushed waste glass as a partial replacement for fine aggregates (sand) while others evaluated the properties of

concrete when fine waste glass is used as a partial replacement for cement. Park et al. (2004) and Sekar et al. (2011) studied the strength characteristics (compressive, flexural and splitting tensile strength) of concrete containing waste glass. The results show that the strength (i.e., compressive, tensile and flexural strengths) decreased as the percent of waste glass increased (Park et al., 2004; Sekar et al., 2011).

Some studies found that finely-grounded glass, which contains 70% of silica and about 10% to 20% of alkalis, can improve the properties of fresh concrete (Vanjare & Mahure, 2012; Khatib et al., 2012). This is due to the fact that the pozzolanic reactivity of waste glass increases as the size of glass decreases, which in turn increase the workability, durability and mechanical properties of concrete structures (Shi et al., 2005; Neithalath, and Schwarz, 2009; Turgut and Yahlizade, 2009; Vanjare & Mahure, 2012; Khatib et al., 2012).

Shi et al. (2005) showed that a concrete mixture prepared with waste glass (15 µm in size) to increase the strength index activity by about 115%. Schwarz et al. (2008) also supported the results of Shi et al. (2005) and reported that a waste glass of 20 µm size was found to provide comparable compressive and tensile strengths compared to a control mixture. Likewise, Afshinnia and Rangaraju investigated the effect of glass powder of size 17 µm and 70 µm on the pozzolanic behavior and ASR mitigation. The results showed that concrete mixes with 20% glass of 17 µm size produced a strength activity index of 37% more than concrete mix containing glass of 70 µm size (Afshinnia and Rangaraju, 2015). These results show that the pozzolanic reactivity of concrete is improved with the use of find waste glass.

Figure 2.6: (a) waste glass in landfill in Wyoming; (b) stockpile of waste glass in West Virginia; (c) crushed glass of size 75μm <size< 5mm; (d) waste glass powder of size <75μm (Amos, 1993)

Table 2.4*:* Cement, sand and the various waste glass chemical features (Soroushian, 2012)

Chemical	**Cement (%)**	**Sand (%)**	**Clear glass**	**Brown glass**	**Green glass**	**Crushed glass**	**Glass powder**
SiO_2	20.2	78.6	72.42	72.21	72.38	72.61	72.2
Al_2O_3	4.7	2.55	1.44	1.37	1.49	1.38	1.54
CaO	61.9	7.11	11.50	11.57	11.26	11.70	11.42
Fe_2O_3	3.0	2.47	0.07	0.26	0.29	0.48	0.48
MgO	2.6	0.46	0.32	0.46	0.54	0.56	0.79
K_2O	0.19	0.42	13.64	13.75	13.52	13.12	12.85
Na_2O	0.82	0.64	0.35	0.20	0.27	0.38	0.43
SO_3	3.9	-	0.21	0.10	0.07	0.09	0.09
TiO_2	-	0.15	0.035	0.041	0.04	-	-

Various researchers examined ASR expansion behavior of concrete containing waste glass; whether as partial replacement of aggregates or cement (Saccani & Bignozzi, 2010; Idir et al., 2010; Maraghechi, et al 2011; Lee et al., 2011; Serpa et al., 2013; Zheng, 2016). It was found that size and dosages as well as chemical properties of waste glass have a great effect on ASR susceptibility. The larger the glass size or dosage, the greater ASR expansion behavior of the concrete mixtures and the greater the alkali content, the higher ASR potential.

Zheng (2016) investigated the effect different sizes of glass powder on ASR expansion (e.g., 50µm and 200µm). Zheng (2016) found that mortar bar with 30% finer glass has length expansion of 0.1% compared to 0.3% expansion when 30% coarser glass was used (Zheng, 2016). Other studies (Nassar and Soloroushian, 2012; Lee et al., 2011) concluded that a glass powder with an appropriate dosage and a size equals to or less than 15µm helped reduce the ASR expansion of concrete.

The ASR expansion can also be mitigated using supplementary cementitious materials (SCMs). The use of SCMs was found an effective approach to reduce ASR expansion. Various SCMs were examined including fly ash, silica fume, slag cement, and Meta-kaolin (Shehata and Thomas, 2000; Venkatanarayanan and Rangaraju, 2011; Venkatanarayanan and Rangaraju 2013; Peterson K., 1992; Boddy et al., 2003; Hester et al, 2005; Beglarigale and Yazici H, 2014; Aquino et al., 2001; Shekarchi et al., 2010). The results showed that the efficiency of using various SCMs depends greatly on both the chemical properties as well as percentage of SCMs. For example, it was found that a meaningful dosage level (e.g., 10% up to 30%) of fly ash (Class C) or slag as SCMs can reduce concrete susceptibility to ASR expansion. However, a balance must be achieved when using such SCMs as this can affect other concrete properties such as workability and early strength (Lane & Ozyildirim, 1999; Shehata & Thomas, 2000). In addition, a sample mix of silica fume as SCMs should be limited as high replacement content may affect fresh concrete properties (Bagheri et al., 2012). Other cementitious materials that also affect workability is the Meta-kaolin (Radlinski & Olek, 2012). High percentage of waste glass and some fly ash type (class C) in concrete found to increase the ASR susceptibility (Shayan & Xu, 2004; Idir R et al., 2010). Therefore, a mixture of two or more SCMs can mitigate ASR expansion and also help to achieve all the required properties of concrete

Several researches investigated the effectiveness of using ternary blend (three cementitious combinations] in concrete. The ternary blend is proposed to mitigate ASR and improve other concrete properties to overcome the shortcoming of using only one SCMs (Erdem and Kırca, 2008; Gesog˘lu et al., 2009; Bagheri et al., 2012; Radlinski and Olek, 2012). It was found that the ternary blend is more beneficial and effective compared to the binary blend in term of mechanical, rheological and durability performance of concrete (Kandasamy and Shehata,

2014; Kaveh and Rangaraju, 2015). For instance, Sheheta and Thomas (2000) conduct a study using a ternary blend of silica fume and fly ash to evaluate ASR mitigation. They concluded that using 10% of silica fume and 30% of fly ash resulted in ASR expansion below 0.04% after 2 years (Shehata and Thomas, 2000). Likewise, Lane and Ozyildirim (1999) used a blend of silica fume and slag and concluded that such blend mitigated ASR expansion and improved early age strength of concrete sample. The effectiveness of ternary blend containing class C fly ash and Meta-kaolin was investigated by Moser et al. (2010). It was concluded that high ASR expansion was measured with the blend of class F fly ash and Meta-kaolin compared to a binary blend containing same amount of Meta-kaolin only (Moser et al., 2010). In 2014, Kandasamy and Shehata found no effect of using a ternary combination of slag and fly ash on concrete expansion compared to individual SCMs at the same dosage level.

From these studies conducted on using ternary blends or combinations of SCMs to mitigate ASR expansion of concrete, it was clear that the ternary blend of slag and high lime fly ash at nominal dosage level has tendency to mitigating ASR expansion without adversely affecting on other properties of concrete. Silica fume and meta-kaolin show a greater tendency to mitigate ASR and effective in supporting other SCMs setbacks. However, the use of silica fume and meka-kaolin in concrete can reduce the workability of concrete. In addition, the silica fume is very expensive. Therefore, there is a need evaluate other materials such as waste glass along with other SCMs (silica fume, slag) to address ternary combination effectiveness. Afshinnia and Rangajaru (2015) studied the efficiency of ternary blends containing fine glass powder in mitigating ASR expansion. The SCMs used were fly ash, meta-koalin, slag and waste glass. The results showed that the use of such ternary blends containing SCMs and glass waste at low percentage reduced ASR expansion and kept other concrete properties unaffected.

2.8 Microstructural Analysis

2.8.1 The Scanning electron microscopic (SEM)

The Scanning Electron Microscopic (SEM) provides high-resolution images of the surface of test materials. The SEM provides higher magnification (> 100,000x) and field depth up to 100 times that of the light microscopes (MEE, 2014). Another crucial advantage of SEM over the light microscope is the added qualitative and quantitative chemical analysis. Such analysis is conducted using an Energy Dispersive X-ray Spectrometer (EDS) attached to the SEM machine. The EDS provides chemical composition and element present in of samples (MEE, 2014; Langan and Wang, 2002).

Numerous research studies were conducted to evaluate the pozzolanic properties of mortar and concrete samples using SEM and EDS. Shao et al. (2000), found that that the fine size of glass powder provides greater pozzolanic activity which significantly improves ASR mitigation compared to the larger sizes of glass powder. This conclusion was also supported by (Kaveh & Rangaraju, 2015; Maraghechi et al., 2012) studies. Likewise, Rajabipour et al. (2010) reported that the ASR expansion doesn't occur at the aggregate-cement paste interface but it happens within the interior of glass or aggregate particles at the micro level. These results are supported by those obtained by Hassan and Rangaraju (2018) when they studied the properties of Portland cement concrete prepared with ground glass fiber as a pozzolan.

Kaveh and Rangaraju (2015) also utilized the SEM in ASR evaluation in concrete samples that have glass powder. The SEM images were used to detect ASR gel in the internal cracks of glass or aggregate particles. The researchers demonstrated that the ASR gel is found predominately at the surface of aggregates rather than inside the particles. They also discovered from SEM images that the binary and ternary blends of SCMs tend to effectively suppress ASR gel compared to the control mix. The microstructural investigation showed that coarser glass particles produce more ASR gel compared to fine glass particles. However, contrary to previous studies, they established that no ASR gel manifested either at the glass-particle interface or around in the cement paste for their mixes. Due to this contradiction, more microstructural investigation or analysis is needed to examine ASR gel at the micro level in mortar samples. Additionally, further research should be carried out to examine SEM analysis on binary and ternary blends containing SCMs and glass powder (used to mitigate

ASR distress) as well as control mixtures as this area is limited in the literature. The expansion behavior at different curing ages should also be investigated using SEM imaging and correlated with the measured expansion.

2.9.2 Thermogravimetric Analysis (TGA)

Thermogravimetric analysis also known as Thermal gravimetric analysis is a comprehensive technique of thermal analysis. It measures the changes in physical and chemical properties of a material when subjected to an increasing temperature over a period of time. These physical properties include phase evolutions, absorption or adsorption and desorption while the chemical properties include oxidation, decomposition or chemisorption (Coat, 1963). Hydration is one of the crucial chemical reactions of cement paste and concrete. The rate of hydration depicts mass conversion at various phases which in turn affects the mechanical properties of cement paste such as strength, toughness, permeability, diffusivity. It can used to study the pozzolanic reactivity of mixtures containing Supplementary Cementitious Materials (SCMs).

Prior to TGA, calometric analysis was utilized to evaluate the hydration rate and pozzolanic activity of cement paste (Zhang et al., 2002; Langan et al., 2002; and De Schutter, 1999). According to De Shutter (1999), the calometric technique cannot be used to evaluate the pozzolanic reactions of blended cement especially at high heat rate, leading to the development of TGA method. The TGA technique is considered the most widely used chemical analysis method to study hydration by studying the mass decomposition with respect to increased temperature and time. For instance, this method was adopted to investigate the rate of hydration of pozzolanic materials such as silica fume, fly ash, slag and meta-kaolin (Frias and Cabrera 2001; Mostafa et al., 2001; Shi and Day, 2000; and Yu et al., 1999). Additionally, it was utilized to study the rate of hydration of blended cement paste containing fly ash (Marsh, 1988) and slag cement (Abo-ElEnein et al., 1974). The mass decomposition of calcium hydroxide at a specific temperature is often monitored to characterize the pozzolanic reaction or hydration rate of cement paste (Kaveh and Rangaraju, 2015). Kaveh and Rangaraju (2015) examined the pozzolanic reactivity of binary and ternary mixes containing glass powder using TGA. The results showed potential benefits of using a ternary blend containing glass powder at only 20% replacement.

CHAPTER THREE: TESTING MATERIALS AND PROTOCOLS

3.1 Introduction

Chapter 3 covers the selection of test aggregates and testing protocols used to assess the ASR susceptibility. A total number of 11 aggregates with different characteristics and sources were selected for both the new proposed 56-day AASTO TP 110 (Miniature Concrete Prism Test [MCPT]) test method as well as 14-day ASTM C1260 (Accelerated Mortar Bar Test [AMBT]). In addition, six different aggregate types out of these 11 tests were also tested using the one-year ASTM C1293 (Concrete Prism Test [CPT]) test method and the six-month unconventional Accelerated Concrete Prism Test (ACPT). Table 3.1 presented the testing matrix for ASR evaluation using various test methods.

3.2 Test Materials

3.2.1 Aggregate Types

A total number of 11 aggregate types were selected for testing ASR expansion (Table 3.1). Some of test aggregates were acquired from different parts of Idaho.

1. *EL- 116c*: acquired from District 3; Terrace gravels of Snake River; East of Bliss, ID.
2. *ORE-8c*: acquired from District 3; Terrace gravels of Snake River; Ontario, Oregon.
3. *Md-45c*: acquired from District 4; Alluvium of Snake River; Southeast of Acequia, ID.
4. *Pw-84c:* acquired from District 5; Gravel and Sand deposits of Bonneville flood; West of Chubbuck, ID.
5. *Ma-22c:* acquired from District 6; Alluvium of Teton River; North side of Rexburg, ID.
6. *Wn-56c:* acquired from District 6; Terrace gravels of Snake River Plain; Eastern of Idaho.
7. *Basalt*: acquired mainly from District 1, ID and part of Washington
8. *Limestone:* acquired from out of state; sedimentary rock
9. *Gabbro:* acquired from out of state; Igneous rock
10. *Manufactured Sand:* acquired from eastern Washington
11. *Granite:* acquired from District 2 (Lewiston); this aggregate was used as a reference aggregate.

The aggregates used in Idaho are El-116c, Ore-8c, Md-45c, Pw-84c, Ma-22c, Wn-56c, manufacture sand and basalt. Table 3.2 provides information about the properties of the test aggregates.

Table 3.1: Aggregates selected for ASR evaluation using different test methods

Aggregates Types	**AMBT (14-day)**	**MCPT (56-day)**	**CPT (1-year)**	**ACPT (6-month)**
Elmore, EI-116c	√√	√√	-	-
Power, Pw-84c	√√	√√	-	-
Minidoka, Md-45c	√√	√√	-	-
ORE-8c	√√	√√	-	-
Madison, Ma-22c	√√	√√	-	-
Wn-56	√√	√√	√√	√√
Basalt	√√	√√	√√	√√
Gabbro	√√	√√	√√	√√
Limestone	√√	√√	√√	√√
Granite	√√	√√	√√	√√
M. Sand	√√	√√	√√	√√

Table 3.2: The properties of each aggregates tested for ASR

Properties	**Different Aggregates types**										
	EI-116c	**ORE-8c**	**Md-45c**	**Pw-84c**	**Ma-22c**	**Basalt**	**Gabbro**	**Granite**	**Lime-stone**	**M. Sand**	**Wn-56**
SGOD	2.69	2.72	2.51	2.55	2.75	2.83	2.6	2.7	2.82	2.64	2.62
SGSSD	2.71	2.74	2.52	2.58	2.76	2.85	2.63	2.71	2.83	2.66	2.64
Absorption, %	0.46		0.42	0.40	0.34	0.38	1.09	0.82	0.35	0.53	0.44
DRUW (kg/m^3)	1403	1568	1557	1531	1566	150 3	1585	1634	1700	1592	161 2
DRUW (Ib/ft^3)	87.5 9	97.89	97.2 0	95.5 8	97.7 6	93.8 3	98.9 5	102. 01	106.13	99.39	100. 63

3.2.2 Portland Cement

A low-alkali cement (ASTM C150 Type I), was acquired from the Pre-Mix concrete plant in Pullman, Washington and was used in this research study. The cement alkali content is 0.49% Na2Oeq. High-alkali cement (ASTM C150 Type I) acquired from Illinois Cement Company, LaSalle, IL, was used in this research study as well. The cement alkali content was 0.82% Na2Oeq with Blaine's fineness of 383 m^3/kg. The autoclave expansion of both low-alkali and high alkali cement was 0.03% and 0.018%, respectively, which is well below 0.8% requirement. The specific gravity is 3.15 for both cement types. Table 3.3 describes the chemical composition of the two cement types.

Table 3.3: Chemical Composition of Cement

	Chemical Composition by mass (%)						
Cement type	SiO_2	Al_2O_3	Fe_2O_3	CaO	MgO	SO_3	Na_2Oe
High-Alkali Cement	19.45	4.85	3.13	61.84	2.92	4.15	0.82
Low-Alkali Cement	20.6	5.1	3.4	64.5	1	3.1	0.49

3.2.3 Reagent

Reagent grade sodium hydroxide (NaOH) beads manufactured by Masers Company Inc., Wood Dale, Illinois were used as a curing agent by mixing 1N (normality) in curing water. This reagent also was used to increase the MCPT concrete samples' alkali level to 1.25% Na_2Oe by weight of cement. (Note: 1N of NaOH is equivalent to 40g of NaOH).

3.3 Test Procedures

Various test methods were used to evaluate aggregate or concrete susceptibility to ASR. In this study, the most prominent test procedures included 1) ASTM C 1260: Accelerated Mortar Bar Test (AMBT), 2) ASTM C 1293: Concrete Prism Test (CPT), 3) AASHTO TP 110: Miniature Concrete Prism Test (MCPT), and 4) Accelerated Concrete Prism Test (ACPT). Table 3.4 provides a summary of the test methods. This section describes these test methods.

3.3.1 Accelerated Mortar Bar Test; AMBT (ASTM C 1260)

The Accelerated Mortar Bar Test ASTM C 1260 was developed to detect potential expansion due to ASR in concrete. Samples 25mm x 25mm x 285mm (1in x 1in x 11.25in) are prepared

in accordance with the standard aggregate gradation of ASTM C33 or ASTM C150. The autoclave expansion of the low alkali cement is limited to 0.03%. The cement to sand ratio is 1:2.25 with a water to cement ratio of 0.47. Prior to mixing, the sand is oven dried and sieved to the particle size distribution required by ASTM C 1260. Twenty-four hours after casting, the test samples are demolded and cured in water for another 24 hours in an oven at 80C. Then, the test samples are immersed in 1N of sodium hydroxide (NaOH) solution at a temperature of 80C for 14 days after curing in water. The zero reading (i.e., first length reading) is recorded with the use of length comparator before immersion of test samples in the NaOH solution. The length readings are recorded after 1, 3, 5, 7, 10 and 14 days of immersion of the test samples in the NaOH solution. An expansion less than 0.10% of the mortar bar indicates non-reactive aggregates. If the average expansion is between 0.11% and 0.30%, the aggregates are considered moderately reactive, while expansion above 0.31% indicates reactive aggregates as presented in Table 3.7.

3.3.2 Concrete Prism Test, CPT (ASTM C 1293)

This method was developed to overcome the limitations of other test methods used to assess aggregates susceptibility to ASR by introducing a concrete test method (instead of aggregate test or mortar bar test). The test method measures the concrete prism change in length. The aggregate gradations for both fine and coarse aggregates used in this test method are provided in Table 3.6. The test involves the use of high-alkali cement with alkali content of 0.90% ± 0.10% and cement content of 420 kg/m^3. In addition, sodium hydroxide (NaOH) is added to the mixing water to raise the cement alkalis to 1.25%. Concrete prisms measuring 75mm x 75mm x 285mm (3in x 3in x 11.25in) are prepared and cured in water for one full year at 38C. The length comparator is used to measure length change at various days (1, 3, 5, 7, 10, 14, 21, 28 56, and every month until 12th month) and the percent expansion is then calculated. As presented in Table 3.7, a concrete sample expansion less than 0.04% after 365 days is considered non-reactive and an expansion greater than 0.241% is considered highly reactive.

3.3.3 Miniature Concrete Prism Test, MCPT (AASTHO TP 110)

The MCPT test procedure was developed to overcome the challenges encountered when using ASTM 1260 and ASTM 1293 test methods. The AASHTO TP 110 test takes about 56

days to complete with an additional 28 days needed in case of slow reacting aggregates. The new test uses concrete prisms measuring 50mm x 50mm x 285mm (2in x 2in x 11.25in) cured in NaOH at 60C. The test also involves the use of high-alkali cement meeting an alkali content of 0.90% ± 0.10% and cement content of 420 kg/m^3. In addition, the sodium hydroxide (NaOH) is added to the mixing water to raise the cement alkalis to 1.25%. AASTHO TP 110 adopted the immersion of test specimens in a NaOH solution to accelerate ASR compared to STM C 1260 (AMBT). The length comparator is used to measure the change in length at various days (i.e., 1, 3, 7, 14, 21, 28, 42, and 56 days) and the percent expansion is calculated. As presented in Table 3.7, a concrete sample expansion less than 0.03% after 56 days is considered non-reactive and an expansion greater than 0.241% is considered highly reactive.

3.3.4 Accelerated Concrete Prism Test, ACPT

This method is a modification of the ASTM C 1293 test. The idea is to reduce the test duration from 1-year to 6 months by subjecting the test samples to a higher temperature of 140F compared to 100F employed for CPT. The test procedure also uses high-alkali cement meeting an alkali content of 0.90% ± 0.10% and cement content of 420 kg/m^3. Also, sodium hydroxide was added to the mixing water to raise cement alkalis to 1.25%. Similar to the 1-year test method, the ACPT samples are 75mm x 75mm x 285mm. The test samples are cured in water for six months at 60^{o}C. Expansion or change in length was measured after 1, 3, 7, 4, 28, 56, 84, 112, 140 and 168 days.

Table 3.4: Summary of ASR Test Procedure

Test Procedure	AMBT (ASTM C1260)	CPT (ASTM C1293)	MCPT (AASHTO TP 110)
Test Type	Mortar Bar Test	Concrete test	Concrete test
Specimen Size	1in x 1in x 11.75in	3in x 3in x 11.25in	2in x 2in x 11.25in
Test Duration	14-day	1-year	56-day – 84-day
Storage Temperature	80^{o}C (176^{o}F)	38^{o}C (100^{o}F)	60^{o}C (140^{o}F)
Storage Environment	IN NaOH soln	100% H20	IN NaOH soln
Initial duration (zero)	24hrs in H20 @ 800C	Nill	24hrs in H20 @ 600C
Cement Type	420kg/m^3 (26lb/ft^3)	420kg/m^3	420kg/m^3
Cement Alkali Content	0.82% +/- 0.1 Na2Oeq	0.82% +/- 0.1 Na2Oeq	0.82% +/- 0.1 Na2Oeq
Alkali Boost	No Alkali boost	1.25% Na2Oeq	1.25% Na2Oeq
Coarse Aggregate	4.75mm – 0.15mm	19mm – 4.75mm	12.5 mm (1/2 in.)
Mix Design			
Water-to-Cement	0.47	0.42 – 0.45	0.45
Dry coarse agg. Vol	Fine aggregate	0.7	0.65

3.4 Specimen Preparation

Table 3.5 presents the mix gradation of mortar bars prepared and tested using ASTM C1293, AASTHO TP 110, and ASTM C 1260. Table 3.6 presents the aggregate graduation requirements of different test methods. For the 14-AMBT method, three replicates of the 1in x 1in x 11.25in specimens were prepared in accordance with ASTM C 1260. Prior to mixing, aggregates (fine and coarse) were collected from source, oven dried and then sieved and batched (well-graded aggregates as shown in Figure 3.1) in accordance with respective aggregate gradation standards (ASTM C136). The water cement ratio used was 0.47. A portable mixer was used for aggregate mixing to ensure thorough mixing without segregation. The mix was then placed in lubricated steel molds and compacted with a tamper rod for consolidation.

Furthermore, in accordance to AASTHO TP 110, concrete prism of 50mm x 50mm x 285mm (2in x 2in x 11.25in). The test involves the use of high-alkali cement meeting an alkali content of 0.90% ± 0.10% and cement content of 420kg/m^3. In addition, sodium hydroxide was added to the mixing water in order to raise cement alkalis to 1.25%. The water-cement

ratio was 0.45. Each mixture was placed in the mold after mixing and compacted. Similar procedure was followed for the CPT test method with water cement ratio of 0.45. Figure 3.2 illustrates the process followed for each preparation. A typical example mix design is provided in Appendix A.

Table 3.5: Mixt design for each testing method

Mix Design at control (kg/m^3)						
Test Method	**W/C**	**Sample-Type**	**Water**	**Cement**	**FA**	**CA**
ASTM C 1260 (AMBT)	0.47	Mortar	207	440	990	-
AASTHO TP 110 (MCPT)	0.45	Concrete	449	997	1780	2320
ASTM C 1260 (CPT)	0.45	Concrete	901	2003	2717	5348

Table 3.6: Aggregate Gradation Requirement (ASTM C441)

AMBT (14-day)		**CPT (1-yr) & ACPT (6-mth)**		**MCPT (56-day)**	
Passing Sieve (FA)	Mass (%)	Passing Sieve (FA)	Mass (%)	Passing Sieve (FA)	Mass (%)
4.75 mm (No. 4)	10	4.75 mm (No. 4)	10	4.75 mm (No. 4)	10
2.36 mm (No. 8)	25	2.36 mm (No. 8)	25	2.36 mm (No. 8)	25
1.18 mm (No. 16)	25	1.18 mm (No. 16)	25	1.18 mm (No. 16)	25
600 μm (No. 30)	25	600 μm (No. 30)	25	600 μm (No. 30)	25
300 μm (No. 50)	15	300 μm (No. 50)	15	300 μm (No. 50)	15
		Passing Sieve (CA)		Passing Sieve (CA)	
		19.0 mm (3/4 in.)	33	12.5 mm (1/2 in.)	57.5
		12.5 mm (1/2 in.)	33	9.5 mm (3/8 in.)	42.5
		9.5 mm (3/8 in.)	33		

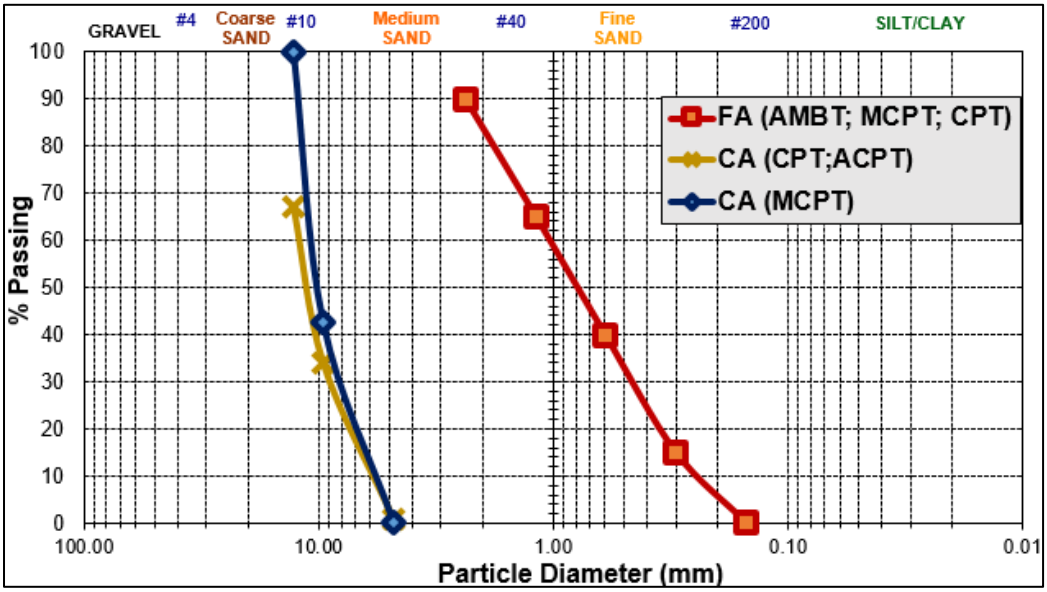

Figure 3.1: Sieve analysis of aggregates

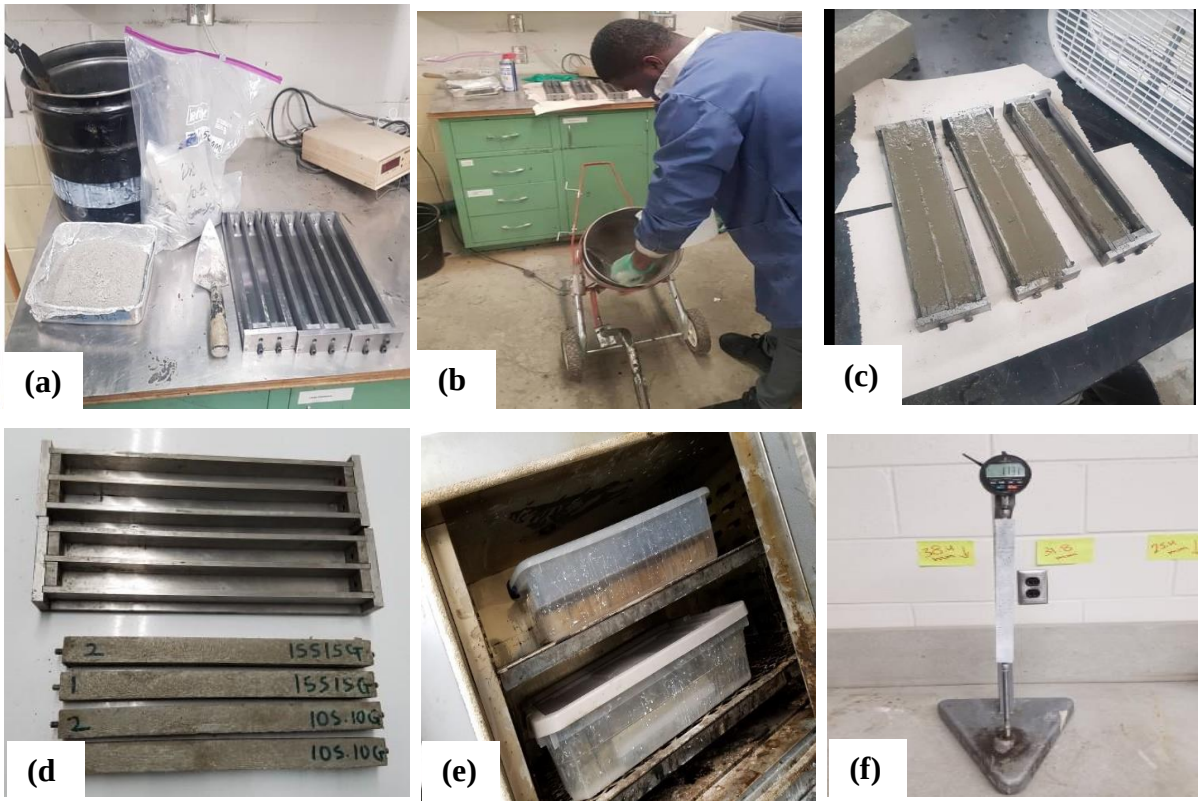

Figure 3.2: (a) aggregate preparation before mixing; b) sample mixing; c) samples prepared for each test method; d) demolding; e) samples placed in the oven; f) expansion measurement using comparator.

3.5 Determination of Length Change (ASTM C 490)

The length change of test samples was measured to assess ASR potential in accordance to ASTM C490. After each test specimen is prepared and cured under the respective test methods, a length comparator (Figure 3.3) is used to measure the change in length of the test specimens at the required age. The comparator cab measures any small variation in specimen length. A reference bar reading is taken prior to measuring the change in length of any test specimen. Equation 3.1 is used to calculate the change in length at any age (*x* days).

$$L\% = \frac{Lx - Li}{G} \times 100 \qquad \text{Eq 3.1}$$

where:

L = Change in Length at *x* age in %,

Lx = Comparator reading of test specimen at *x*-age minus comparator reading of reference bar at *x* age in inches

Li = Initial comparator reading of specimen minus comparator reading of reference bar at that time in inches

G = Nominal Gauge Length, 10 inches.

The calculated length change for each specimen is expressed to nearest 0.001% and the average values are to nearest 0.01%.

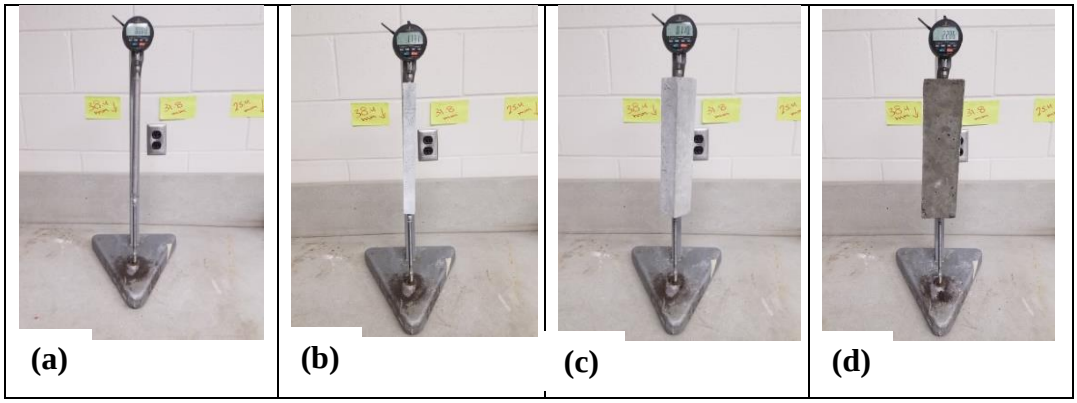

Figure 3.3: The length comparator apparatus for measuring (a) reference reading; b) AMBT sample; c) MCPT sample and d) CPT sample

The degree of ASR reactivity of the test aggregates can be determined based on expansion calculations. Table 3.7 summarizes aggregate reactivity classification for each method used in this study. The classification is used to separate non-reactive aggregate from reactive aggregates. For the 14-day AMBT method (ASTM C1260), a concrete sample expansion less than or equal to 0.1% after 14 days is considered to be non-reactive and an expansion greater than 0.10% is considered to be reactive (whether moderately or reactive or very highly reactive). However, for the 56-day MCPT (AASTHO TP 110) and 1-year or 6-month CPT (ASTM C1260) methods, an expansion less than 0.03% is considered as a non-reactive and an expansion greater than 0.241% is considered highly reactive.

Table 3.7: Classification of aggregate reactivity due to ASR

Reactivity	**14-Day AMBT (%)**	**56-day MCPT (%)**	**1-yr CPT &6-mth ACPT (%)**
Non-reactive	≤ 0.10	≤ 0.03	≤ 0.04
Slow/Low Reactive		$0.031 > X \leq 0.040$	
Moderately reactive	$0.10 < X \leq 0.30$	$0.041 < X \leq 0.12$	$0.04 < X \leq 0.12$
Highly reactive	$0.31 < X \leq 0.45$	$0.121 < X \leq 0.240$	$0.121 < X \leq 0.24$
Very highly reactive	> 0.45	> 0.24	> 0.24

CHAPTER FOUR: ASR EVALUATION AND ANALYSIS

4.1 Introduction

A total number of 11 aggregates were tested to assess the ASR potential using AASHTO TP 110 also known as the Miniature Concrete Prism Test (MCPT) and ASTM C 1260 (Accelerated Mortar Bar Test [AMBT]) method. Similarly, six aggregates of different lithology were tested using the 1-year Concrete Prism Test (CPT) and 6-month Accelerated Concrete Prism Test (ACPT). The selection of aggregates was based on their characteristics, availability, previous laboratory studies, usage in highway concrete structures, and field performance. Based on the measured expansion, the degree of aggregates' reactivity determined using Table 3.7 for each test method. Five different reactivity levels are determined including non-reactive, slow/low reactive, moderately reactive, highly reactive, and very highly reactive. Note, unlike the 14-day AMBT testing, a Low/Slow reactivity was integrated into the aggregate reactivity classification for the MCPT method. Any aggregate in this category is likely to have very low or slow ASR expansion, which simply means a distress (expansion or crack) potentially begins to occur in concrete after 10 to 15 years of construction. Similarly, it is recommended to extend the testing period to 84 days instead of the 56 days to measure the actual status of the aggregate in question.

Relating the laboratory testing with field performance, the following gives a description of each reactivity (see Table 4.1) state in respect to time at which distress begins to emerge after construction. These levels are defined as follows.

- *Non-reactive aggregates*: refers to aggregates that exhibit no sign of expansion in concrete due to ASR. Such aggregates have the tendency to go beyond 30 years without distress.
- *Low/slow reactive aggregates*: refers to aggregates that display sort of ASR distress in concrete at nominal after 10 years from the date of construction.
- *Moderate reactive aggregates*: refers to aggregates that are in between the low and highly reactive region and are expected to show ASR distress in concrete between 5 and 10 years from the date of construction.

- *Highly and very highly reactive*: refers to aggregates with a potential of high expansion due to ASR. The aggregates are expected to show ASR distress in in less than 5 from the date of construction.

This section discusses the results of ASR evaluation using various test methods and examines the correlation between them.

4.2 The ASR Rate of Expansion

Five aggregates (both coarse and fine) with different levels of reactivity were specifically selected study the rate of expansion using the 56-day MCPT method. These aggregates are four reactive aggregates (i.e., El-116c, ORE-8C, Md-45c, Pw-45c, and Ma-22c). The percentage increment of expansion that occurs in MCPT test samples after 3, 7, 14, 21, 28, 42, 56, and 84 days for each aggregate is shown in Figure 4.1 and Figure 4.2 for fine and coarse sizes, respectively. The results showed that coarse aggregates had an approximately uniform net expansion between the reading intervals. Meanwhile, for the fine aggregates, the net expansion increased substantially from 3 days to 14 days and then decreased to a steady state beyond 14 days. This can be explained by the fact that fine aggregates expand more compared to coarse or larger aggregates at early age because fine particles have a higher surface area that expedites the ASR reaction and expansion.

It can be observed that most of the ASR expansion occurs between 7 and 21 days in the MCPT method. The average expansion rate for the reactive aggregates from day 1 to 84 days is 0.07% while aggregates with expansion ≤ 0.12 (non-reactive or moderately reactive) after 84 days have an average expansion rate of 0.008%. On the other hand, we recorded a similar rate of expansion of 0.062% and 0.008% for reactive and non-reactive coarse aggregates respectively between 1 to 84 days testing (Figure 4.2).

From the 14-day AMBT results, the rate of expansion was also evaluated for the same set of fine aggregates. There was a constant increase in net expansion with age for AMBT as shown in Figure 4.3. For 6-month and 1-year CPT testing methods, the rate of expansion was inconsistent between reading intervals which reflects field performance. The results of the 6-month ACPT and 1-year CPT methods are provided in Appendix D1 and E1.

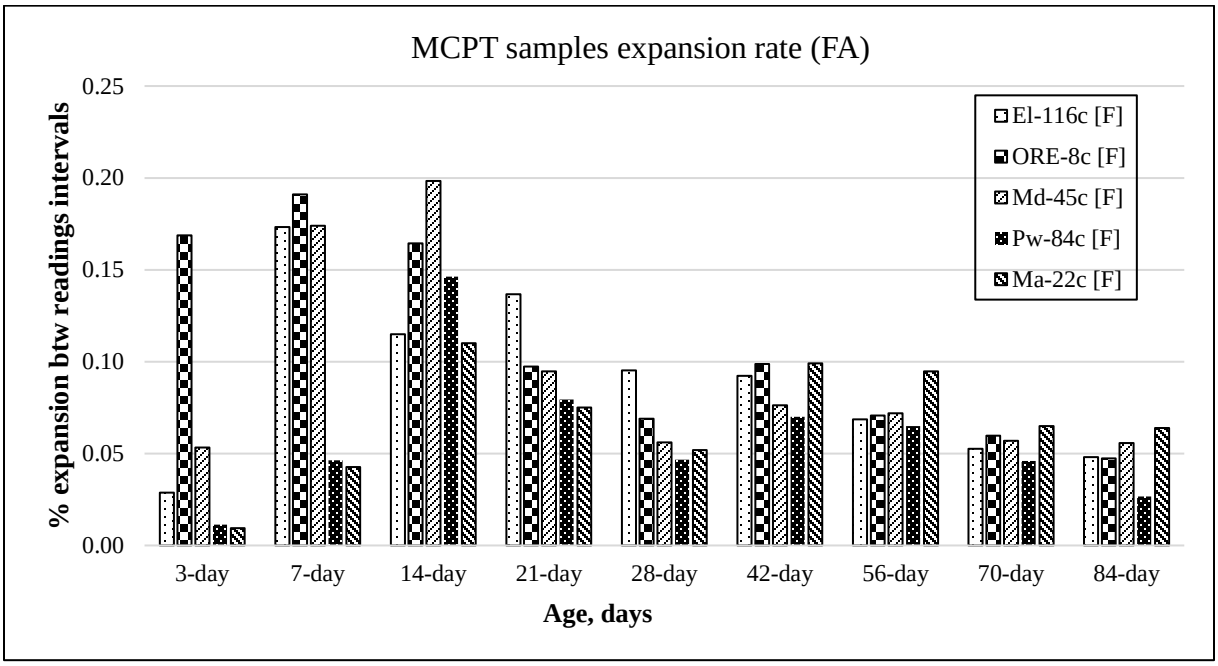

Figure 4.1: 56-day MCPT expansion rate for FA, %

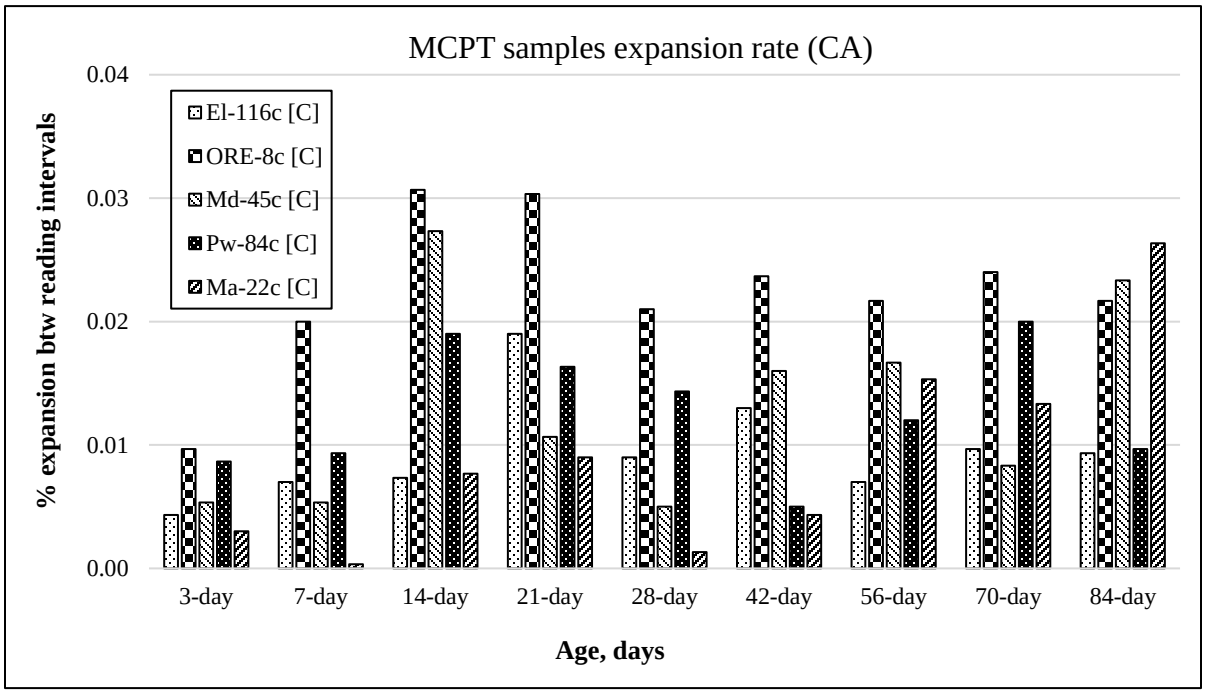

Figure 4.2: The 14-day AMBT expansion rate for CA, %.

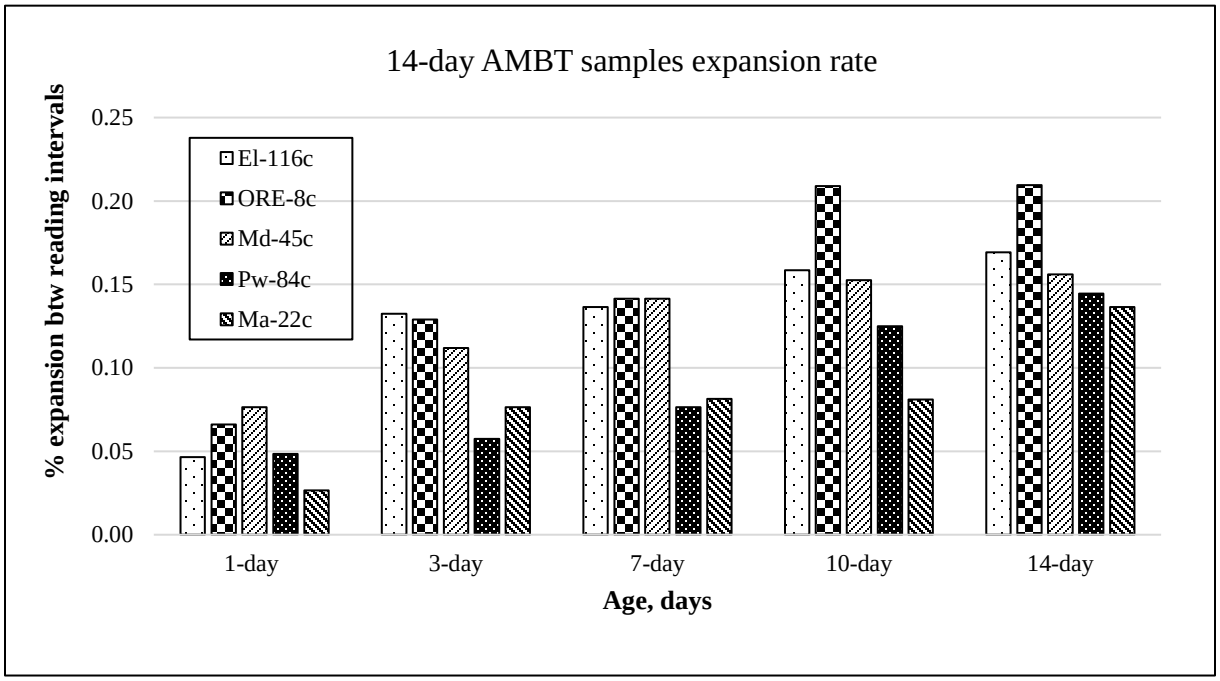

Figure 4.3: 14-day AMBT expansion results

4.3 Aggregate Expansion Results

As discussed earlier, the ASR potential of test aggregates were evaluated using 14-day AMBT, 56-day AASTHO TP 110, 1-year ASTM C2393 and 6-month revised ASTM C2393. This section presents the results of from each test method.

4.3.1 Evaluation of ASR Potential using MCPT Method

The change in length of each specimen was measured using the length comparator at zero, 1, 3, 7, 10, 14, 21, 28, 42, 56, 70, and 84 days and the calculated percent expansion was then plotted against age (days). The 56-day MCPT expansion results for nine coarse aggregates (CA) (in availability of aggregates) and 11 fine aggregates (FA) are showed in Figure 4.4 and Figure 4.5, respectively. Figure 4.6 and 4.7 show percent expansion versus age for coarse and fine aggregates, respectively. Similarly, the concrete prism expansion for coarse aggregate is also displayed in Figure 4.7. Figure 4.8 shows an example of test samples before and after the MCPT test.

The results showed that the coarse aggregate (CA) passed the 0.04% non-reactive expansion requirement at the end of 56 days except granite rocks with an expansion of 0.025%. However, four aggregates (i.e., Ma-22c, Basalts, Wn-56 and Limestone) show moderate reactivity to ASR with an expansion percent of 0.081%, 0.08%, 0.097%, and 0.66%,

respectively. The ORE-8c, Md-45c, Pw-84c were found to be highly reactive with percent expansion of 0.21%, 0.14%, and 0.14%, respectively which exceeds the 0.12% requirement. El-116c was at the border between being moderate and highly reactive with percent expansion of 0.12% after 56 days and 0.14% after 84 days. We can see from Figure 4.6 that expansion is directly proportional to age. However, the rate of expansion differs from one aggregate to another. ORE -8c had a steep slope compared to the rest of the aggregates. This aggregate was acquired from the western Snake River which has high silica content.

The results of fine aggregates (Figure 4.5 and 4.7) show that all aggregates with the exception of granite were above the 0.04% non-reactivity expansion threshold at 56 days. Based on the results, all aggregates are also considered reactive. For instance, El-116c, ORE 8c, Md-45c, Wn-56, Pw-84c and Ma-22c are all regarded as very highly reactive aggregates because their 56-day percent expansion is above 0.24% (Figure 4.5). The use of such aggregates in concrete is very deleterious to concrete structures. Similar to coarse aggregates, the percent expansion increased with age (Figure 4.7). The granite rocks (a non-reactive $\leq$0.04) showed a relatively straight line from control to 84 days of testing. ORE 8c aggregates yielded the highest expansion of 0.99% at 56 days and 1.10% after 84 days which is in agreement with the coarse aggregate expansion.

Most of the specimens' expansion occurred at an early age between 7 days and 21 days for the fine aggregates specimens and between 14 and 21 days for CA. These results specify the transition from a latent stage (at the point where aggregate's siloxane bridges are broken) to the active period when the silica swelling gel begins to form. Lastly, the expansion behavior of non-reactive fine aggregates (i.e., granite) is linear across the age with an expansion of 0.023% recorded at the 56-day reading. Table 4.1 summarizes the expansion results for all test aggregates including fine and coarse aggregates using the MCPT method. Appendix B provides the expansion measurements for the test aggregates.

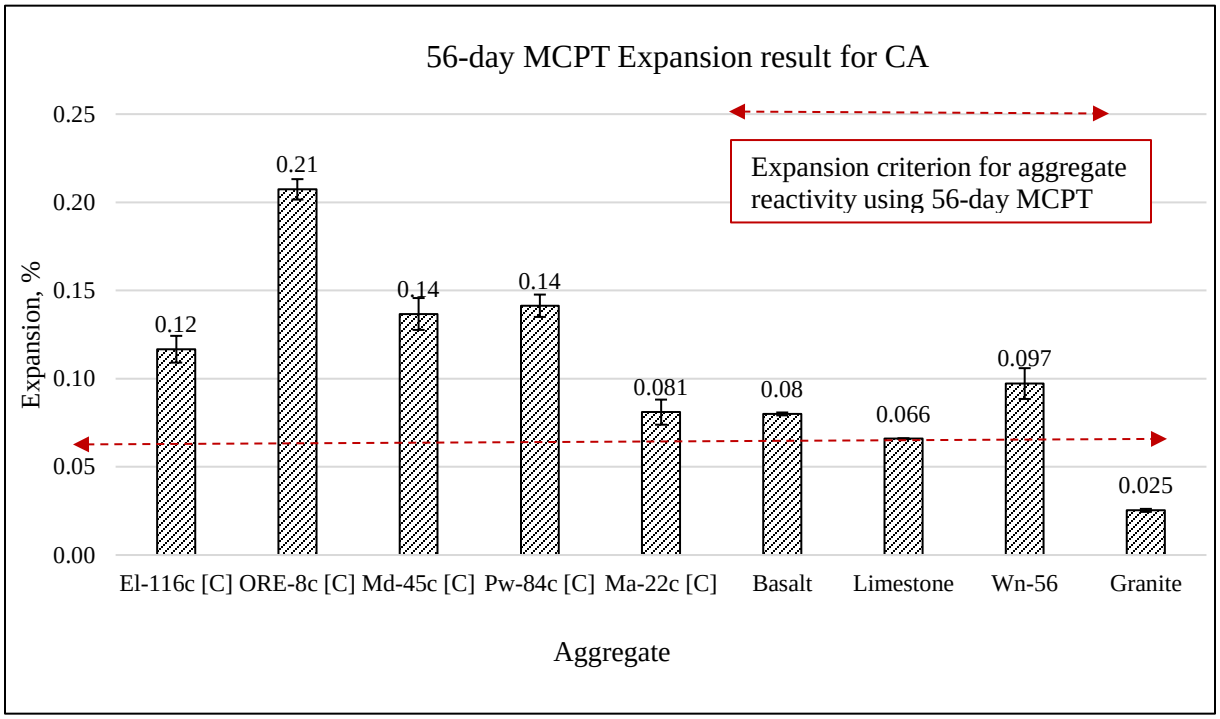

Figure 4.4: 56-day MCPT expansion results for coarse aggregates

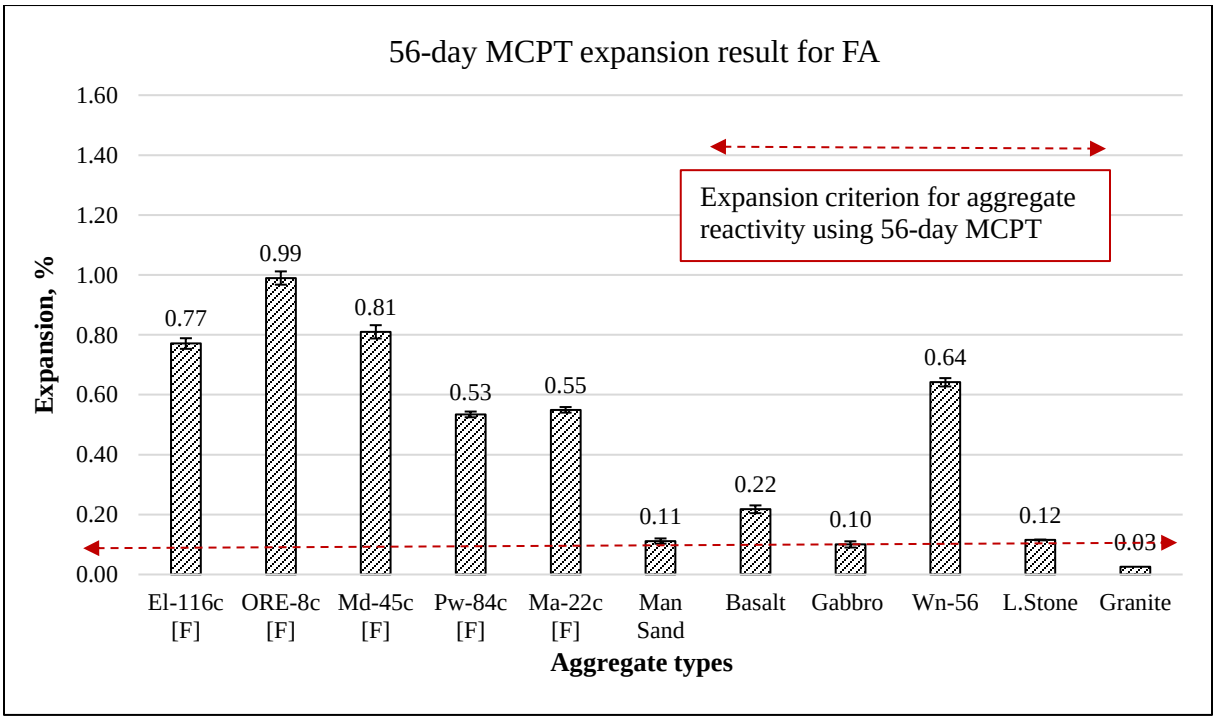

Figure 4.5: 56-day MCPT expansion results for fine aggregates

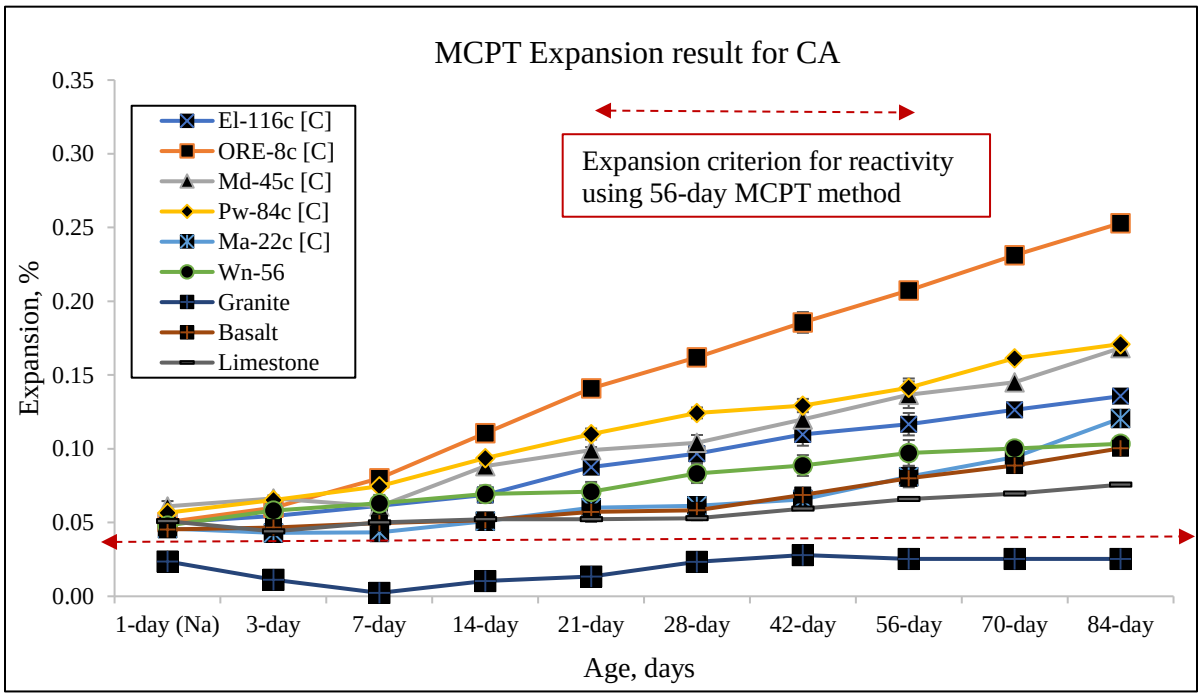

Figure 4.6: MCPT percent expansion vs. age for coarse aggregates

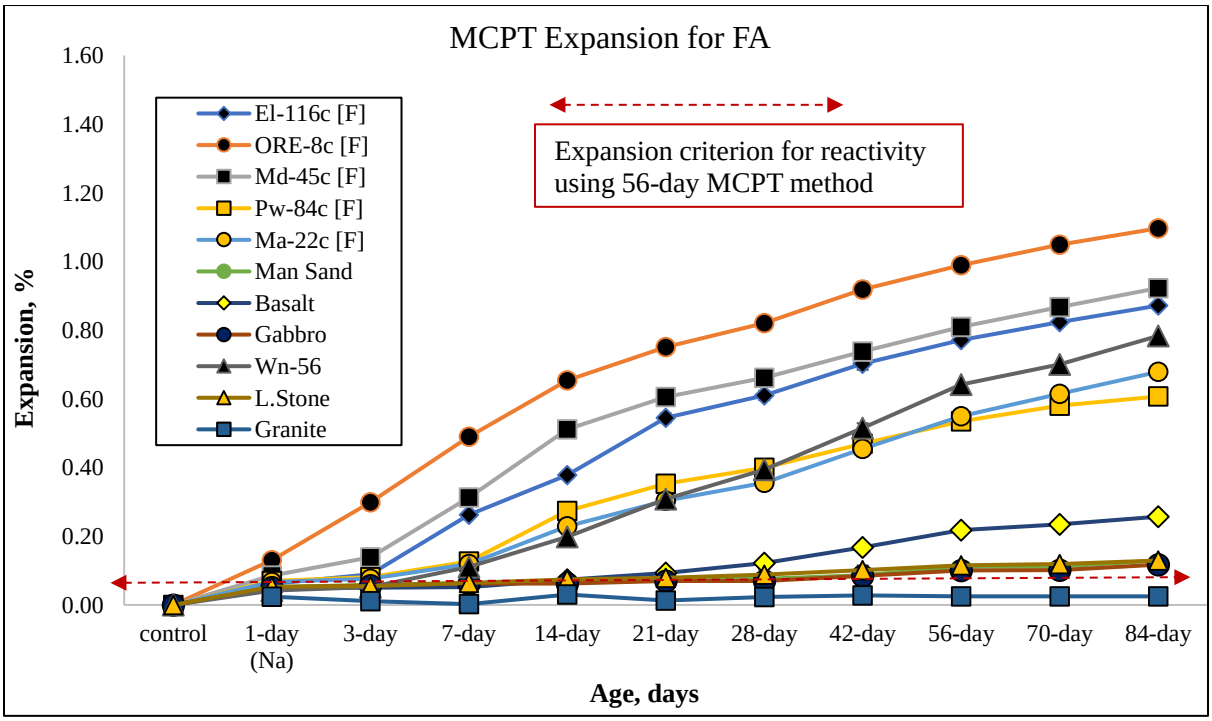

Figure 4.7: MCPT percent expansion vs. age for fine aggregates

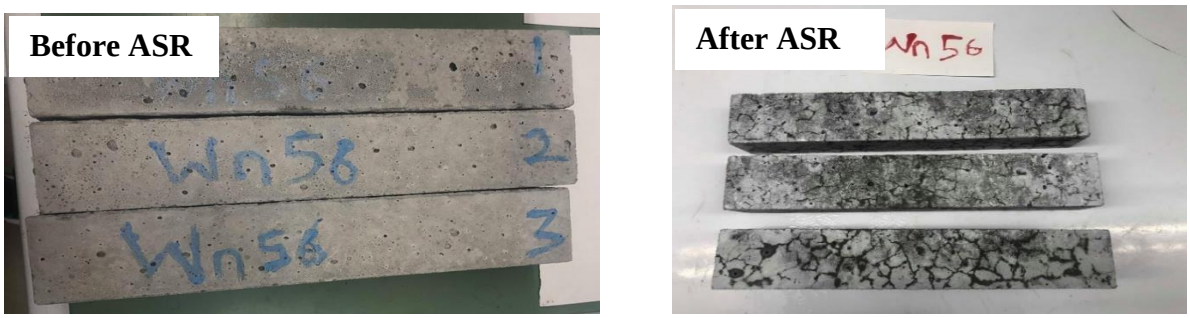

Figure 4.8: Concrete samples before and after expansion

4.3.2 Evaluation of aggregate using the AMBT Method

A total number of 11 fine aggregates were tested using the 14-day Accelerated Mortar Bar Test (AMBT) method in accordance with ASTM C1260. Since the test specimens used in the AMBT test are made of mortar, only fine aggregates are tested. Figure 4.9 depicts the 14-day expansion results while Figure 4.9 shows expansion rate or how age affects the expansion for the test aggregates. Following the ASTM requirements, result shows that all aggregates that were found to be very highly reactive using the MCPT method were also found to be very highly reactive using the AMBT method (El-116c, ORE-8c, Md-45c, Pw-45c, Ma-22c, and Wn-56c). Each aggregates expansion exceeded the threshold (0.45%) except Pw-45c aggregate which is considered to be highly reactive with 0.33% expansion. Additionally, manufactured sand was found to be moderately reactive using both 14-day AMBT and 56-day MCPT methods.

Granite, limestone, and gabbro were found to be non-reactive with expansion of 0.009%, 0.049% and 0.07% respectively. It should be noted that only granite was found to be non-reactive using the MCPT method. These results show a little discrepancy between the two test methods (i.e., MCPT and AMBT). The difference in the results could be due to the small expansion threshold of 0.04% specified in the MCPT method compared to the 0.10% threshold specified in the AMBT method. Therefore, an adjustment should be made on the AASTHO TP 110 ASR expansion threshold for non-reactive aggregates. Furthermore, the results showed that, as one expects, the percent expansion of each aggregate increased with age (Figure 4.10). The expansion rate was similar to the MCPT expansion rate. The expansion rate was predominant at 14-day testing, particularly for the reactive aggregates. Granite, limestone, and gabbro (non-reactive aggregates) were found to experience very low

expansion with age. Figure 4.11 shows an example of test samples before and after the AMBT test. Table 4.1 summarizes the expansion results using the AMBT method. Appendix C provides the expansion measurements for the test aggregates.

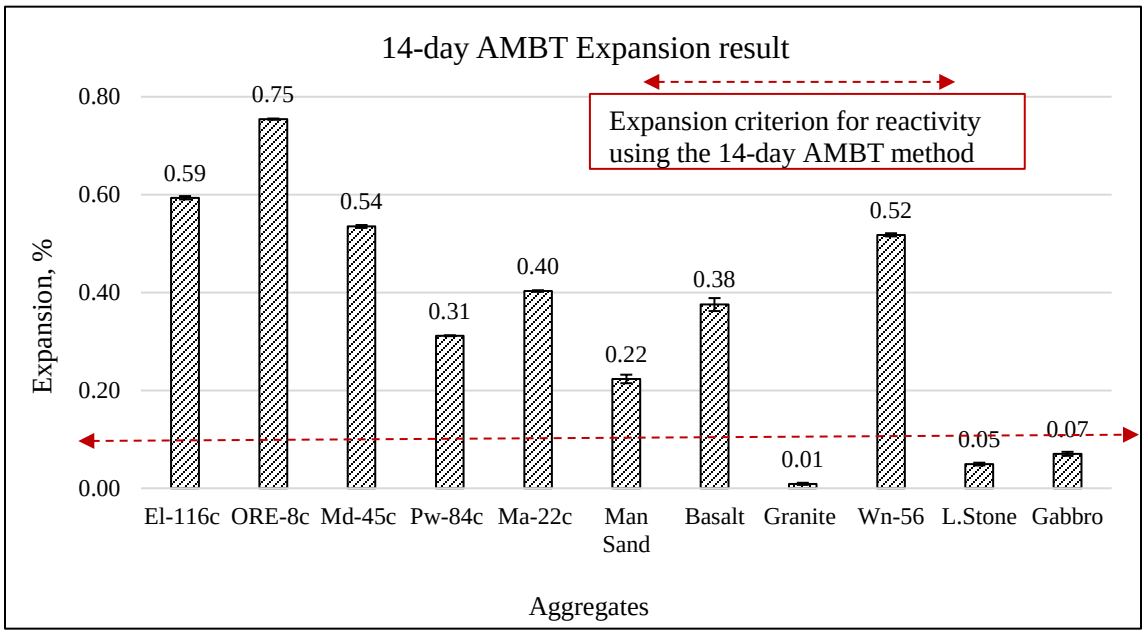

Figure 4.9: 14-day AMBT expansion result for 11 aggregates, %.

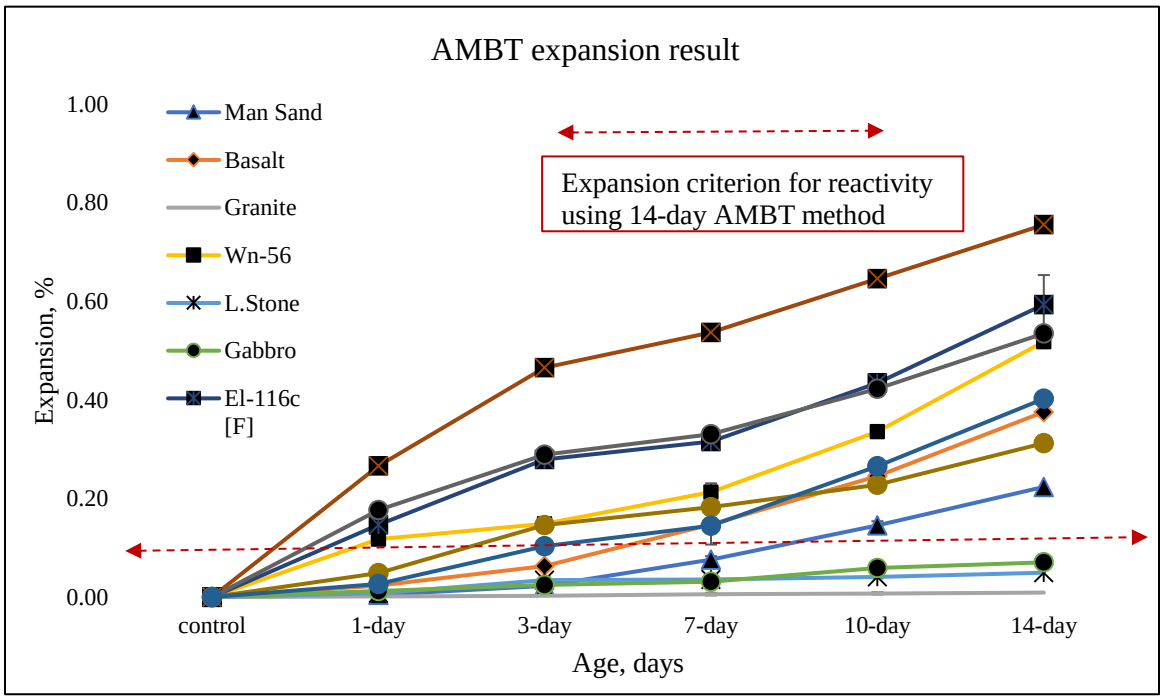

Figure 4.10: Percent expansion using AMBT versus age.

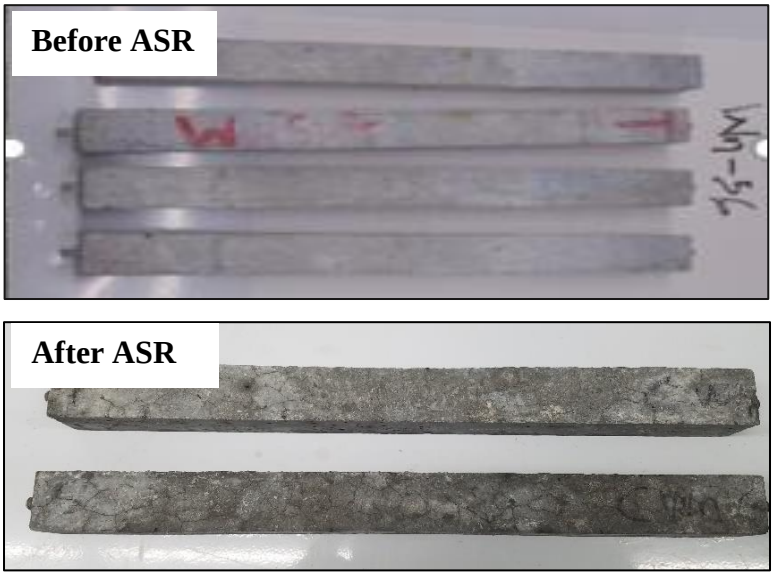

Figure 4.11: Mortar bar test samples before and after expansion (Wn-56)

4.3.3 Evaluation of aggregate using the CPT methods

Six different aggregates were evaluated using both the 1-year CPT and 6-month ACPT test methods in accordance to ASTM C 1293 standard. The temperature and duration for conditioning the test specimens are different in both test methods (i.e., 1-year CPT and 6-month ACPT). The conditioning temperature for the 1-year CPT is 38C while it is 60C for the 6-month ACPT methods. Also, the test is conducted for one full year for the CPT while it is conducted for 6 months for ACPT. Only six aggregate types were tested using the 1-year CPT and 6-month ACPT test due to limited amount of reference aggregates provided by Idaho Transportation Department. For the 6-month ACPT results, all six aggregates exceeded the 0.04% ASR threshold for non-reactive aggregates excluding granite rock (0.0293% expansion). The granite rock was found non-reactive which is in good agreement with the results obtained from both the 14-day AMBT and 56-day MCPT.

Wn-56c aggregate had the highest expansion rate of 0.1% after 6 months as shown in Figure 4.12. Similarly, the expansion results for the 1-year CPT follow that of 6-month ACPT results. However, for most aggregates, the 1-year CPT expansion results were found to be slightly higher compared to the ACPT expansion results. These results are in good agreement to previous findings of Ideker et al. (2010). Also, the Wn-56 aggregates was found to have

the highest expansion rate for the 1-year CPT method while granite rock was found to be non-reactive. The results of both methods (i.e., 1-year CPT and 6-month ACPT) followed a similar pattern for the test aggregates. These results suggest that the 6-month ACPT test can substitute for the 1-year test which addresses one of the major concerns namely the long testing time of 1-year CPT test. Meanwhile, the author recommend testing additional aggregates to validate such correlation.

The expansion results versus age using 6-month ACPT and 1-year CPT method are shown in Figure 4.13 and Figure 4.14, respectively. It clear that there is a similar trend between the two test methods, where concrete prisms experience a sudden increase in expansion and the rate of expansion increases with time steadily. Such expansion behavior is consistent with field performance (Salwocki, 2016). Appendix D and E include the expansion results for all test aggregates.

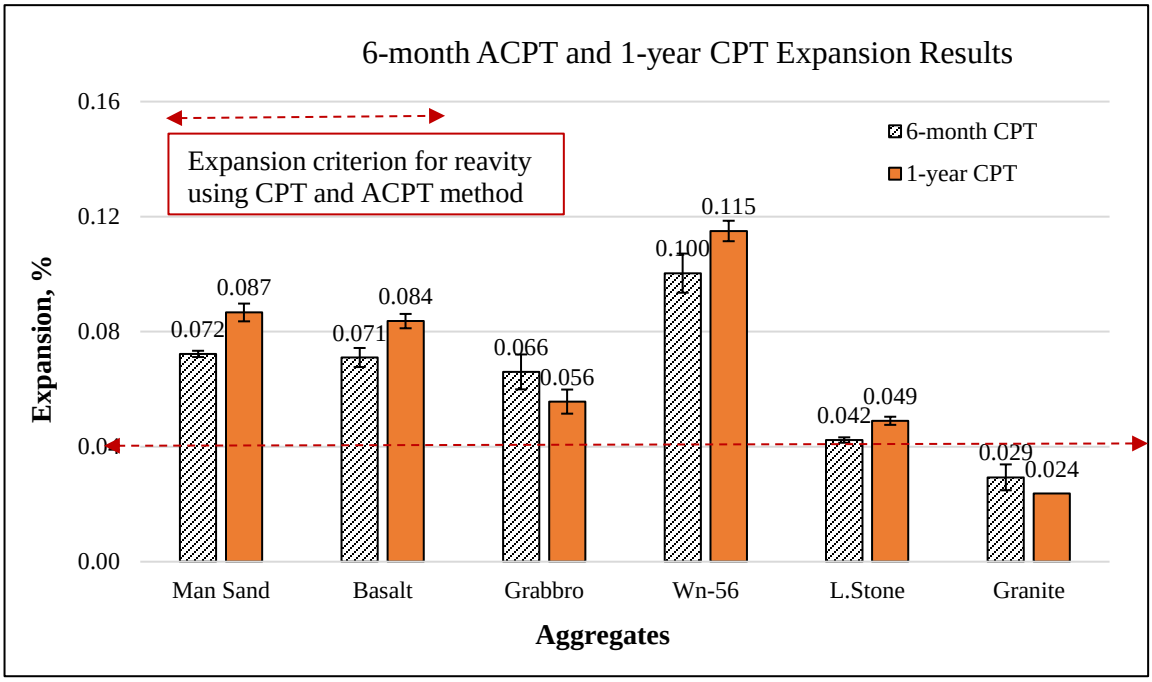

Figure 4.12: 6-month and 1-year CPT expansion result for 6 aggregates, %

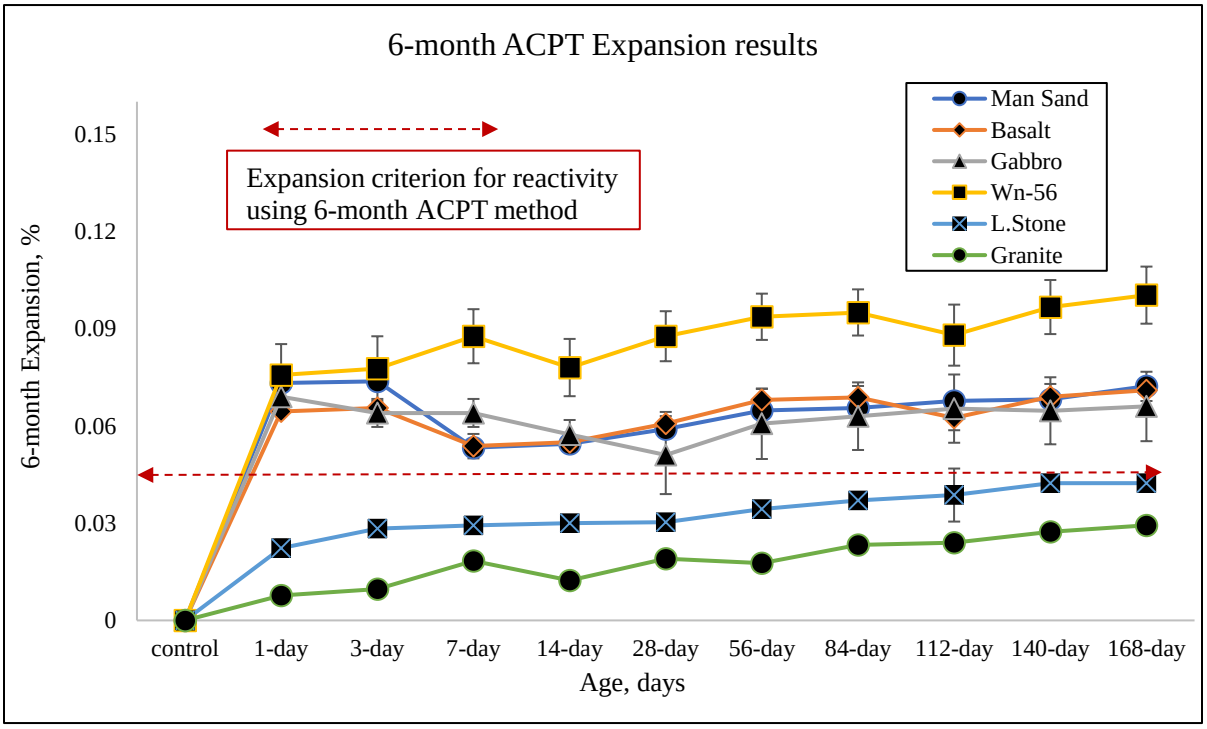

Figure 4.13: Percent expansion using 6-month ACPT versus age

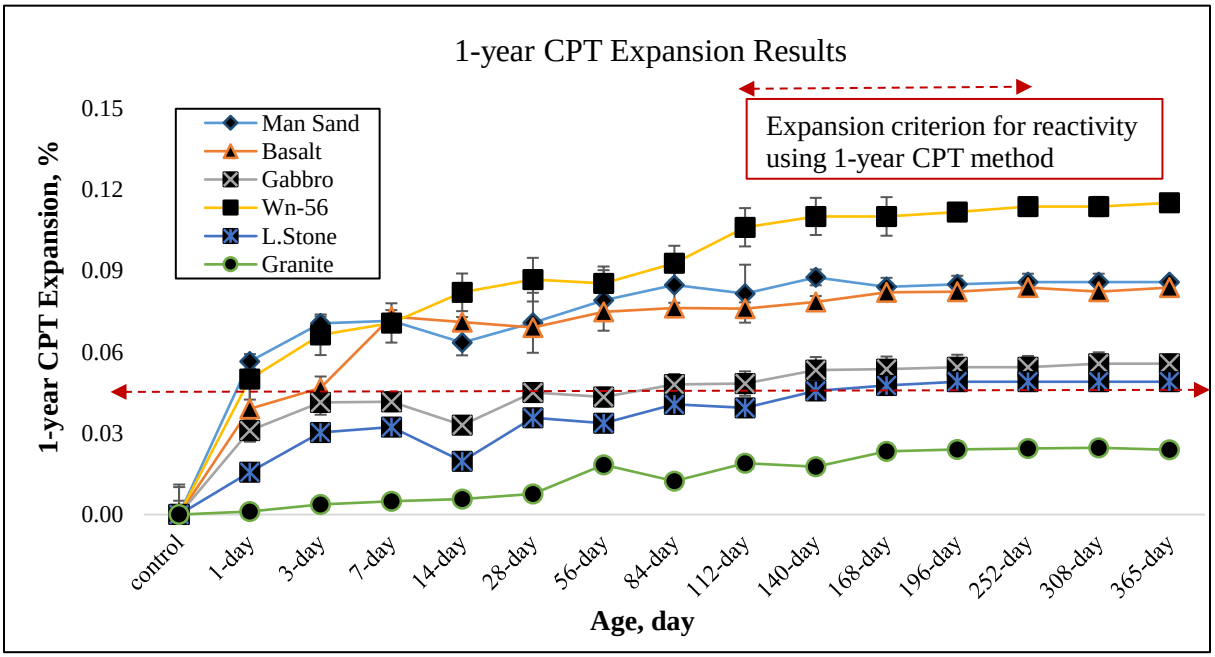

Figure 4.14: Percent expansion using 1-year CPT versus age

Table 4.1: Summary of expansion results for different test methods

Aggregates	56-Day MCPT		14-Day AMBT		6-Month ACPT		1-Year CPT	
	Expansion,%	**COV**	**Expansion,%**	**COV**	**Expansion,%**	**COV**	**Expansion,%**	**COV**
El-116c [F]	**0.77**	2.30	**0.57**	1.43				
ORE-8c [F]	**0.99**	2.23	**0.68**	0.64				
Md-45c [F]	**0.81**	2.74	**0.54**	1.51				
Pw-84c [F]	**0.53**	1.78	**0.33**	2.47				
Ma-22c [F]	**0.55**	1.69	**0.40**	0.55				
Man Sand	**0.11**	7.82	**0.22**	3.91	**0.072**	1.51	**0.086**	3.63
Basalt	**0.22**	5.96	**0.38**	3.54	**0.071**	4.67	**0.084**	2.59
Gabbro	**0.10**	10.30	**0.07**	2.00	**0.066**	4.67	**0.056**	7.53
Wn-56	**0.64**	2.16	**0.52**	0.62	**0.100**	8.78	**0.115**	3.09
Limestone	**0.12**	6.04	**0.05**	5.81	**0.047**	1.99	**0.049**	2.89
Granite	**0.02**	3.39	**0.01**	5.84	**0.029**	5.33	**0.024**	0.52
Non-Reactive	≤ 0.04		< 0.10		≤ 0.04			
Moderate Reactive	0.041< X ≤ 0.012		0.10< X ≤ 0.30		0.041< X ≤ 0.12			
Highly Reactive	0.121< X ≤ 0.240		0.30< X ≤ 0.45		0.121< X ≤ 0.240			
Very Highly reactive	> 0.241		> 0.45		> 0.241			

4.4 Correlation of Among Various Test Methods

The author examined the correlation between various tests methods used to assess the ASR potential in this study. This section shows and discusses the correlation of the results.

4.4.1 Correlation between ASR Potential of FA and CA using MCPT Method

Figure 4. 15 shows the correlation between fine and coarse aggregate as evaluated using the 56-day MCPT method. The results show good correlation with an R-squared value of 0.76. Nine aggregates with different reactivity levels were considered in this correlation with an expansion threshold for non-reactive aggregates set as 0.04% according to the AASTHO TP 65. These results indicate that the fine aggregates have higher expansion compared to coarse aggregate. This is attributed to the large surface area of fine aggregates compared to coarse aggregates. These findings are in good agreement with previous studies by Farny and Kosmatka (1997) and Thomas et al. (2007). Equation 4.1 presents a relationship between the expansion of coarse aggregates ($Expansion_{CA}$) and the expansion of fine aggregates ($Expansion_{FA}$) measured using The MCPT method. This correlation can be used to predict the expansion of coarse aggregates from fine aggregates and vice versa as needed.

$$Expansion_{CA} = 0.1379(Expansion_{FA}) + 0.0344 \qquad \text{Eq. 4.1}$$

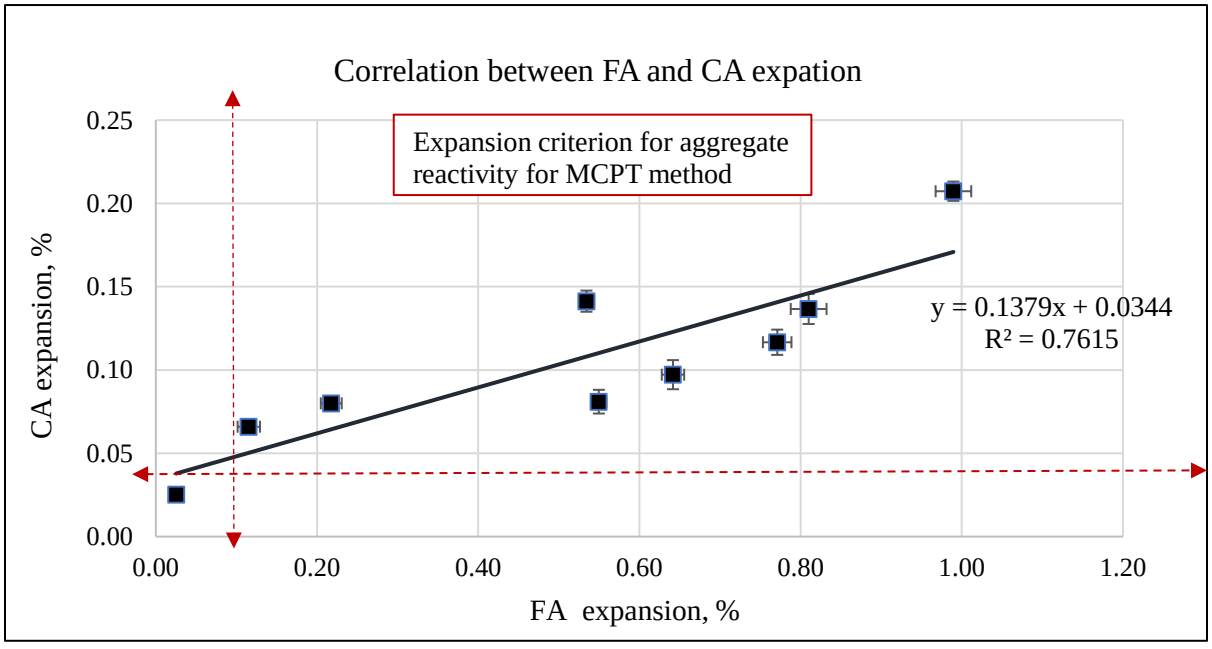

Figure 4.15: Correlation between MCPT expansion of coarse aggregates (CA) and fine aggregates (FA)

4.4.2 Correlation between MCPT and AMBT method

The correlation between 56-day MCPT method and 14-day AMBT test results for 11 aggregates with different reactivity levels is shown in Figure 4.16. Figure 4.16 shows that there is a good correlation with an R-squared value of 0.88 which indicates strong relationship between the two test procedures. However, the correlation was even higher (R-squared of 0.95) when considering only very highly reactive aggregates (with expansion of 0.24% and above) (Figure 4.17). Equation 4.2 presents a relationship between the MCPT expansion and AMBT expansion. This correlation can be used to predict MCPT expansion (56-day testing) from AMBT expansion (14-day testing) and it clearly shows the validity of using the AMBT to assess the reactivity of aggregates to ASR.

$$\text{Expansion}_{MCPT} = 0.632(\text{Expansion}_{AMBT}) + 0.0628 \qquad \text{Eq. 4.2}$$

These results show better correlation compared to the findings of Latifee and Rangaraju (2014). Based on the correlation between both test methods, it is recommended to adopt the AMBT method over the MCPT method since it takes less testing time. Meanwhile, further testing should be conducted on aggregates from different sources. Also, it is recommended to adjust the expansion threshold for classifying reactive aggregate using MCPT to 0.1% baseline was considered to provide better correlation with the AMBT method.

The expansion limit of 0.040% (very low) set to classify aggregates tested with MCPT method, should be modified as many aggregate considered to be low or moderately reactive with other method was seen to be highly reactive with this method.

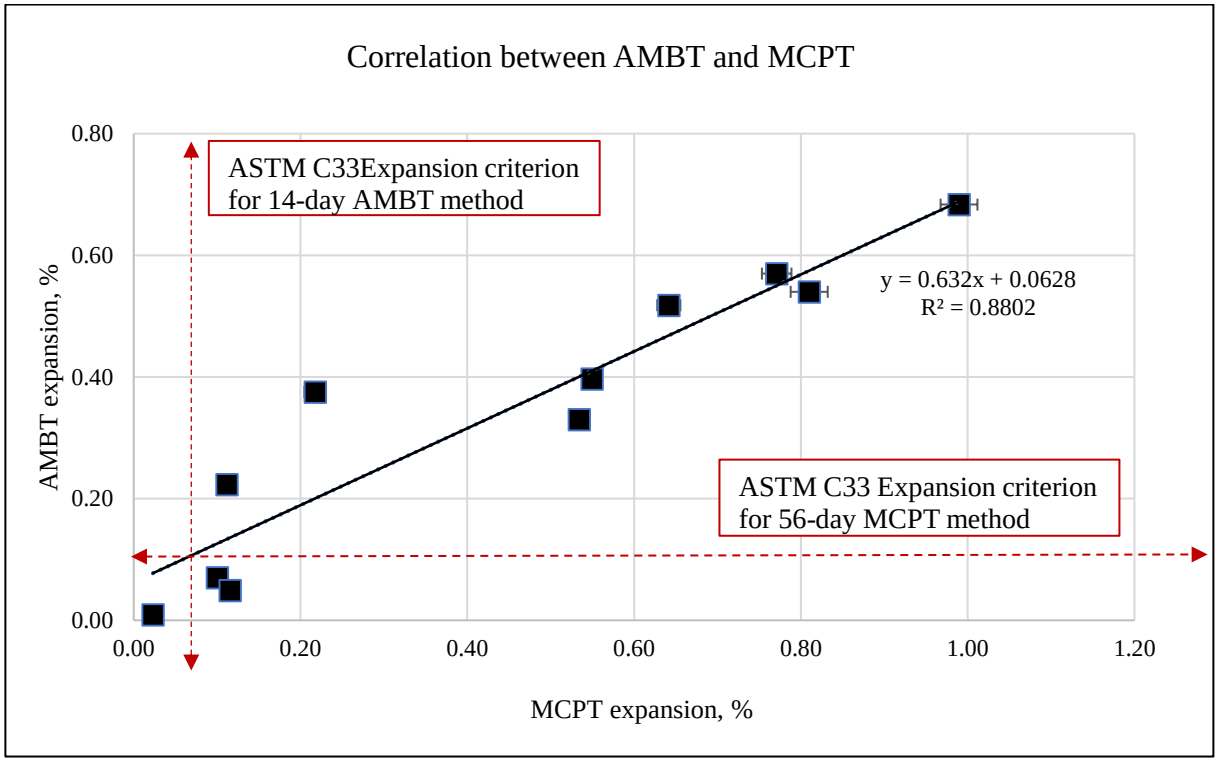

Figure 4.16: Correlation between the 14-day AMBT and 56-day MCPT

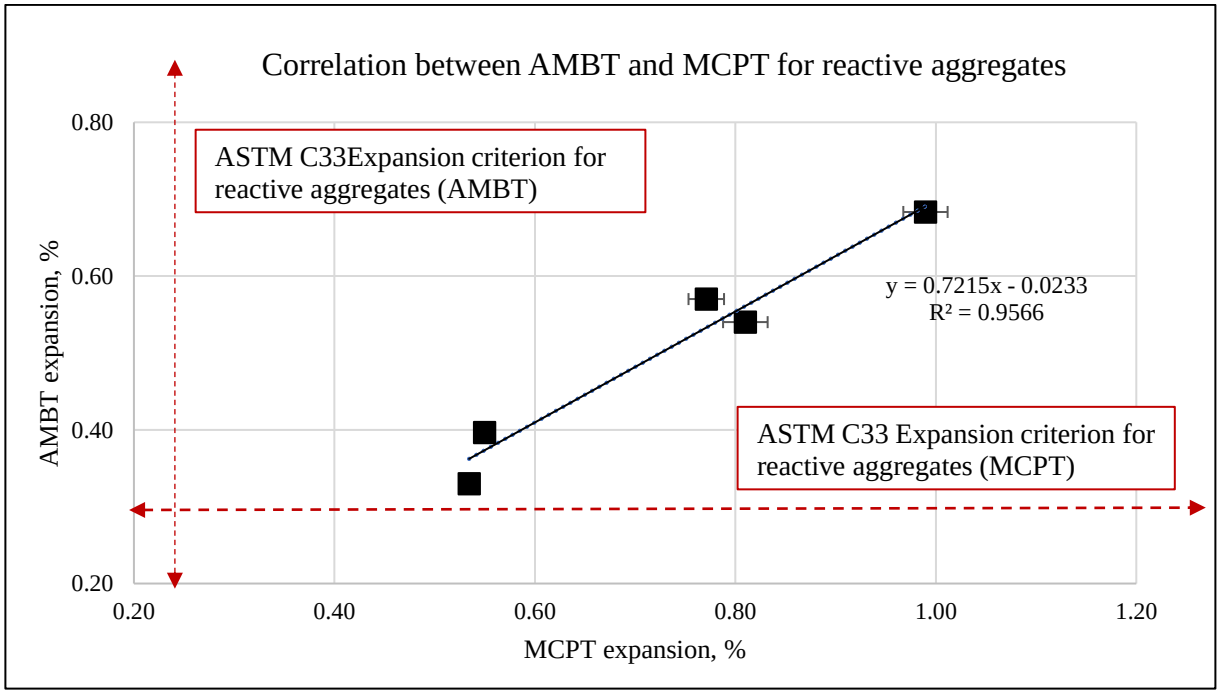

Figure 4.17: Correlation between AMBT-MCPT for 5 reactive aggregates

4.4.3 Correlation between MCPT and CPT method

The correlations between 56-day MCPT and 6-month ACPT expansion results and between 56-day MCPT and 1-year CPT for the test aggregates are shown in Figure 4.18 and 4.19, respectively. For both MCPT and CPT test methods, the expansion limit to distinguish reactive from non-reactive aggregates is specified at 0.04% by AASTHO TP 65. This threshold (i.e., 0.04% expansion) indicates when the concrete prism begins to show signs of distress. From Figure 4.18, there is a high degree of correlation between the MCPT and 6-month ACPT with an R-squared value of 0.71. Likewise, an R-squared value of 0.69 was also found from the MCPT and 1-year CPT (Figure 4.19). It should be noted that some aggregates which were found to be very high reactive aggregate under the MCPT method after 56 days (e.g., Wn-56, Basalt) were found to have a moderate reactivity using the 1-year CPT method. Based on this result, the 56-day MCPT expansion can be strongly correlated to the 365-day CPT expansion and could be adopted for assessing aggregate susceptibility to ASR. Equation 4.3 and 4.4 present the relationship between MCPT and CPT, and between MCPT and ACPT, respectively. These relationships can be used to predict the corresponding expansion after 6 months (ACPT) and 1 year (CPT) after 56 days of testing using MCPT method.

$$\text{Expansion}_{\text{ACPT(6-month)}} = 0.0907(\text{Expansion}_{\text{MCPT(56-day}}) + 0.046 \qquad \text{Eq. 4.3}$$

$$\text{Expansion}_{\text{CPT(1-year)}} = 0.1197(\text{Expansion}_{\text{MCPT(56-day}}) + 0.0447 \qquad \text{Eq. 4.4}$$

These results are in good agreement with findings of Latifee and Rangaraju (2014). Based on these results, it could be concluded that the MCPT method can be adopted ahead of the one-year CPT to save time or alkali leaching. It is recommended to adjust the expansion threshold for classifying reactive aggregate when using MCPT method as some aggregates tested to be less reactive in CPT were very reactive using MCPT.

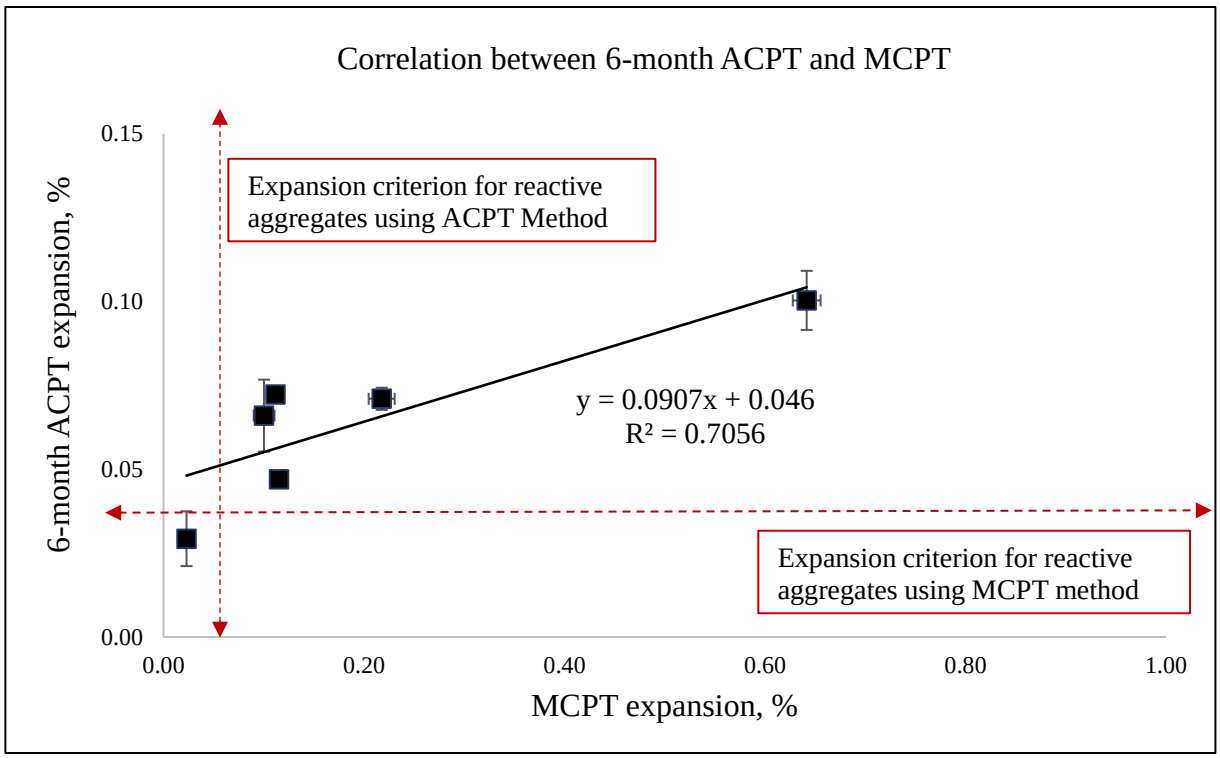

Figure 4.18: Correlation between MCPT and 6-month ACPT

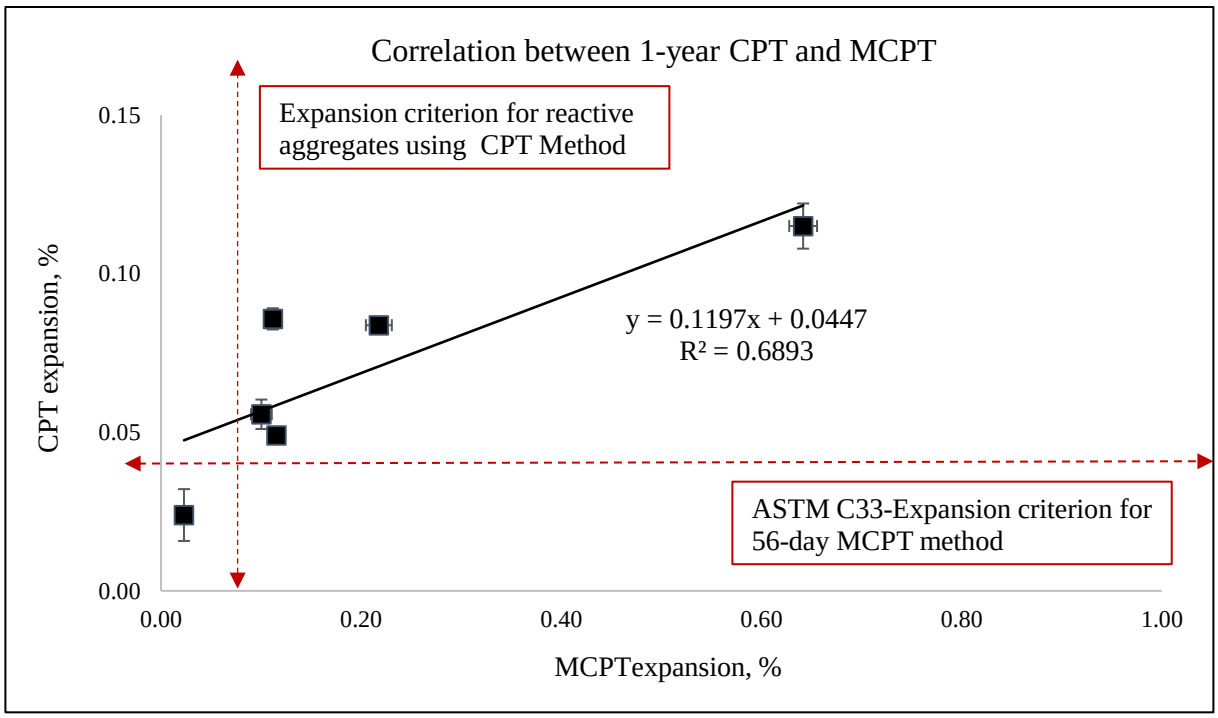

Figure 4.19: Correlation between MCPT and 1-year CPT

4.4.4 Correlation between AMBT and CPT method

Similarly to the result gotten from the MCPT and CPT method, the correlation of 14-day AMBT and 1-year or 6-month CPT also produced a high degree of correlation of despite the expansion limit as required by AASTHO PP 65 to distinguish reactive from non-reactive aggregates is different from each method. The correlation between the two tests is given in equations 4.5 and 4.6 below. Also, such correlation can be used to predict CPT expansion (365-day testing) from AMBT expansion (14-day testing) and it clearly shows the validity of using the AMBT to assess the reactivity of aggregates to ASR. No previous correlation was obtained between the AMBT and CPT methods in the literature. Thomas et al. (2006) suggested using the 14-day AMBT for accepting aggregates and not for rejecting aggregates.

$$\text{6-month CPT} = 0.1048(\text{AMBT}) + 0.0426 \quad (R^2 = 0.741) \qquad \text{Eq. 4.5}$$

$$\text{1-year CPT} = 0.1489(\text{AMBT}) + 0.038 \quad (R^2 = 0.8703) \qquad \text{Eq. 4.6}$$

4.4.5 Correlation between 6-month ACPT and 1-year CPT Methods

Figure 4.20 examines the correlation between the 1-year CPT and 6-month ACPT methods. A strong correlation with an R-squared value of 0.94 was found between both methods. The expansion limit to differentiate non-reactive from reactive aggregates is specified at 0.04% according to the ASTM C33 standard. Equation 4.7 presented the relationship between both CPT and ACPT expansions.

$$\text{Expansion}_{\text{ACPT(1-year)}} = 1.2924(\text{Expansion}_{\text{CPT(6-month)}}) - 0.0143 \qquad \text{Eq. 4.7}$$

Such strong correlation between 6-month ACPT and 1-year (CPT) suggests that 6-month ACPT can be used to reduce the time of testing from 1 year to 6 months. This also also in goo agreement with the work of (Thomas et al., 2006). However, further research and testing need to be conducted to verify this finding using additional number of aggregates. The summary of these result is presented in Table 4.2.

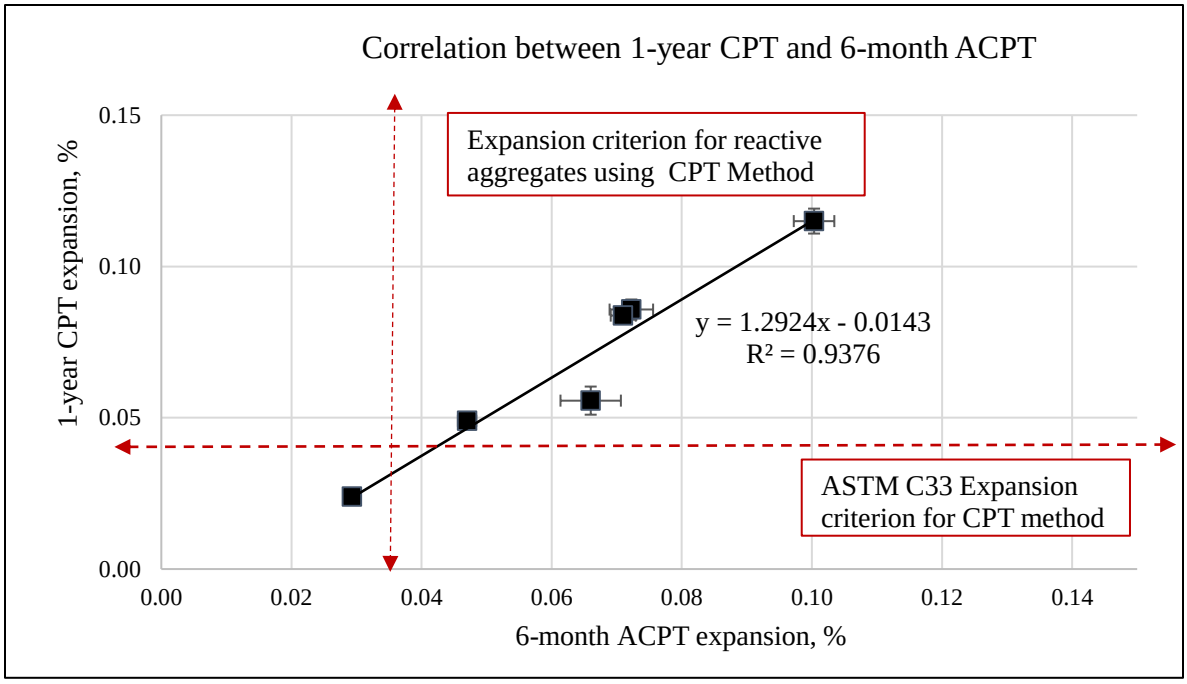

Figure 4.20: Correlation between CPT (1-year) and ACPT (6-month)

Table 4.2: Summary of correlations between various test methods

Correlation	Test Method	Equation (linear eqn)	R-square	Status
AMBT-MCPT	14-day vs 56-day	y = 0632x + 0.0628	**0.8802**	**Excellent**
ACPT-MCPT	6-month vs 56-day	y = 0.0907x + 0.046	**0.7056**	**Good**
ACPT-AMBT	6-month vs 14-day	y = 0.1048x + 0.0426	**0.7410**	**Good**
CPT-AMBT	1-year vs 14-day	y = 0.1489x + 0.038	**0.8703**	**Excellent**
CPT-MCPT	1-year vs 56-day	y = 0.1197x + 0.0447	**0.6893**	**Good**
CPT-ACPT	1-year vs 6-month	y = 12924x - 0.0143	**0.9376**	**Excellent**

Further statistical analyses were performed to determine and assess the correlation between various methods. The Pearson correlation coefficient (r) was examined. This correlation predicts a linear correlation using the mathematical equation (Equation 4.8) and has values between -1 and +1 (Zhu et al., 2017). A positive correlation coefficient represent a direct increasing relationship and vice versa. A Microsoft Excel tool was used to calculate the Pearson correlation coefficient (r) as presented in Table 4.4. The Pearson correlations confirmed that the 14-day AMBT, 56-day MCPT, 6-month ACPT and 1-year CPT test methods are highly correlated which confirms the findings of the linear relationships.

$$r = \frac{n(\sum xy) - (\sum x)(\sum y)}{\sqrt{[n\sum x^2 - (\sum x)^2][n\sum y^2 - (\sum y)^2])}} \quad \text{Eq. 4.8}$$

where:

x and *y* are correlation variables (performance indices).

n is number of mixtures.

Table 4.3: Correlation between ASR methods using Pearson analysis

ASR Methods	14-day AMBT	56-day MCPT	6-month ACPT	1-year CPT
14-day AMBT	1.00			
56-day MCPT	0.94	1.00		
6-month ACPT	0.89	0.84	1.00	
1-year CPT	0.94	0.83	0.97	1.00

CHAPTER FIVE: ALKALI-SILICA REACTION MITIGATION MEASURES

5.1 Introduction

Based on the results of Chapter 4, most of tested aggregates were found to be very reactive and susceptible to ASR distress. Therefore, there is a need to establish a mitigation approach to minimize distress cause by ASR when reactive aggregates are used in concrete materials. Further research was conducted to investigate different approaches to effectively mitigate ASR using Supplementary Cementitious Materials (SCMs) and waste glass powder as a partial replacement of cement. SCMs are proven to reduce ASR distress effectively due to the rapid pozzolanic reactivity in concrete (Venkatanarayanan & Rangaraju, 2011, 2013; Boddy et al., 2003; Shekarchi et al., 2010). Likewise, waste glass powder or crushed brick powders derived from industrial waste contain some pozzolans amd can assist in mitigating ASR distress (Turgut & Yahlizade, 2009; Vanjare & Mahure, 2012; Khatib et al., 2012, Afshinnia & Rangaraju, 2015). In addition using glass powder can reduce the amount of materials sent to landfills and cut down carbon emission from cement production (H. Du & K.H. Tan, 2013).

The author examined the use of SCMs and glass powder in reducing ASR expansion. The evaluation included SCMs and glass powder at various binary and ternary combinations. Chapter 5 provides information about test materials (i.e., aggregates, SCMs, and glass powder) and test methods (i.e., AMBT and MCPT) used in the laboratory testing program. In addition, the flow test was employed to study the workability of mortar samples prepared with SCMs and glass powder. The strength activity index (SAI) was measured for each sample to characterize for the concrete mechanical properties. In addition, the Scanning Electronic Microscopic (SEM), Energy-Dispersive X-ray (EDX) spectral analysis were also introduced to investigate pozzolanic reactivity, ASR gel formation, microstructural and chemical analysis and of specimen prepared with glass powder and other SCMs.

5.2 Materials and Test Methods

5.2.1 Aggregates Types

Three different reactive aggregates (i.e. Wn-56, basalt, and manufactured sand), and one non-reactive aggregate (i.e., granite) were used in this mitigation study as shown in Figure 5.1.

These aggregates includes:

- *Wn-56:* acquired from North-central, Snake River Plain.
- *Basalt*: acquired mainly from District 1, ID and part of Washington
- *Manufactured sand:* acquired from Eastern Washington and North Idaho.
- *Granite*: acquired from the Lewiston, Idaho. Granite was used as the reference aggregate.

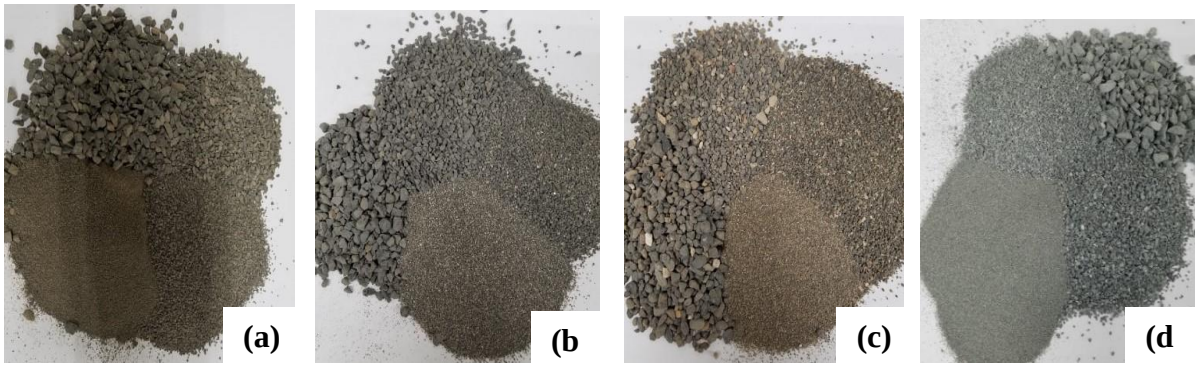

Figure 5.1: Reactive aggregates considered a) Wn-56; b) Basalt rocks; c) Manufactured Sand; d) non-reactive aggregates (granite)

5.2.2 Portland Cement and Reagent

The Portland cement used in the ASR mitigation study was the same type described earlier in Section 3.2.2. Sodium hydroxide (NaOH) was also used as a curing agent as described in Section 3.2.3.

5.2.3 Waste Glass Powder

The glass powder used in the ASR mitigation study was a finely-grounded soda lime glass manufactured by BRQ Inc., Boise, ID (Figure 5.2b). The average powder size is 10 μm with a specific gravity of 2.45. The chemical composition of glass powder is shown in Table 5.1.

5.2.4 Slag Cement

A grade 100 ground granulated blast furnace hlag (GGBFS) was used in accordance with ASTM C989. The slag cement (Figure 5.2c) has a specific gravity of 2.93 and Blaine fineness of 5810 cm^3/g and was obtained from Diversified Mineral Inc., California. The chemical composition of the slag cement is presented in Table 5.1

5.2.5 Silica Fume

This study, used a high-performance densified silica fume or Sikacrete-950 DP (Figure 5.2d) obtained from Sika Corporation, New Jersey. The silica fume particles have an average diameter less than 1 μm, specific gravity of 2.26 and a minimum of 85% SiO_2, meeting the requirements of ASTM C1240. Table 5.1 shows the chemical composition of the silica fume compared to other SCMs.

Table 5.1: Chemical Composition of slag, silica fume and glass powder

Suppl. Cementitious Mat. (SCMs)	**Chemical composition (%)**						**Specific gravity**
	SiO_2	Al_2O_3	Na_2O	Fe_2O_3	CaO	MgO	
Slag	34.2	13.68	-	0.75	41.41	6.74	2.93
Silica Fume	92	0.47	0.27	0.53	0.89	1.67	2.26
Glass Powder	71.86	1.45	17.16	0.71	6.58	2.04	2.45

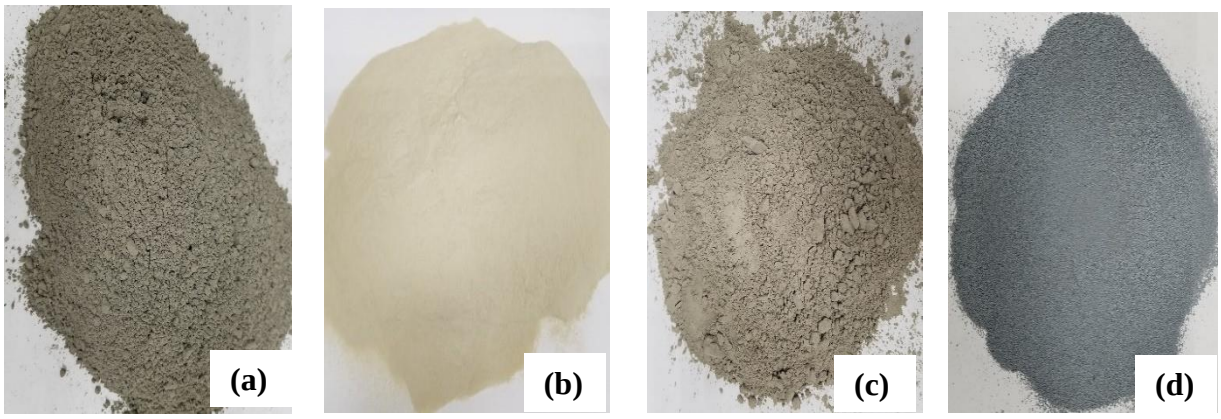

Figure 5.2: a) Portland cement; b) glass powder; c) slag; d) silica fume

5.3 Mixture Proportions

The author developed and executed a comprehensive testing program to evaluate ASR mitigation using SCMs and glass powder. Table 5.2 presents the testing program. The mix proportions include SCMs with or without glass powder at both binary and ternary levels. Different characteristics were evaluated including workability, strength activity index, and ASR expansion. A total number of 16 different mixes were developed and tested as presented in Table 5.2. Different SCMs were used including silica fume and slag as well as glass powder with different percentages were used in preparing the mixes. The binary mix was

considered when cement was partially replaced with slag, silica fume and glass powder up to 30% while the ternary mix at 20% and 30% dosage level was considered with slag and glass powder or silica fume and glass powder, An example of the mixture proportion at 10, 20 and 30% replacement with pozzolans is shown in Table 5.3 while Table 5.4 show the mix proportion used in the ASR expansion testing using the 14-day AMBT and 56-day MCPT method, respectively. The blended mix of cement and sand for flow test and strength test is presented in Table 5.5. For the themogravemetric analysis, five mixtures were examined as presented in Table 5.6.

Table 5.2: Relative mix proportion containing SCMs with or without glass powder

Mix No	**Mixture ID**	**Cementitious Materials (%)**				
		Cement (%)	**Slag (%)**	**Silica Fume (%)**	**Glass Powder (%)**	**Total Replacement (%)**
1	Control	100	-	-	-	
2	10G	90	-	-	10	10
3	20G	80	-	-	20	20
4	30G	70	-	-	30	30
5	10S	90	10	-	-	10
6	20S	80	20	-	-	20
7	30S	70	30	-	-	30
8	10SF	90	-	10	10	10
9	20SF	80	-	20	20	20
10	30SF	70	-	30	30	30
11	10S10GP	80	10	-	10	20
12	10SF10GP	80	-	10	10	20
13	10S200GP	70	10	-	20	30
14	10SF20GP	70	-	10	20	30
15	15SF15GP	70	15	-	15	30
16	15SF15GP	70	-	15	15	30

Table 5.3: Design mix proportion for mortar samples for AMBT testing

Materials (kg/m3)	**Mix proportion example**							
	Control	**10GP**	**20S**	**30SF**	**10S10GP**	**10SF10GP**	**10S20GP**	**15SF15G**
Water	207	207	207	164	164	164	164	164
Sand	990	990	990	990	990	990	990	990
Cement	440	396	352	308	352	352	308	308
Slag	-	-	88	-	44	-	44	-
Silica fume	-	-	-	132	-	44	-	44
Glass powder	-	44	-	-	44	44	88	88

Table 5.4: Design mix proportion for MCPT testing

mix proportion @ control							
Material	**Water**	**Cement**	**Sand**	**Coarse**	**Glass**	**Slag**	**Silica fume**
Amount(kg/m^3)	733	1777	2408	4792	-	-	-

Table 5.5: Aggregate gradation for flow and strength test

mix proportion @ control							
Material	**Water**	**Cement**	**Sand**	**Glass**	**Slag**	**Silica fume**	**Sample size**
Amount(kg/m^3)	277	554	1237	-	-	-	Cube
Amount(kg/m^3)	1740	3480	7831	-	-	-	Cylinder

Table 5.6: Aggregate gradation for TGA Testing

Mix ID	**Cement, % (g/m^3)**	**Additives, % (g/m^3)**	**W/c**
Control	100 (855)	0	0.45 (384)
20GP	80 (684)	20 (171)	0.45 (384)
20Si	80 (684)	20 (171)	0.45 (384)
20SF	80 (684)	20 (171)	0.45 (384)
10S10GP	70 (599)	30 (256)	0.45 (384)
10SF20GP	70 (599)	30 (256)	0.45384)

5.4 Specimen Preparation

The same mix prepared for the strength test was also used to test the fresh characteristics of mortar samples (i.e., workability or flow test). For the compressive cube test, a total number of 189 cubes were produced and tested. This number include 144 cubes for 16 mitigation mixtures and 45 extra cubes in order to compare the sample performance after cured in 1N

NaOH solution with the strength of control mix. The mix ratio of cement to fine aggregate (sand) of 1:2.25 by volume was used with particles passing No. 4 through No. 100 in according with ASTM C 33 (Table 5.4). A water-to-cement (w/c) ratio of 0.49 was used which was based on the consistency and stability of the control mix (Ramamurthy et al., 2009). A portable mortar mixer was used for sample mixing without segregation. The mix was then placed in the lubricated steel mold and compacted with a tamper rod to minimize void and even consolidation.

For the expansion test, 16 different mixes with three replicates each containing SCMs with or without glass powder (made of 1in x 1in x 11.25in mold) were prepared in accordance to ASTM C 1260 standards with the use of one reactive aggregate type (Wn-56). Five selected mixtures produced using reactive Wn-56 aggregates were also evaluated using two additional reactive aggregates to verify the effectiveness of the mitigation procedure. Table 5.7 presents an overview to the laboratory experiment; properties evaluated, aggregates considered, and testing method.

Table 5.7: Summary of laboratory experiments

Aggregates used	Properties	Testing Method	Sample size	No of Mix
Wn-56	Durability (ASR)	AMBT	1-in x 1-in x11.25-in	16 (All Mix)
		MCPT	2-in x 2-in x11.25-in	5 (CTRL, 20GP, 10S10GP, 10S20GP, 10SF10GP, 15S15GP)
	Workability	Flow Test	2-in x 2-in x2-in	16 (All mix)
	Strength	Cube Test	2-in x 2-in x2-in	16 (Al mix)
	Pozzolanic Activity	TGA		6 (CTRL, 20G, 20S, 20SF, 10S10GP, 10SF10GP)
	Microstructural Analysis	SEMs		3 (CTRL, 30GP, 10S10GP)
		EDX		3 (CTRL, 30GP, 10S10GP)
Basalt & Man. Sand	Durability (ASR)	AMBT	1-in x 1-in x11.25-in	5 (CTRL, 20GP, 10S10GP, 10S20GP, 10SF10GP, 15S15GP)

5.5 Test Methods

The AMBT (Section 3.3.1) and MCPT (Section 3.3.2) test methods were used to evaluate the effectiveness of SCMs and glass powder to mitigate the ASR in reactive aggregates. Figures 5.3 and 5.4 show the sample preparation and testing used in the ASR mitigation study using AMPT and MCPT test methods, respectively. The MCPT was conducted on few selected mix containing SCMs and glass powder to correlate its mitigation results with the 14-day AMBT mitigation results. In addition, the researcher conducted additional testing, including flow test, strength activity index, thermogravimetric analysis, scanning electron microscopy (SEM), and energy-dispersive X-ray (EDX) spectral analysis to examine the effects of SCMs and glass powder on various properties and chemical composition of concrete materials. This section provides an overview of these test methods and techniques.

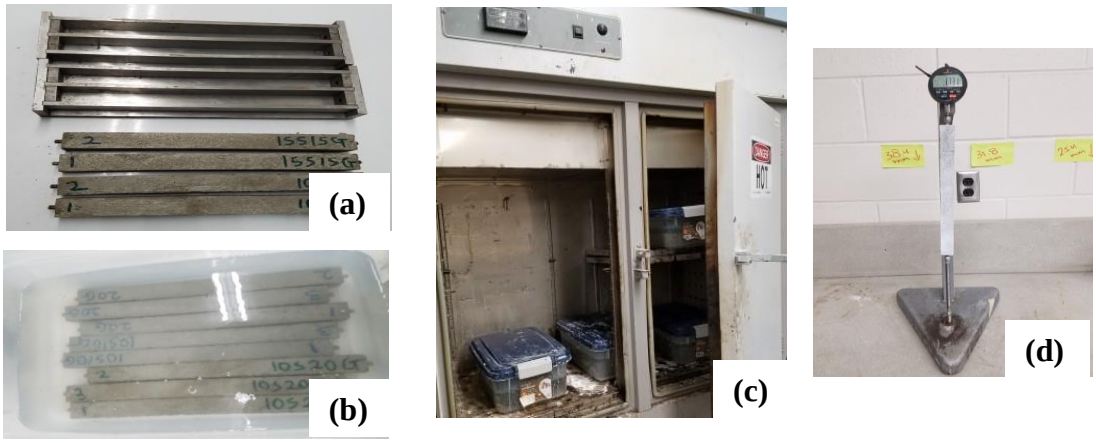

Figure 5.3: a) 14-day AMBTs' sample preparation; b) specimen cured in NaOH solution; c) sample placed in oven; d) Expansion measurement using the length comparator

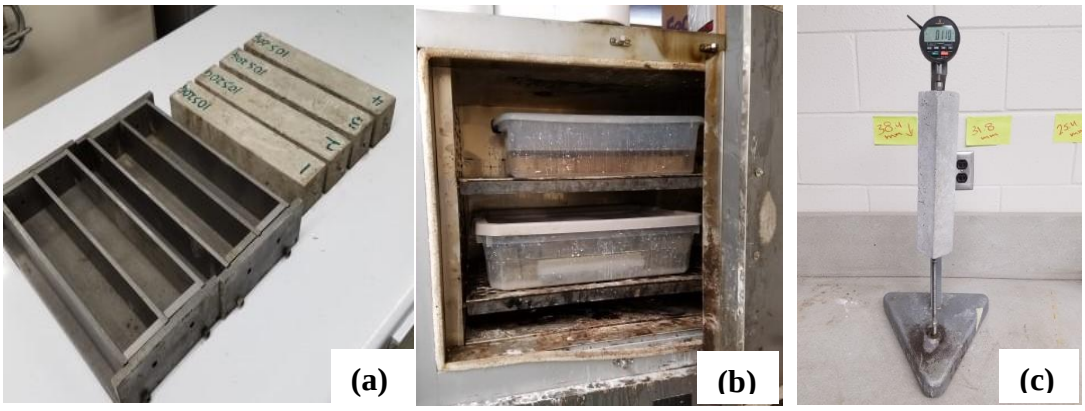

Figure 5.4: a) MCPT sample preparation; b) sample placed in oven; c) expansion measurement using the length comparator

5.3.1 Flow Test

The flow test is conducted in accordance with ASTM C1437 on each test mixture to determine the consistency and workability of mortar bar samples. Although the workability performance of test samples itself doesn't have a direct benefit on ASR mitigating, the fresh mortar flowability test is important to ensure good consolidation of test specimens. In this test, a steel cone is placed at the center of a vibrating table and filled with a fresh mortar in two layers. Each layer is compacted with 20 strokes of a tamper rod follow by exerting 25 drops within 15sec on the mix (Figure 5.5a). The percent flow of each mixture is determined by measuring the mortar sample diameter from three locations (Figures 5.3b to 5.3d) using Equation 5.1. The percent flow is then evaluated as resulting increase in average base diameter of the mortar mass expressed as a percentage of the original base diameter.

$$\text{Percent Flow} = \frac{\text{Davg} - \text{Do}}{\text{Do}} \text{ x } 100 \qquad \text{Eq. 5.1}$$

where:

Davg = Average base diameter after 25 drops

Do = Original base diameter (i.e., 4 in)

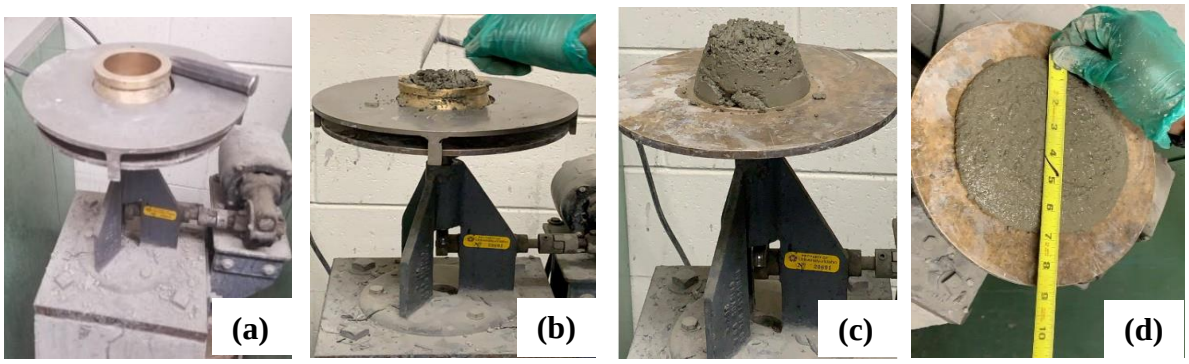

Figure 5.5: a) Flow test table; b) fresh mix placed in the cone mold; c) sample subjected to vibration; d) flow measurement.

5.3.2 Strength Activity Index (ASTM C311)

The compressive strength or strength activity index of mortar cubes is conducted in accordance with ASTM C 311. This test was used in this study to evaluate and compare the pozzolanic activity of each mixture blended with SCMs and waste glass powder at binary and ternary combination level. In this test, a 2-in steel cubes was filled with fresh mortar in two layers and each layer was compacted using 20 strokes of a tamper rod. A total of 16 mixtures (Table 5.2) with 6 replicates each were tested at both 7 and 28 days (96 in total). Theses mixes contain various amounts of SCMs and glass powder as a partial replacement of Portland cement (Table 5.2). The cubes were placed inside a curing room at a standard room temperature and relative humidity. After 24 hours, the test specimens were demolded, cured in a lime-saturated water tank at room temperature (Figure 5.6). The compressive strength of test mortar specimens were measured after 7 and 28 days using a 300-kip concrete compression machine (MC-300PR) at the rate of 35psi/sec (Figure 5.6d). The strength activity index is calculated using Equation 5.2.

$$\textit{Strength Activity Index (SAI)} = \frac{X}{Y} \text{ x } 100\% \qquad \text{Eq. 5.2}$$

where:

X= average compressive strength of different mixtures (N/mm^2)

Y = average control compressive strength of mortar sample (N/mm^2).

Furthermore, the compressive strengths of cylindrical concrete samples of selected mixes were also measured and compared to those of mortar cubes. Lastly, the strength activity index of selected samples was also investigated after curing in 1N NaOH solution (replicating harsh conditions). This is conducted to determine the strength after ASR and the results were compared to the strength of mortar cubes cured in water.

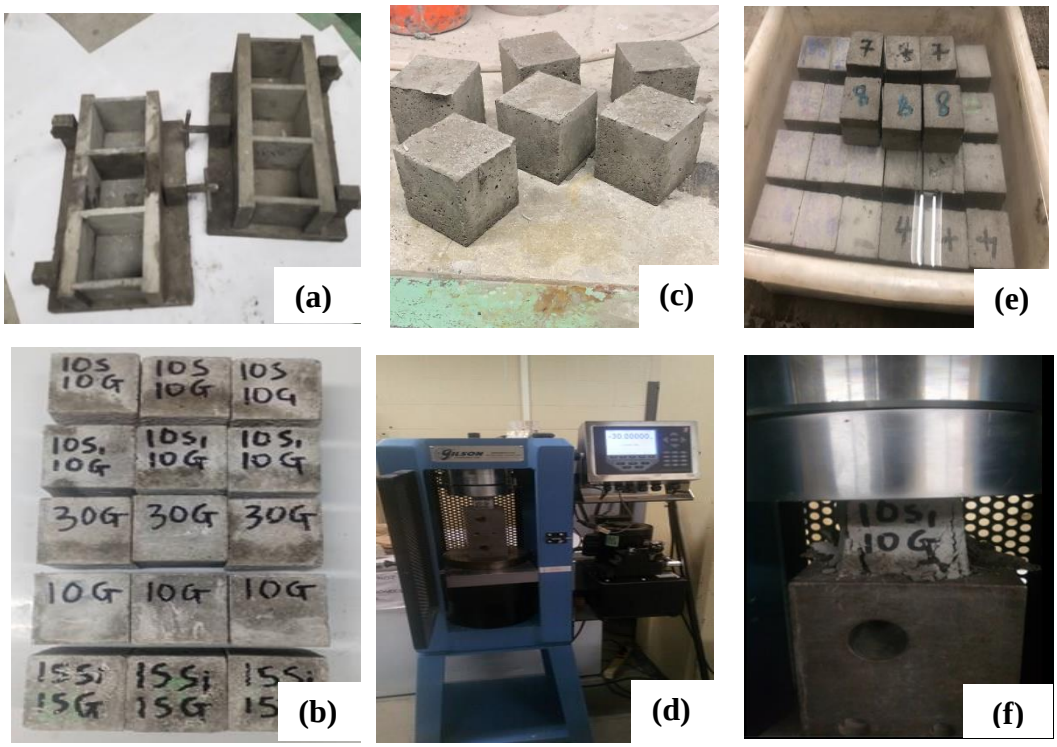

Figure 5.6: Cube compressive test 4-in cube mold (a); sample prepared (b); samples cured and ready for testing (c & d; specimen testing (e & f).

5.3.3 Thermogravimetric analysis (TGA)

The thermogravimetric analysis (TGA) was used in this study to compute the pozzolanic reactivity of test specimens. TGA technique operates through gradual heating of the mortar paste (placed on a furnace pan) from the ambient temperature to 800^{o}C. The mass decomposition is monitored with respect to temperature and time. The percent decomposition of the inorganic compound calcium hydroxide, $Ca(OH)_2$ from each cement paste was evaluated to characterize the pozzolanic reaction or the hydration rate. The percent $Ca(OH)_2$ decomposition is measured by subjecting the cement paste to a range of temperatures between 440C and 520C (824F - 968F) at 10^{o}C/min. A total number of eight cement pastes with best binary and ternary blends were prepared and the percent $Ca(OH)_2$ decomposition was evaluated. Prior to testing, a 2-in thick cement paste was cured in lime-saturated water according to Table 5.8 for 14 and 28 days (Villain et al., 2007; Pane and Hansen, 2005; Afshinnia and Rangaraju, 2015). Paste pieces of test samples were grounded until an average thickness of 0.02 in is acquired. Figure 5.7 show the test procedure for the TGA experiment.

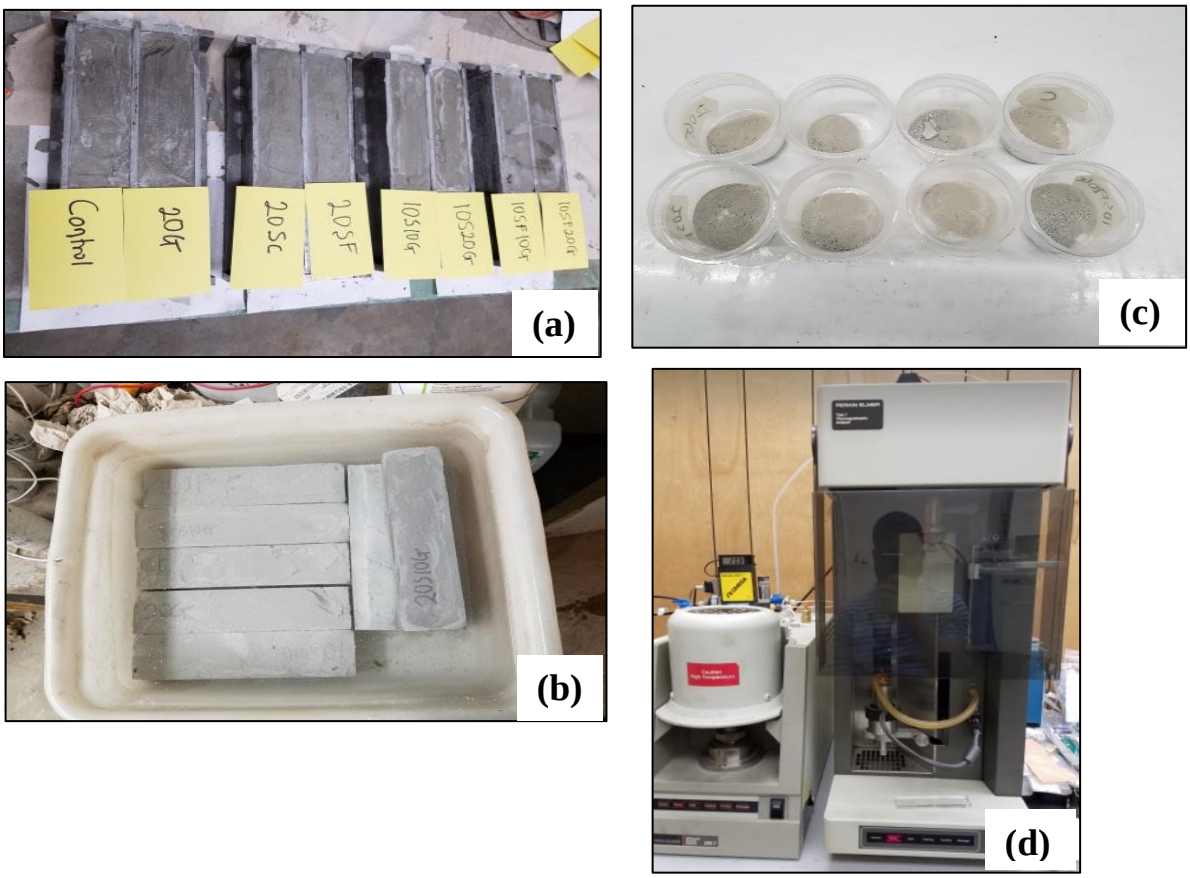

Figure 5.7: a) Cement paste sample preparation; b) sample curing; c) Core part of test samples; d) Testing using the TGA

5.3.4 Scanning Electron Microscopy (SEM) and Energy-Dispersive X-ray Spectral Analysis (EDX)

Scanning electron microscopy (SEM) is a mechanism for taking high-resolution imaging performed on polished section of concrete surface. Therefore, SEM and EDX were adopted to capture the formation of swelling gel due to ASR as well as the chemical configuration of mortar samples. The effect of using SCMs with and without glass powder on formation of ASR gel was evaluated. This microstructural examination was conducted after 28 days on 1in x 1 in x 11.25in samples tested using the AMBT method (ASTM C 1260). The AMBT samples were mixed, cast, and cured in a NaOH solution for 28 days in accordance with ASTM C 1260 and prepared for SEM and EDX analysis.

Sample preparation prior to imaging is very important. 10-mm thick cross section was cut with diamond blade saw and then dried for 2 days. A smaller sample (2-mm thick) was trimmed, ground and polished with fine grits (i.e., from #8 to #2000) diamond discs. Lastly,

the polished samples were coated with carbon before placing the test samples in SEM. The samples were scanned using the backscatter mode at voltage of 15-kV and current of 1-nA. These conditions provided good image contrast as a function of elemental composition, as well as surface topography (see Figure 5.8).

The Energy-Dispersive X-ray Spectral analysis, which is attached to the SEM machine, was performed to study the quantitative chemical composition of the test samples. The EDX techniques detects x-rays emitted from the sample to characterize the elemental composition of the analyzed volume. At least three different locations (close to one another) were examined for chemical analysis.

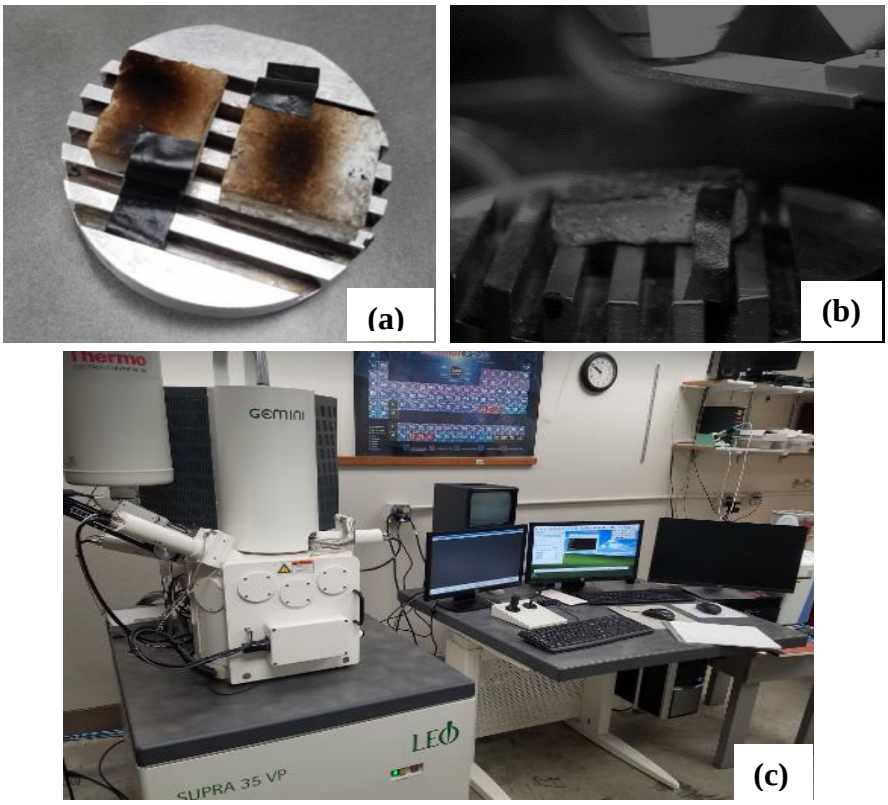

Figure 5.8: a) Sample prepared for SEM analysis; b) sample's image in the machine; c) Testing machine set up for SEM

CHAPTER SIX: ASR MITIGATION RESULTS AND ANALYSIS

6.1 Introduction

This chapter discusses the results of the ASR mitigating study using SCMs and glass powder at various binary and ternary combinations. First, the flow test was conducted to study the workability of various produced mortar mixes and their compressive strength was measured by testing mortar cubical samples. The ASR expansion was measured using the AMBT and MCPT methods. Additionally, this research utilized advanced characterization techniques including themogravimetric analysis (TGA), scanning electronic microscopic (SEM) imaging, and energy-dispersive X-ray (EDX) spectral analysis to investigate pozzolanic reactivity, ASR gel formation, and microstructural and chemical analysis of mortar specimens prepared with glass powder and other SCMs. The results of these tests are discussed in Chapter 6.

6.2 Flow (workability) Test

The workability results using the flow table, discussed in Chapter 5, for the 16 mixtures are presented in Table 6.1. Figure 6.1 shows the partial replacement of cement at binary level with slag, silica fume (SF) and glass powder (GP) at 10, 20, and 30 percent. The workability of binary blends containing GP and slag increased with percent replacement. Mixes with 30% GP mix had the highest flow value of 7.98 in (10% more than the control mix). Meanwhile, the flow value decreased with the increase in SF. Mixes with 30% SF had a 35% reduction in flow value compared to the control mix. Mixes with low flow values correspond to difficulty in mixing. These results are in good agreement with the findings in the literature. Park et al. (2005) reported that the reduction in workability of mixes prepared with silica fume could be due to the large surface area of silica fume since silica fume particles range between 15,000 to 30,000 m^2/kg. Hassan and Rangaraju (2015) and Rangaraju et al. (2016) showed that mixes prepared glass powder and slag had better workability. This could be due to the smooth surface textures of glass powder and slag which improve the workability.

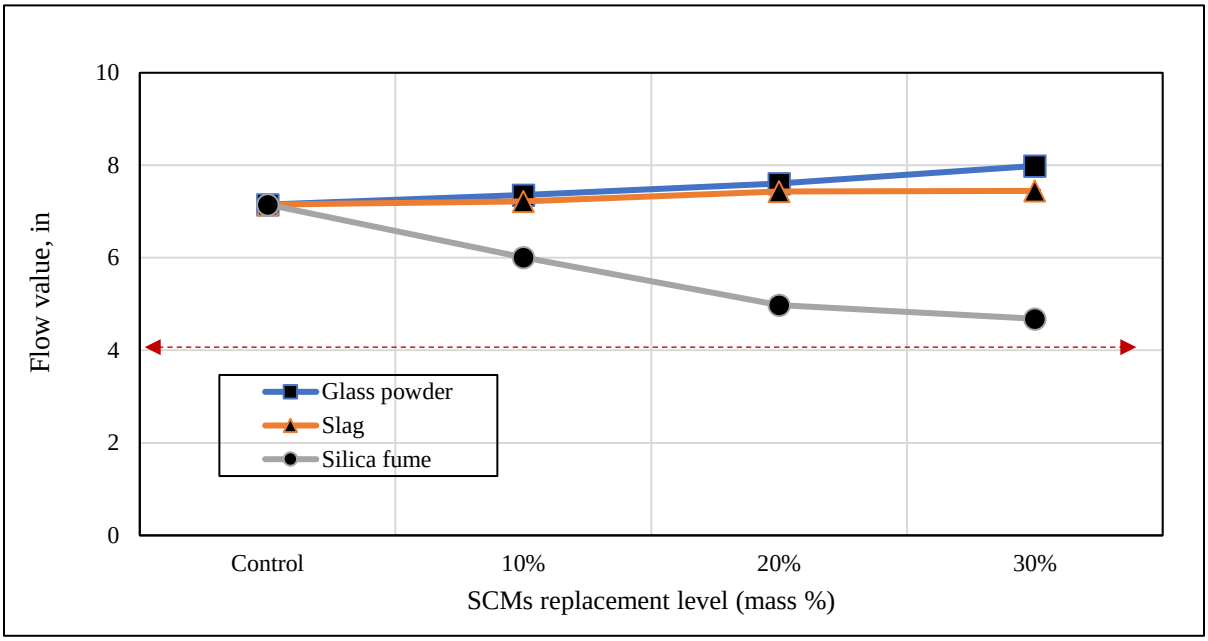

Figure 6.1: Flow values for glass powder, slag, and silica fume mixes

Table 6.1: Flow values for the test mixtures

Mixture ID	Initial (in)	10 drops (Avg-in)	25 drops (Avg-in)	Percent flow	STD Error
Control	4.00	5.67	7.15	**79**	0.9399
10GP	4.00	5.36	7.36	**84**	0.7150
20GP	4.00	5.50	7.61	**90**	1.1365
30GP	4.00	5.69	7.99	**100**	1.1960
10S	4.00	4.94	7.22	**81**	1.0528
20S	4.00	5.29	7.44	**86**	0.6236
30S	4.00	5.59	7.45	**86**	0.5523
10SF	4.00	4.36	6.01	**50**	0.67453
20SF	4.00	4.15	4.98	**24**	0.3535
30SF	4.00	4.00	4.68	**17**	0.5892
10S10GP	4.00	5.68	7.83	**96**	2.0665
10SF10GP	4.00	4.34	6.11	**53**	2.9598
10S200GP	4.00	5.65	7.73	**93**	2.3570
10SF20GP	4.00	5.02	6.67	**67**	2.5685
15S15GP	4.00	5.68	7.89	**97**	2.8358
15SF15GP	4.00	4.19	5.18	**30**	3.2441

In general, ternary blends made of glass powder show a better flowability performance compared to binary blends as shown in Figure 6.2 and 6.3. The percent flow of ternary mixes made with slag and glass powder at higher replacement percentage (i.e., 20% and 30%) increased by 15% and 12%, respectively compared to the control mix. Also, mixes made with glass powder and slag had higher flow values compared to mixtures made with glass powder and silica fume. These results agree with the findings by Hassan and Rangaraju (2015) and Kaveh and Rangaraju (2015). The ternary blends of glass powder and silica fume (at 10%) displayed improved workability compared to binary blends with 10%, 20%, or 30% of silica fume. Only one mix (i.e., 10SF20G) produced the best ternary mix containing silica fume.

Analysis of Variance (AVOVA) and Tukey Honest significant difference (HSD) at 95% confidence level were performed to examine the mixes that are statistically different from one another. Mixtures sharing the same letter are not statistically different while mixtures with dissimilar letters show a significant difference. The percent flow of most mixtures containing pozzolans at binary and ternary stage are significantly different from the control statistically, expect for 10S mix. Generally, it can be concluded that mixes made with slag and/or glass powder are not significantly different from one another compared to mixtures made with silica fume. For example, mix with 30% silica fume with a letter “G” is far different from mix containing 30% glass powder or 30% slag with letters “A” and “C”, respectively (Figure 6.2 and 6.3).

All mixes had better workability compared to the control mix expect 20SF, 30SF, and 15SF15GP which showed reduced workability. Mixes 30GP, 10SF10GP, and 10SF20GP had higher percent flow of 99.7%, 96%, and 96%, respectively and better workability compared to the control mix. A clear example of a mix with slag + GP and SF + GP workability is shown in Figure 6.5.

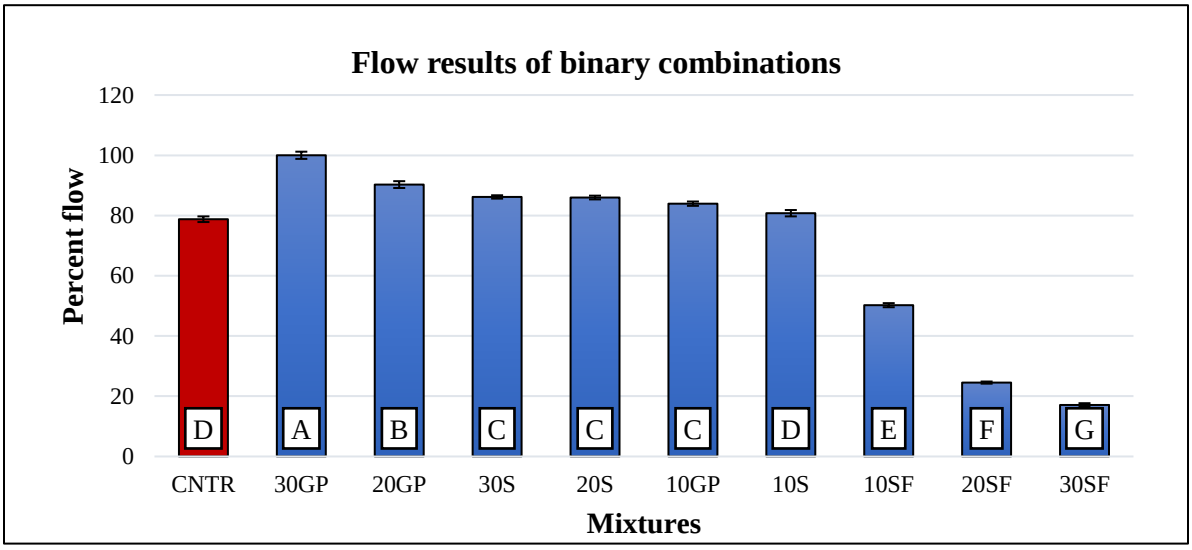

Figure 6.2: Flow percentage of mortar sample at binary replacement

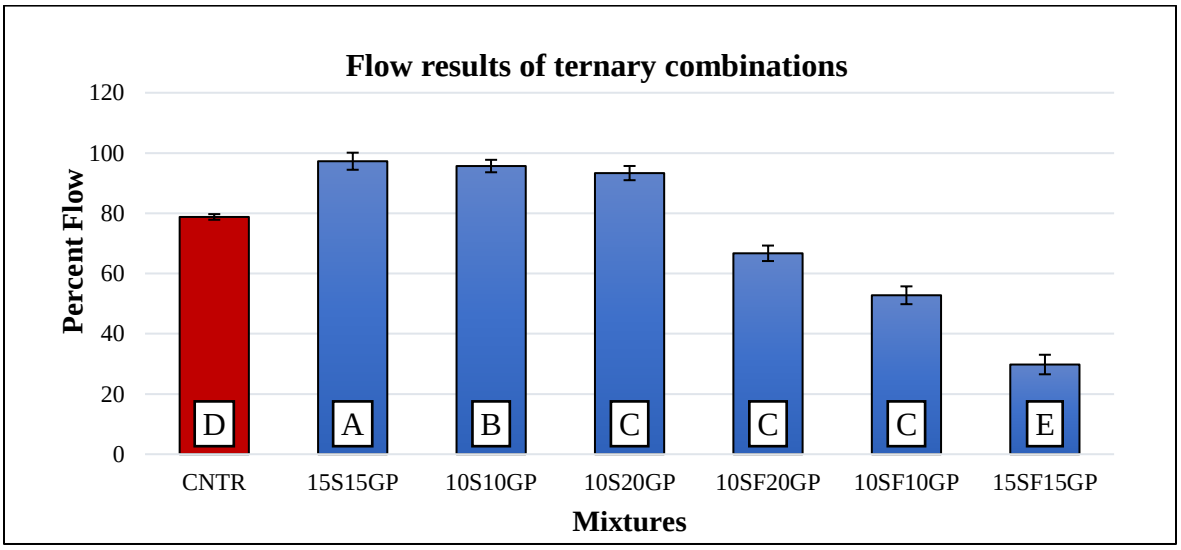

Figure 6.3: Flow percentage of mortar sample at ternary replacement

The images taken using the scanning electronic microscope (SEM) for various mixes can be used to understand the effect of pozzolans and glass powder on workability. The particle shape of slag cement was found to be angular with some slight spherical shape. The silica fume and waste glass powder were found to be spherical and angular in shape respectively as shown in Figure 6.4. The angular shape of slag and glass powder could cause lower water absorption capacity and increased workability. Meanwhile, the spherical shape

and large surface area of silica fume could make room for partial absorption of water and reduce the required water for lubrication leading to reduced workability (Kaveh and Rangaraju, 2015, Arowojolu, et al, 2019).

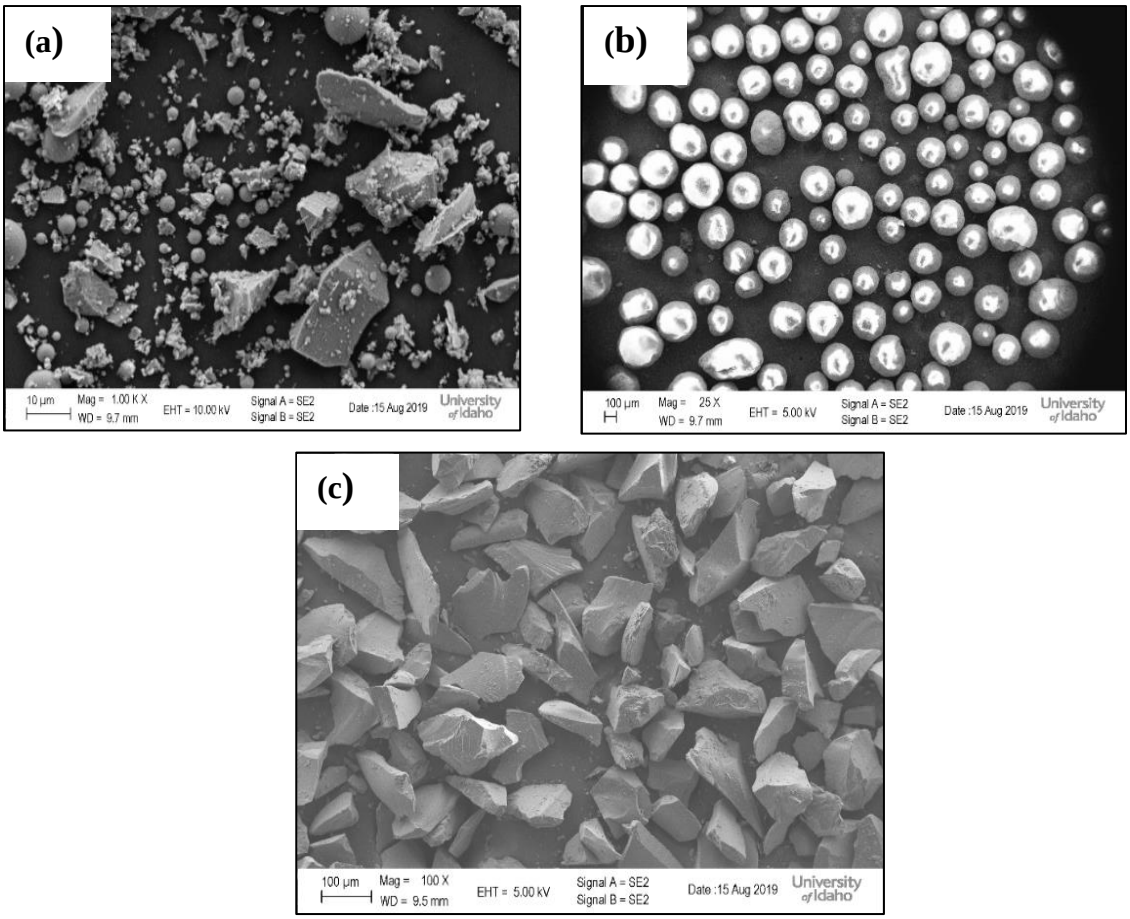

Figure 6.4: SEM images of a) slag; b) silica fume (b), and c) glass powder

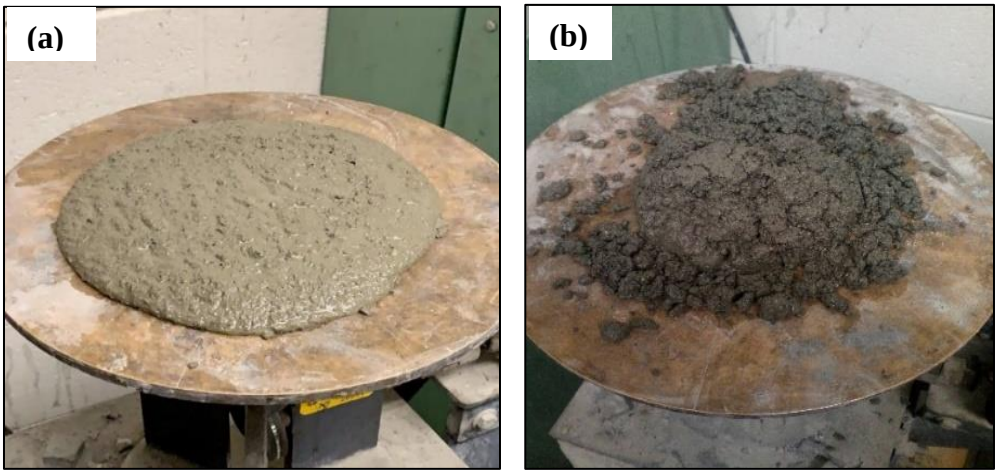

Figure 6.5: Mortar flow containing a) glass powder and slag; b) glass powder and silica fume

6.3 Strength Activity Index (SAI)

The strength-activity index (SAI) was determined to evaluate the pozzolanic reactivity of mortar and concrete samples containing SCMs with and without glass powder (at both binary and ternary mixtures). In addition, the SAI of samples prepared with SCMs and glass powder were compared to the control mix. The SAI results for 16 different mixes are summarized in Table 6.2. Figure 6.6 depicts the 7-day and 28-day strengths measured for various binary and ternary blends. Generally, the compressive strength increases proportionally with curing age as shown in Figure 6.6. The control mix at 28 days possess 7% increase in strength compared to 7-day strength, while mixtures with SCMs at binary and ternary levels had an average increment of 32%. The results demonstrate that using SCMs in concrete mixtures substantially increased the strength over time. The binary mixtures containing 10%, 20% and 30% glass powder (GP) have a 28-day strength activity of 95%, 79% and 60%, respectively. These results showed that strength decreases steadily with percent replacement of glass powder in the mix. The reduction in SAI is due to the reduction in pozzolanic behavior of glass powder at higher percentages [Sadati and Khayat, 2017; Rangaraju et al, 2016; Olaniyi et al., 2019)]. Based on the results of SAI shown in Figure 6.6, the replacement of cement by glass powder should be limited to 20% since the SAI of 30% was less 75% which is the minimum threshold per ASTM C618.

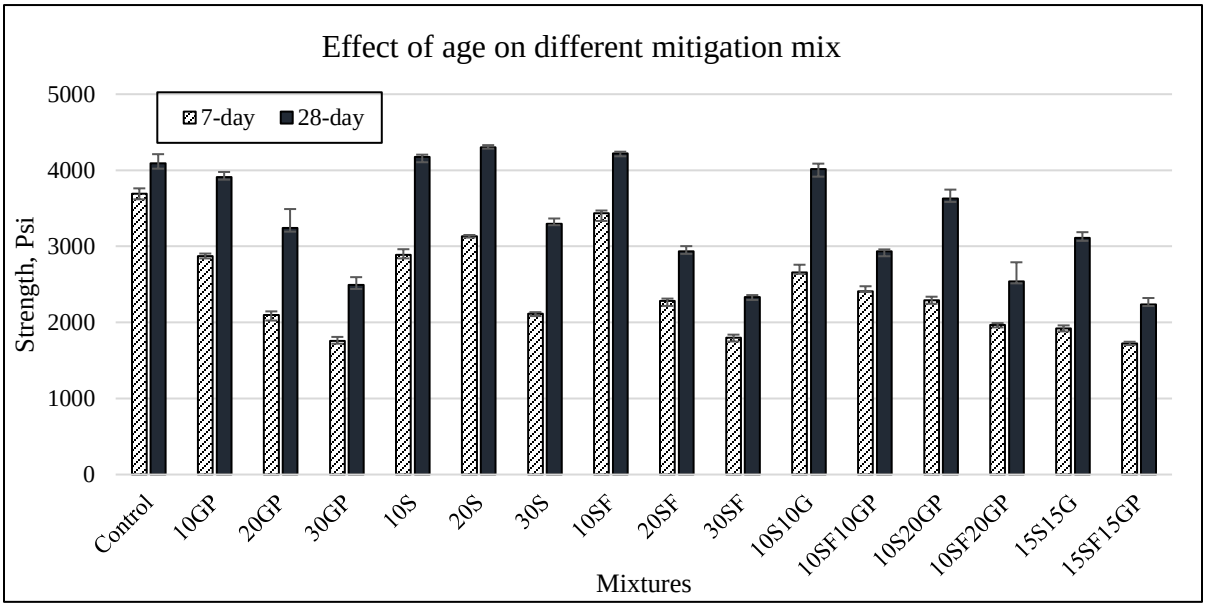

Figure 6.6: Strength of each mixture at 7 and 28 days

Table 6.2: SAI result for 16 mortar mixtures

S/N	Mixture ID	Avg 7-day strength	Avg 28-day strength	Percent increase (%)	Avg. SAI (STD error)
1	**Control**	**3690**	**4093**	**9.84**	**100**
2	10GP	2873	3909	26.49	**99 (4)**
3	20GP	2097	3242	35.32	**79 (8)**
4	30GP	1758	2492	29.47	**61 (4)**
5	10S	2890	4178	30.82	**102 (4)**
6	20S	3132	4301	27.18	**105 (4)**
7	30S	2115	3298	35.88	**81 (2)**
8	10SF	3434	4221	18.65	**103 (1)**
9	20SF	2281	2933	22.21	**72 (3)**
10	30SF	1801	2334	22.83	**57 (1)**
11	10S10GP	2659	4016	33.80	**98 (4)**
12	10SF10GP	2411	2935	17.86	**72 (1)**
13	10S20GP	2292	3630	36.87	**89 (5)**
14	10SF20GP	1966	2538	22.55	**62 (7)**
15	15S15GP	1921	3112	38.26	**76 (4)**
16	15SF15GP	1724	2238	22.95	**55 (3)**

For mixes prepared with silica fume (SF), there is a substantial difference between the strength after 7 and 28 days. This is because silica fume increases the rate of cement hydration hence increasing the early age strength (ACI Committee 234, 2012). Meanwhile for mix made with slag, the results showed that incorporating slag (S) at the binary level of 10% and 20% increased the strength by only 2% and 5%, respectively. The strength decreased by 19% when 30% of slag was used compared to the strength of control mix as shown in Figure 6.7. This reduction in strength at higher percentage of slag cement could be due to the rate of strength gain. The rate of strength gain for mixtures prepared with slag cement is lower compared to control mix because the hydration properties of slag is subordinate to that of OPC concrete (ACI 234, 2012).

The use of 10% silica fume (SF) increased the strength slightly (SAI of 103%), but the SAI decreased greatly to 72% and 57% at higher percentages of 20% and 30%, respectively which is lower than the minimum SAI threshold of 75% according to ASTM C618. The strength improvement in mixes with 10% silica fume is due to the physical effect from micro filler action and chemical reaction from pozzolanic materials. These pozzolanic and filler actions could result in primary binder (cement) replacement when higher dosages of SF are introduced, hence, causing strength reduction as noticed for both 20% and 30% replacement. Therefore, the use of 20% replacement of slag along with 10% of silica fume (SF) would provide better performance, and this combination is recommended. Figure 6.8 shows the SAI results of ternary blends, mixtures containing glass powder (GP) and slag (S) at any percent replacement produce a clear synergistic effect and maintain the compressive strength above the requirement per ASTM C618 as shown in Figure 6.8. For example, the 28-day SAI of mortar cubes of 10S10GP (10% slag and 10% glass powder) and 10S20GP (10% slag and 20% glass powder) were 98% and 89%, respectively. Comparing these results with binary blends (e.g., 30% glass powder, 30% slag, or 30% silica fume), it can be seen that ternary blend (e.g., 10% slag and 20% GP) produces mixes with higher SAI (i.e., 89%). While the SAI values for binary blends with 30% glass powder, 30% slag, or 30% silica fume were 28%, 9% and 32%, respectively lesser than the 10S20GP.

A similar trend was also observed when comparing the compressive strength of ternary blends at 20% replacement (e.g. 10S10GP) with 20% slag or 20 GP and 20SF. Comparing all ternary blends with 30% cement replacement only, mixtures containing slag and glass powder produce a satisfactory strength while the strength of mixtures containing silica fume and ground powder was very low and therefore not recommended. Based on the statistical analysis conducted using the Tukey HSD, most mixtures at 10% replacement with cement is not statistically different from the control samples (mixture share same letters). However, there are substantial significant differences in strength of mixtures at higher replacement level except 20% slag (20%S). More importantly, mixtures with 30% silica fume had significant lower strengths compared to all mixtures except 30% glass powder (30%GP) as shown in Figure 6.7. At the ternary level, mixes made with silica fume are statistically different from other SCMs combinations. Mixtures containing slag and glass powder

generally showed little or no significant difference compared to the control mix. This statistical results are consistent with the percent flow presented and discussed in Section 6.2.

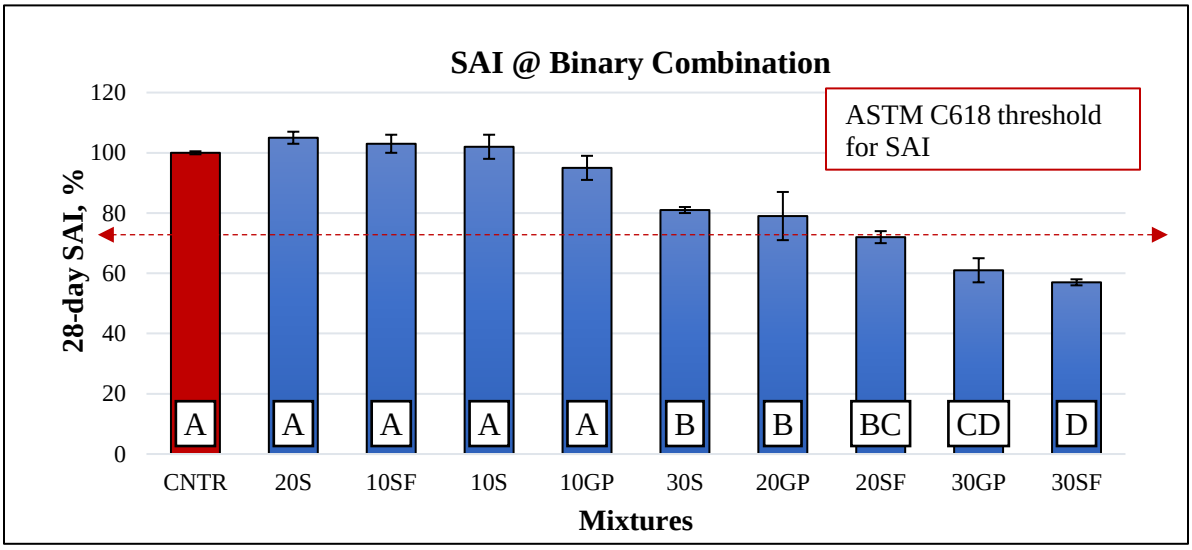

Figure 6.7: SAI percentage of mortar sample at binary replacement

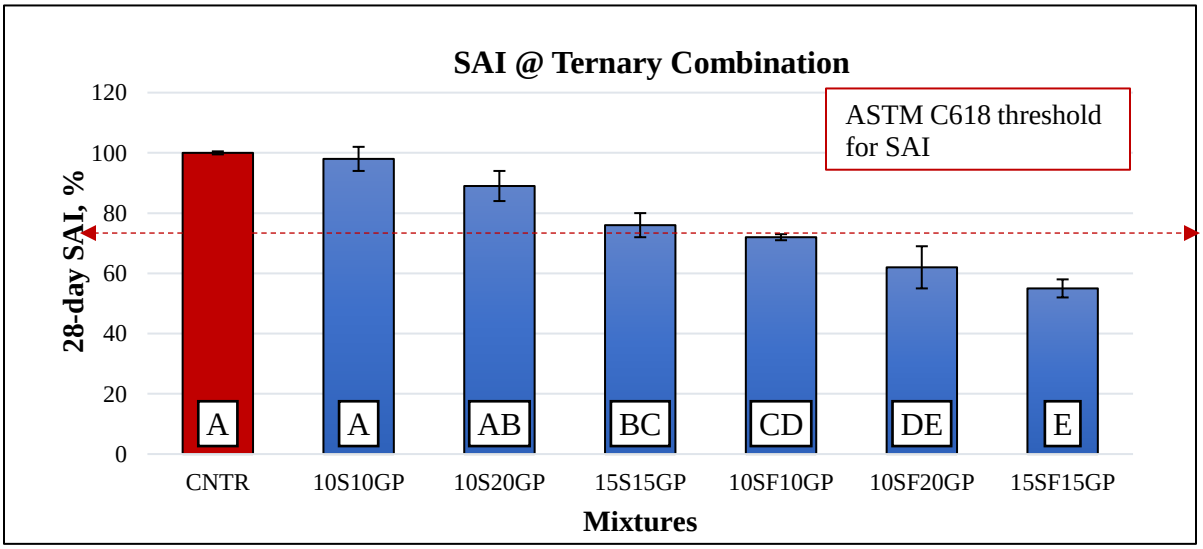

Figure 6.8: SAI percentage of mortar sample at ternary replacement

Figure 6.9 shows the compressive strength of selected mortar cubes tested after 14 days and 28 days of curing in a sodium hydroxide solution at 80^{o}C. The results were also compared to the strength of mortar cubes cured at room temperature in water (see Figure 6.10). This comparison was performed to evaluate the effect of ASR expansion on mortar samples as well as the effect of curing conditions. Contrary to the strength results of samples cured in

water (Figure 6.7), the compressive strength decreased with curing age. For instance the control mix experienced 18% reduction in strength after 28 days compared to the strength after 14 days (Figure 6.9), while the Binary and ternary combinations of slag and glass powder have an average reduction of 5% to 18%, respectively. The strength of mixtures containing silica fume reduced by half after 28 days. This is because the exposure of test specimens to this aggressive environment of sodium hydroxide at a high temperature of 176^{o}F over a period of time weakens the internal structure of the mortar samples, leading to a reduction in strength. Likewise, as shown in Figure 6.10, a reduction in strength was also observed in specimens cured under harsh conditions (i.e., NaOH at 176^{o}F) compared to specimens cured in water at the ambient temperature. Mixtures prepared using silica fume experienced a significant reduction (i.e., 50%). Poon et al., (2006) indicated that silica fume with higher porosity can contribute to the inferior strength of concrete. The results of mixtures prepared with silica fume agree with the results obtained by Poon et al. (2006). Tukey HSD showed that there is a significant difference in strength values for mixtures cured in water compared to those cured in sodium hydroxide except two mixtures (20GP and 10S20GP) Meanwhile, in respect to the curing medium, only the 14-day strength of mix containing 20% GP was not statistically different compared with the 28-day strength.

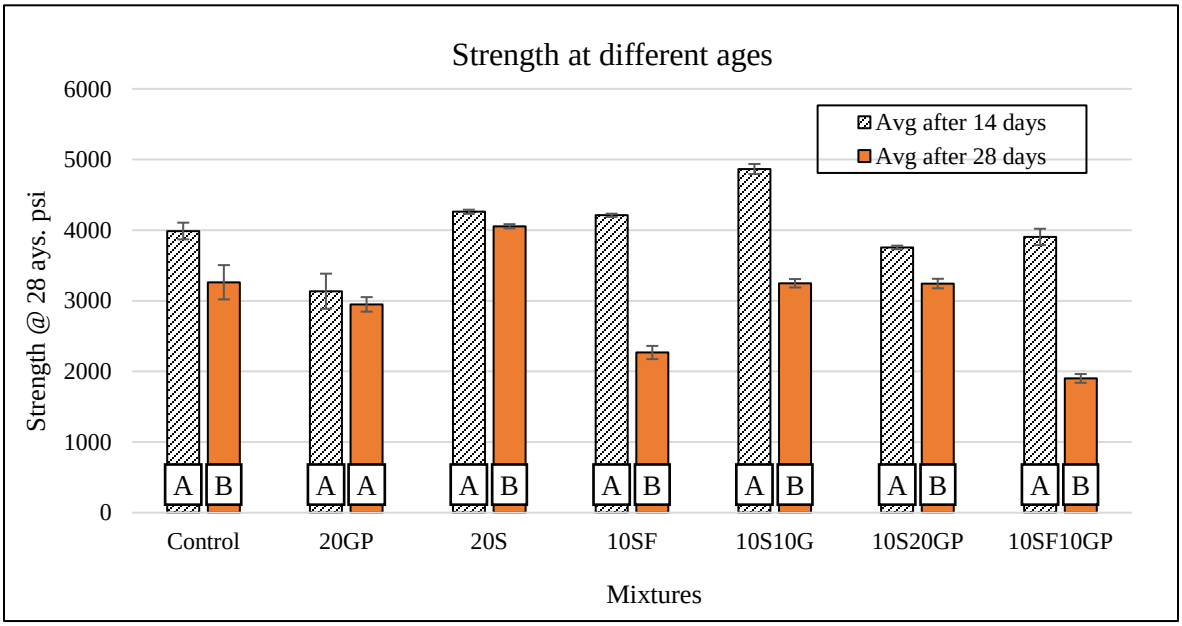

Figure 6.9: Strength comparison when cured in NaOH solution (note: compare 14-day strength to 28-day strength for each mix separately)

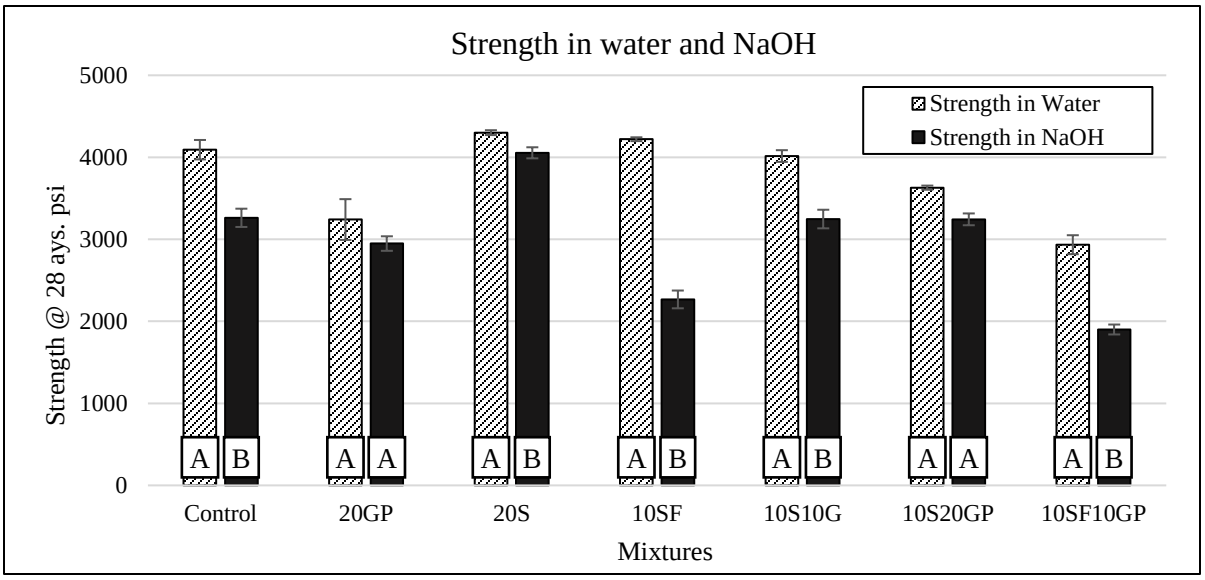

Figure 6.10: Strength after 14 and 28 days in aggressive conditions (note: compare strength in water to strength in NaOH for each mix separately)

6.4 ASR Mitigation Using Glass Powder, Slag and Silica Fume

6.4.1 Binary Combination

One of main research objectives was to evaluate how we can effectively mitigate ASR expansion and distresses especially when highly reactive aggregates are used for construction. This study examined using glass powder, slag cement and silica fume in ASR mitigation in mortar bar samples. A binary blend prepared by partially replacing the cement with SCMs (e.g., silica fume, slag) was investigate. Test samples were prepared using Wn-56 (reactive aggregate) and other SCMs materials as presented in Table 6.3. Several mortar bar samples containing binary blend were prepared and tested using the 14-day AMBT in accordance with ASTM C1260. Figure 6.11 and Figure 6.12 show the expansion performance of mortal bar containing only slag cement and silica fume respectively as partial replacement with cement at 0%, 10%, 20% and 30%. The results show a gradual reduction in the expansion for samples prepared with different percentages of slag cement and silica fume. Samples with slag perform better in term of ASR reduction compared to specimens with silica fume. This better performance from specimens made with slag is associated with the reduction in the alkalinity level of pore solution where the fine particles of slag (small surface area) aggressively react with pore solution from mortar samples especially at early stages while the large surface area particles of silica fume made it difficult for this reaction to

occurs. Beyond 14 days, the rate of expansion (beyond 14 days) of mixtures containing slag and silica fume is minimal compared to control mixtures.

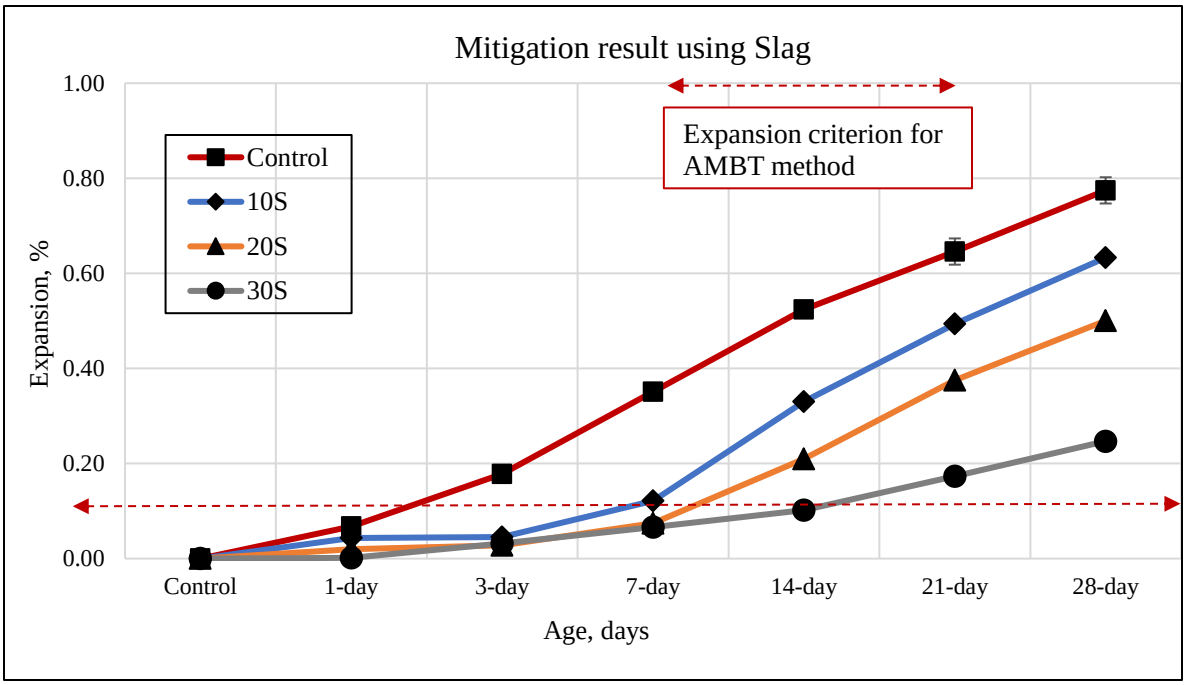

Figure 6.11: Expansion behavior of mortar bar containing slag cement

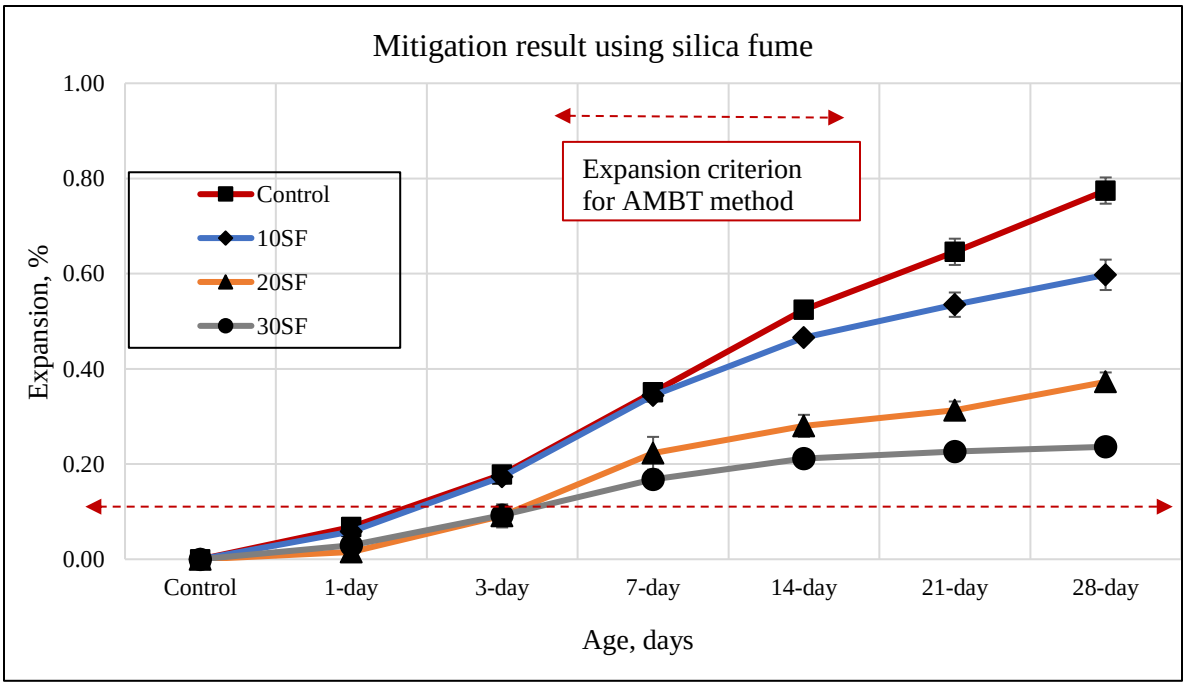

Figure 6.12: Expansion behavior of mortar bar containing silica fume

The use of glass powder as a partial replacement for Portland cement in concrete mix was able to reduce the ASR expansion to a level below that the maximum threshold (i.e., 0.10% requirement). Figure 6.13 shows the expansion behavior of specimen containing 0%, 10%, 20% and 30% of glass powder (GP). After 14-day testing, the expansion values were 0.33%, 0.12% and 0.0478% for blends with 10%, 20% and 30% glass powder. There was a significant reduction in ASR expansion at a higher dosage of glass powder. Moreover, beyond 14 days, there is only little expansion noticed. The utilization of glass powder in mortar or concrete mixtures was found to cause immediate pozzolanic reaction and the calcium hydroxide content is consumed resulting to ASR suppression (Liu et al., 2015; Lee et al. 2011). In addition, glass powder discharges a small amount of alkalis (much lower than that of cement) resulting in minimal alkali in pore solution from cementitious materials (Xiong, Q., 2006). Glass powder contains silica; however, only large sizes (i.e., size > 300 µm) contain greater amount of SiO2 which then dissolves into the solution to form C-S-H gel causing ASR gel (Rajabipour et al., 2010; Mirzahosseini and Riding 2015). However, fine particles of glass powder (similar to the one used in this study [10 µm]) only undergo pozzolanic reaction which completely dissolves in the solution (Liu et al., 2015; Lee et al. 2011). The fine particles of glass powder dissipate a higher percentage of calcium (Ca2+) in both pozzolanic reaction and hydration products causing insufficient presence of SiO2 to form the ASR gel according to Shayan and Xu (2006).

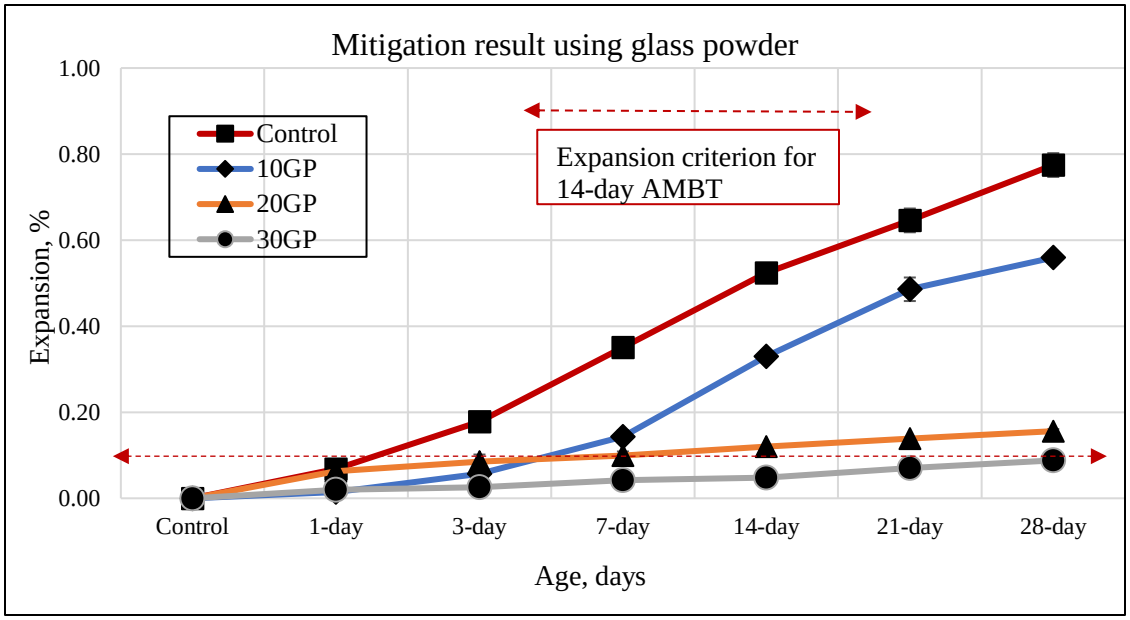

. Figure 6.13: Expansion behavior of mortar bar containing glass powder

6.4.2 Ternary Combination

In addition to the binary blends, several ternary blends were also developed and evaluated as presented in Table 6.3. These ternary blends were designed using glass powder and slag and silica fume. Figure 6.14 and 6.15 shows the ASR expansion results for the ternary blends. It can be seen that blends of slag and glass powder generally mitigate ASR expansion whether at 20% or 30% replacement levels. For instance, an expansion value of 0.11%, 0.1%, and 0.11% was recorded for 10% slag and 10% glass powder (10S10GP), 10% slag and 20% glass powder (10S20GP) and 15% slag and 15% glass powder (15S15GP) respectively, falling exactly at the border line of 0.10% expansion threshold. Blends containing silica fume and glass powder were found to reduce ASR expansion substantially, with expansion of 0.12%, 0.19%, and 0.16% for 10% slag and 10% GP (10SF10GP), 10% slag and 20% GP (10FS20GP) and 15% slag and 15% GP (15SF15GP), respectively (Figure 6.15). However, the expansion was not below the required threshold. The results show that the use of mixtures with slag and glass powder provide better performance over mixtures with silica fume and glass powder. Furthermore, similar rate of expansion was observed beyond 14 days of testing for all ternary blends at 20% and 30% dosages.

In summary, mixtures containing only glass powder or slag (as a partial replacement of cement) at binary blend effectively mitigate ASR expansion. However, due to negative effects on fresh properties (workability) and the required strength of concrete, the dosage should be limited to 20% when using glass powder at binary level. Additionally, the percent of slag should be limited up to 30%. However, to achieve overall concrete performance, we recommend the use of maximum 20% slag. The use of 10% replacement of slag or silica fume generally improves the concrete properties and also slightly reduces ASR expansion. For ternary blends, the mix containing 10% slag and 10% glass powder can be used to efficiently suppress ASR without jeopardizing the fresh and mechanical properties of concrete. Also 30% cement replacement (e.g., 10S20GP and 15S15P) can be employed as well. Table 6.3 summarizes the expansion results for 16 various mixes.

The statistical analysis and Tukey HSD presented in Figure 6.16 showed all mixtures prepared with pozzolans are statistically different from the control mix. Similar to the mitigation results, mixtures with higher dosages of SCMs showed better performance

compared to mixtures with lower dosages of SCMs. For instance, the ASR expansion for most binary and ternary blends (e.g., 20GP, 30GP, 30S, 10S10GPand 10S20GP) with letter "H" were significantly different compared to that of the control with letter "A". These results indicate the effectiveness of the ASR mitigation strategies discussed in this chapter.

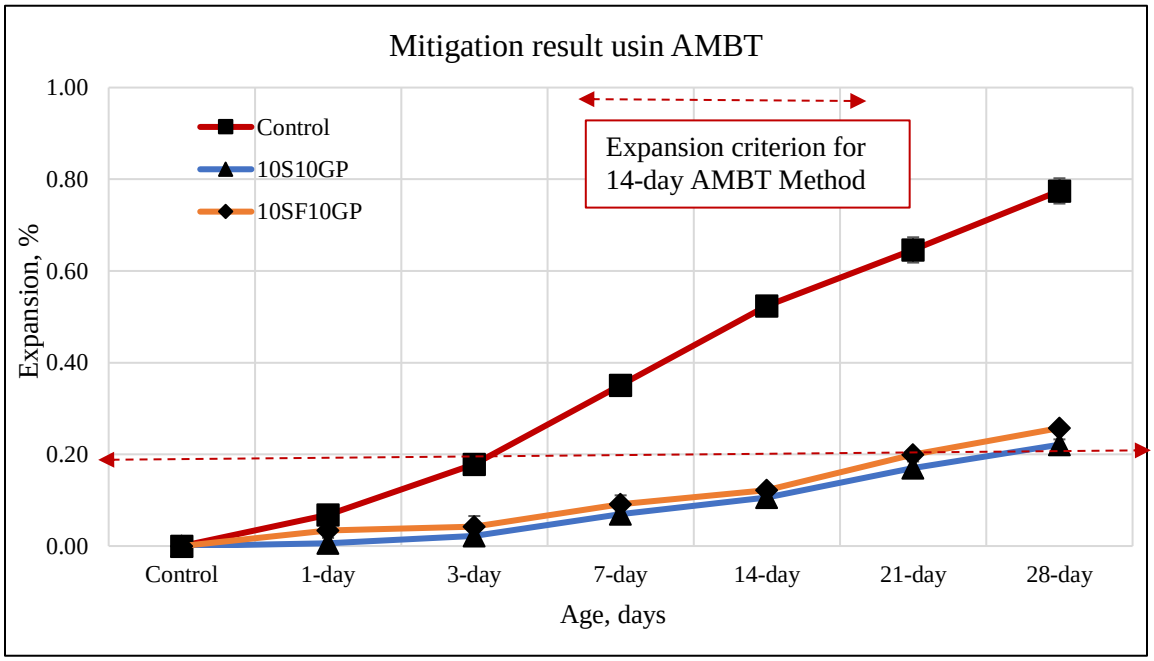

Figure 6.15: Expansion behavior of mortar bar with ternary mix up to 20% dosage

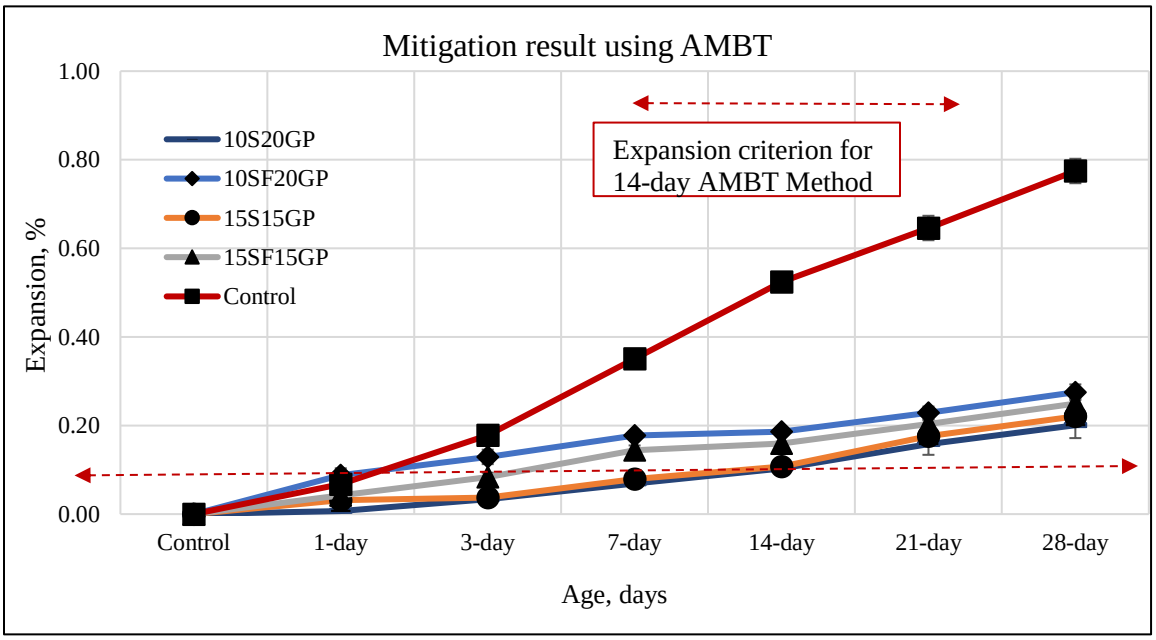

Figure 6.16: Mitigation behavior of mortar bar with ternary mix up to 30% dosage

Table 6.3: Mitigation data result for 16 mortar mixtures

Mixture ID	ASR Expansion result			
	14-day	STDerror	28-day	STDerror
Control(Wn-56)	**0.52**	**0.008**	**0.77**	**0.028**
10GP	0.33	0.010	0.56	0.002
20GP	0.12	0.002	0.16	0.005
30GP	0.05	0.001	0.09	0.005
10S	0.33	0.012	0.63	0.034
20S	0.21	0.013	0.50	0.014
30S	0.10	0.003	0.25	0.010
10SF	0.47	0.010	0.60	0.032
20SF	0.28	0.023	0.37	0.020
30SF	0.21	0.002	0.24	0.012
10S10GP	0.11	0.001	0.22	0.012
10SF10GP	0.12	0.002	0.26	0.003
10S20GP	0.10	0.010	0.20	0.029
10SF20GP	0.19	0.001	0.28	0.018
15S15GP	0.11	0.007	0.22	0.014
15SF15GP	0.16	0.004	0.25	0.012

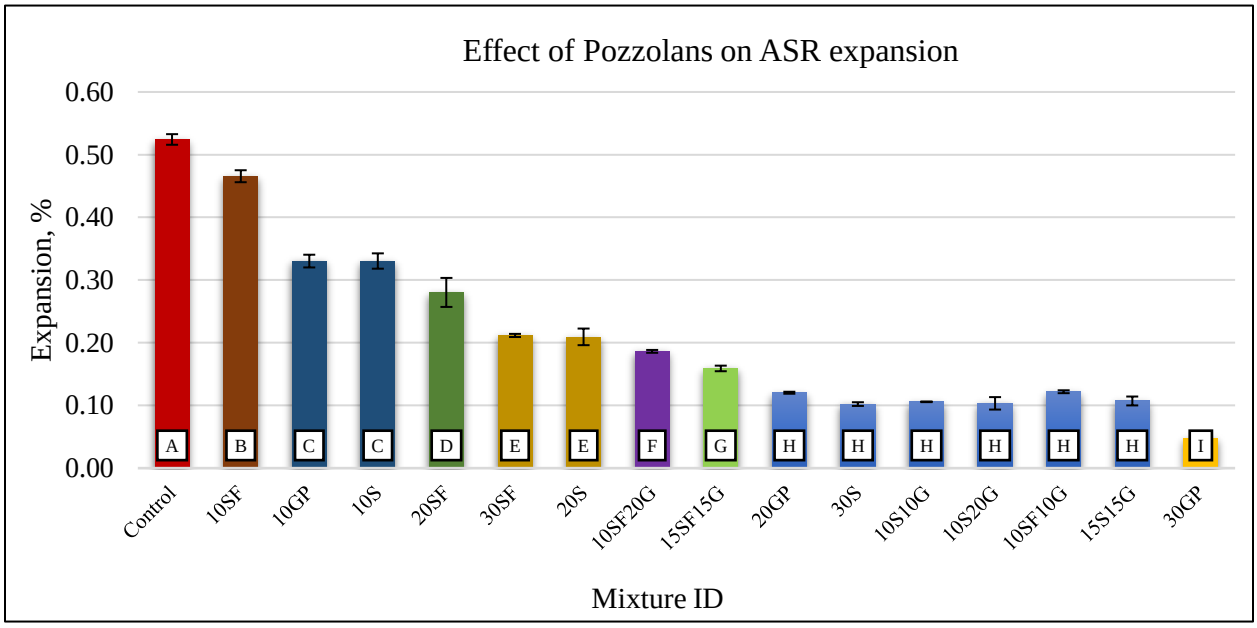

Figure 6.16: Mitigation data result for 16 mortal mixtures

6.4.3 Mitigating ASR using Additional Reactive Aggregates

This study examined the use of the best binary and ternary combinations (found to reduce ASR of Wn-56 aggregates) with two additional reactive aggregates (i.e., basalt rocks and manufactured sand). Basalt has an expansion rate of 0.39% while manufactured sand has a 0.23% expansion after 14-day using AMBT test methods. Figures 6.17 and 6.18 shows the results of ASR expansion for basalt and manufactured sand mortar bar samples. The results clearly showed that all binary and ternary mixtures at 20% or 30% replacement showed reduced ASR expansion compared to the control mixture and the expansion was below the expansion limit (i.e., 0.01%). Furthermore, a low expansion rate was observed past the 14-day testing period and up to 28 days of testing. Similar results were also obtained for the manufactured sand which is considered a moderately reactive aggregate compared to basalt. The average percentage reduction in ASR expansion was 0.18% and 0.35% after 14 days and 28 days, respectively (Figure 6.18).

Figure 6.19 shows the correlation between the expansion of Wn-56c and the other two aggregates (basalt and manufactured sand) using various binary and ternary combinations. The expansion was measured using the AMBT method after 14 days of testing. Strong correlation was found with R^2 of 0.933 and 886 for basalt and manufactured sand, respectively. Figure 6.20 shows the mitigation results for the control mixture and five different mixtures. These results show the effectiveness of binary and ternary combinations in ASR mitigation irrespective of the degree of aggregate reactivity.

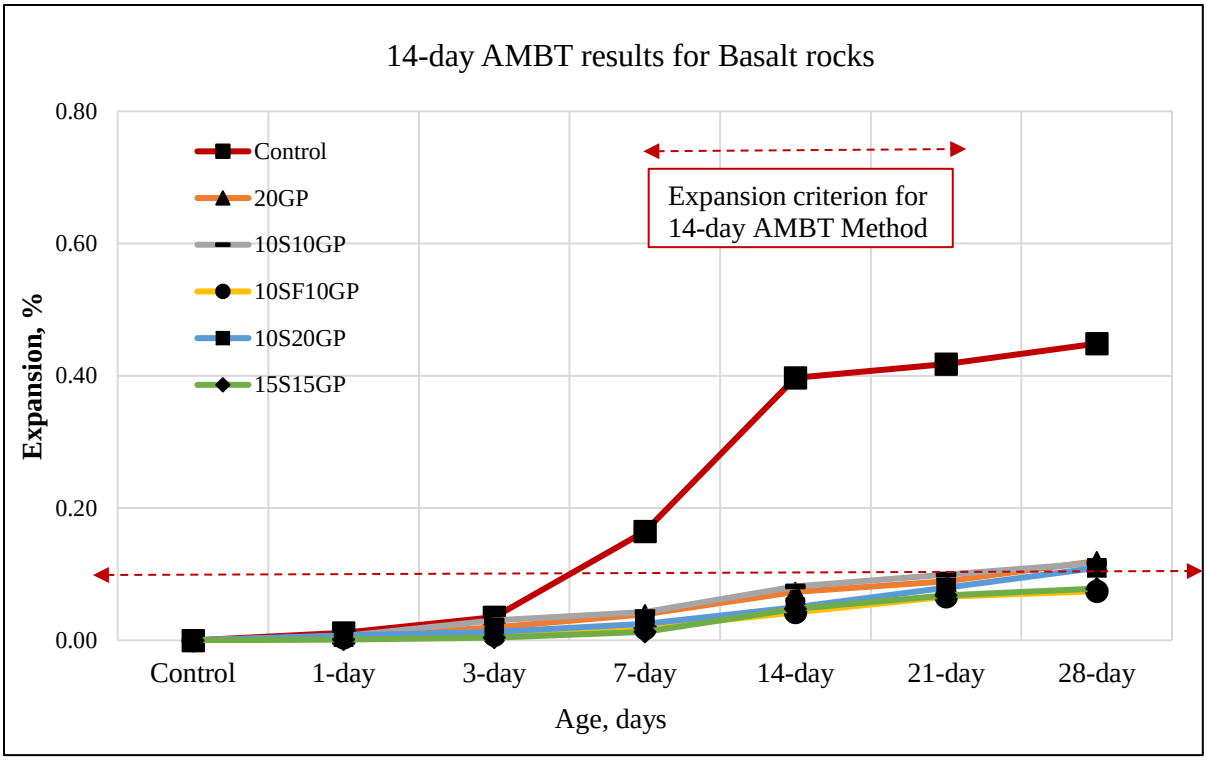

Figure 6.17: Mitigation behavior of mortar bars of basalt rock

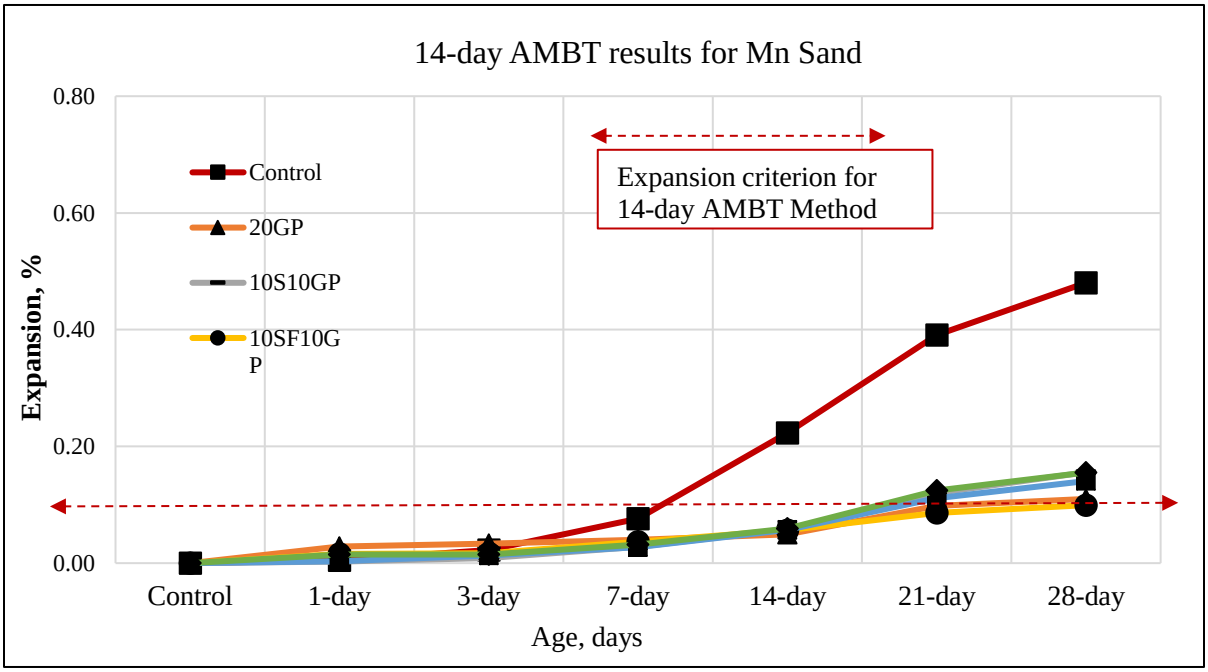

Figure 6.18: Mitigation behavior of mortar bars of manufactured sand

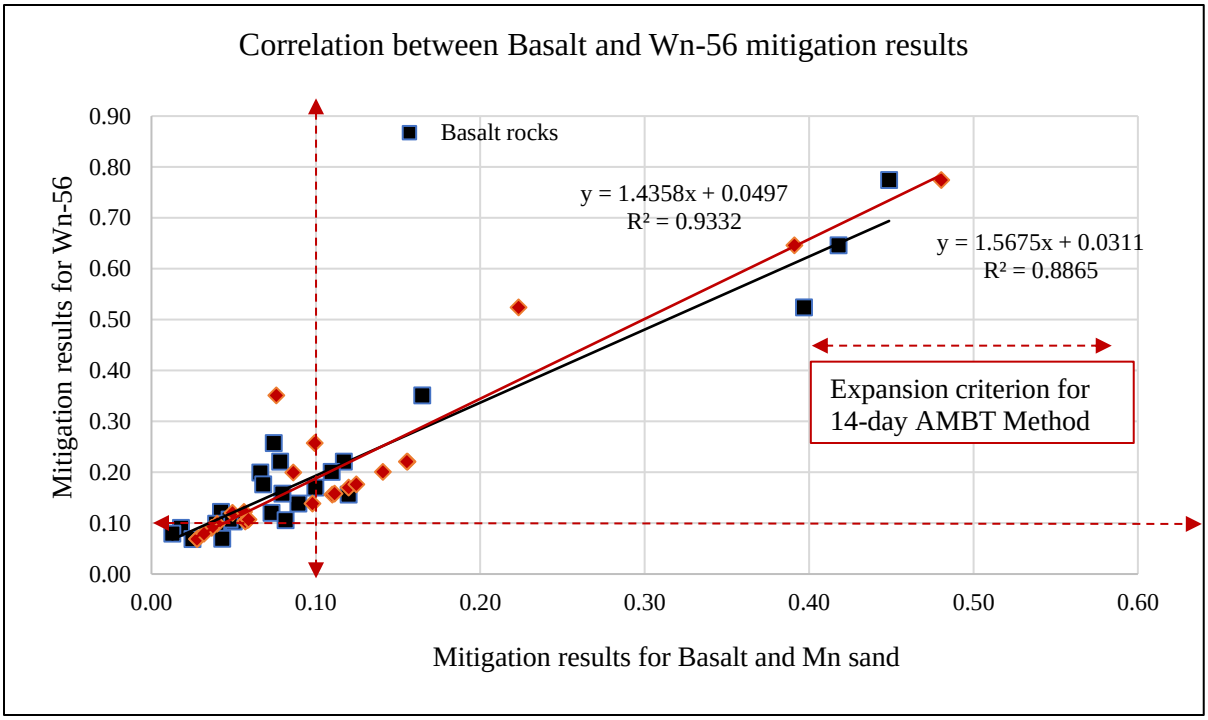

Figure 6.19: Correlation between Wn-56 with Ba and Mn sand aggregates

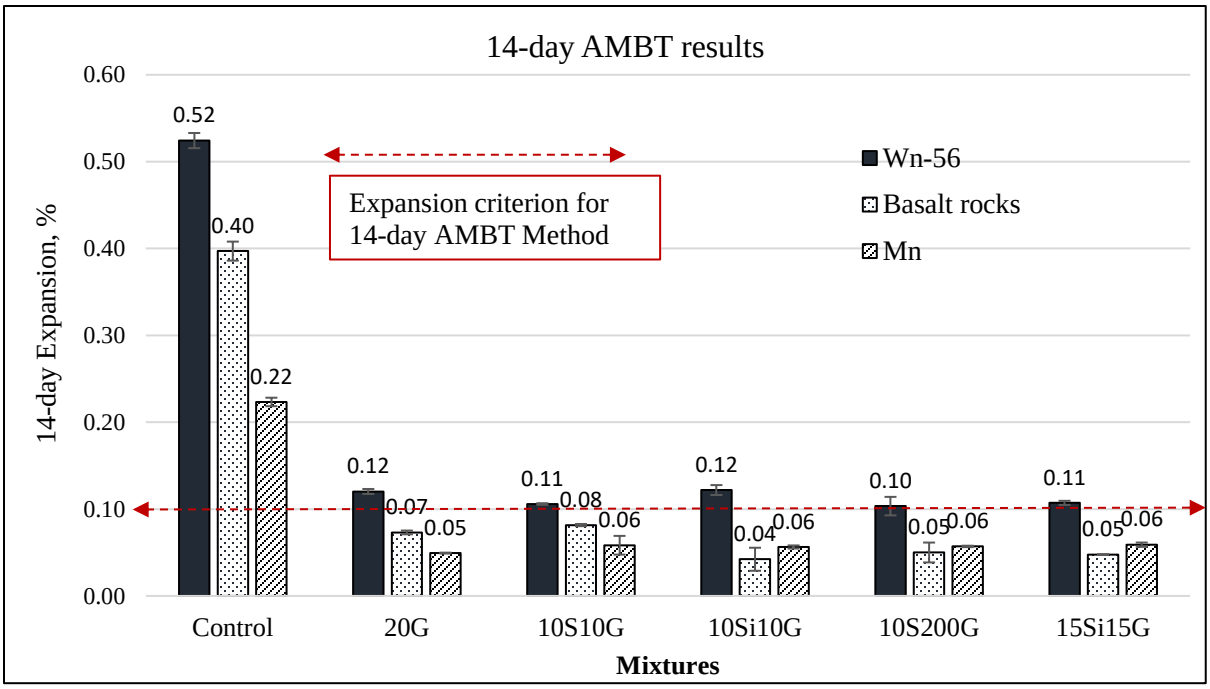

Figure 6.20: Mitigation result for reactive aggregates for control and various mixes

.4.4 ASR Mitigation using MCPT

Figure 6.21 shows the expansion results of selected concrete prisms at control (without any SCMs) and mixtures containing SCMs and glass powder measured using the MCPT method (i.e., AASHTO TP 110). MCPT expansion should be limited to 0.04% or below for nonreactive aggregates. This part of study was conducted to evaluate ASR expansion using the 56-day MCPT for various mixtures (Figure 6.21) and the results were compared to 14-AMBT test methods. The MCPT (56-day testing) expansion results were in good agreement with the 14-day AMBT results for each mixture. As shown in Figure 6.21 and 6.22, all test mixtures at 20% replacement or 30% replacement reduced the ASR expansion by about 75% to 83%. These results show that the effectiveness of different mitigation blends can be assessed using with either the 14-day AMBT or 56-day MCPT methods. Additionally, this the MCPT can be used to assess the ASR mitigation of both reactive fine and coarse aggregates. The AMBT can be used to assess only the fine portion of the aggregates. Similar to the correlation established between 14-day AMBT and 56-day MCPT (Figure 6.23), there was also a strong correlation ($R^2 = 0.99$) between AMBT and MCPT expansion results for the mitigation tests. These results showed clearly that 14-day AMBT can be used to assess various mitigation blends, which is advantageous since it takes less time compared to the 56-day MCPT method.

The Tukey HSD results indicated that all mixtures prepared with pozzolans were statistically different from the control mix. Test mixtures made with 20% glass powder were not statistically different from the test mixtures made with 10% silica fume and 10% glass powder or 10% slag and 10% glass powder (Figure 6.21). Similar to the AMBT mitigation results, mixtures with 30% replacement level performed better than mixtures with 20% replacement and they were statistically different from one another.

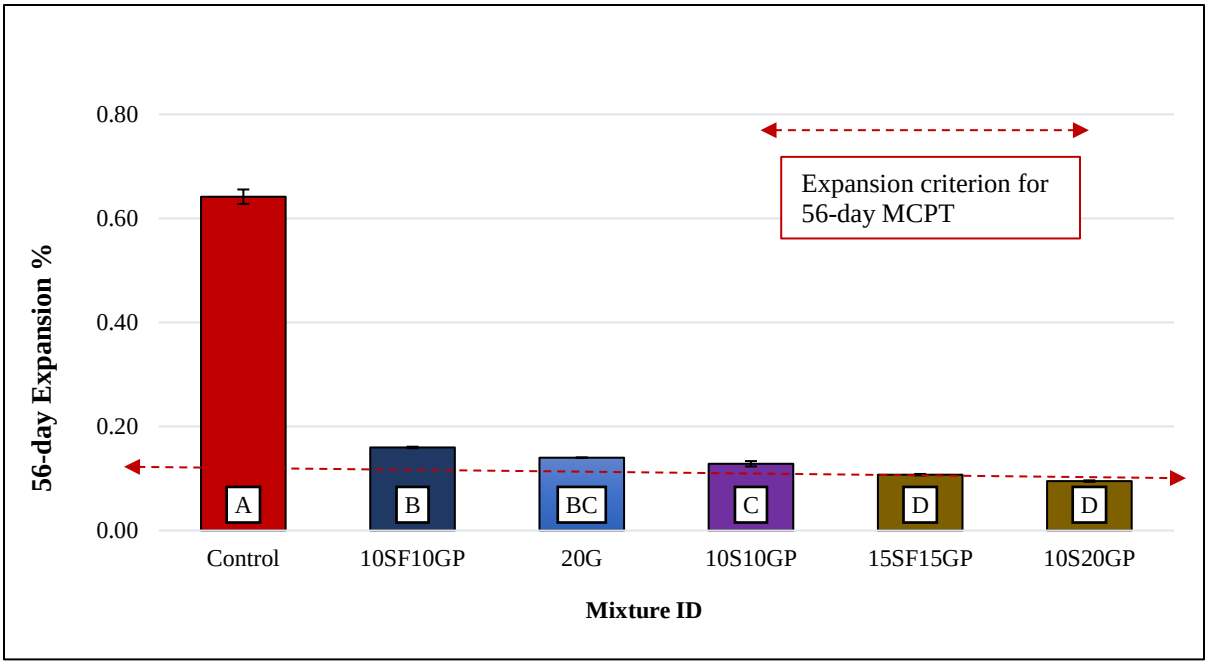

Figure 6.21: Mitigation results using MCPT method for control (Wn-56) and various mixes

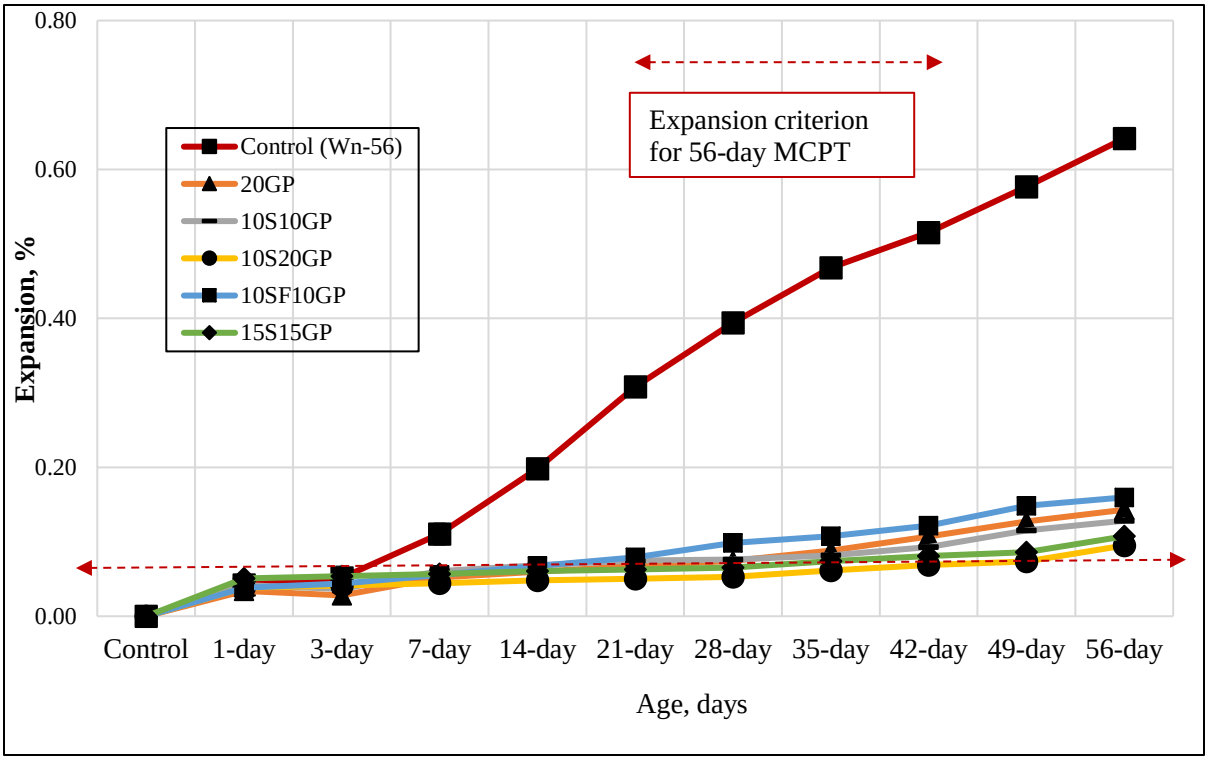

Figure 6.22: Mitigation behavior of concrete prisms using MCPT method

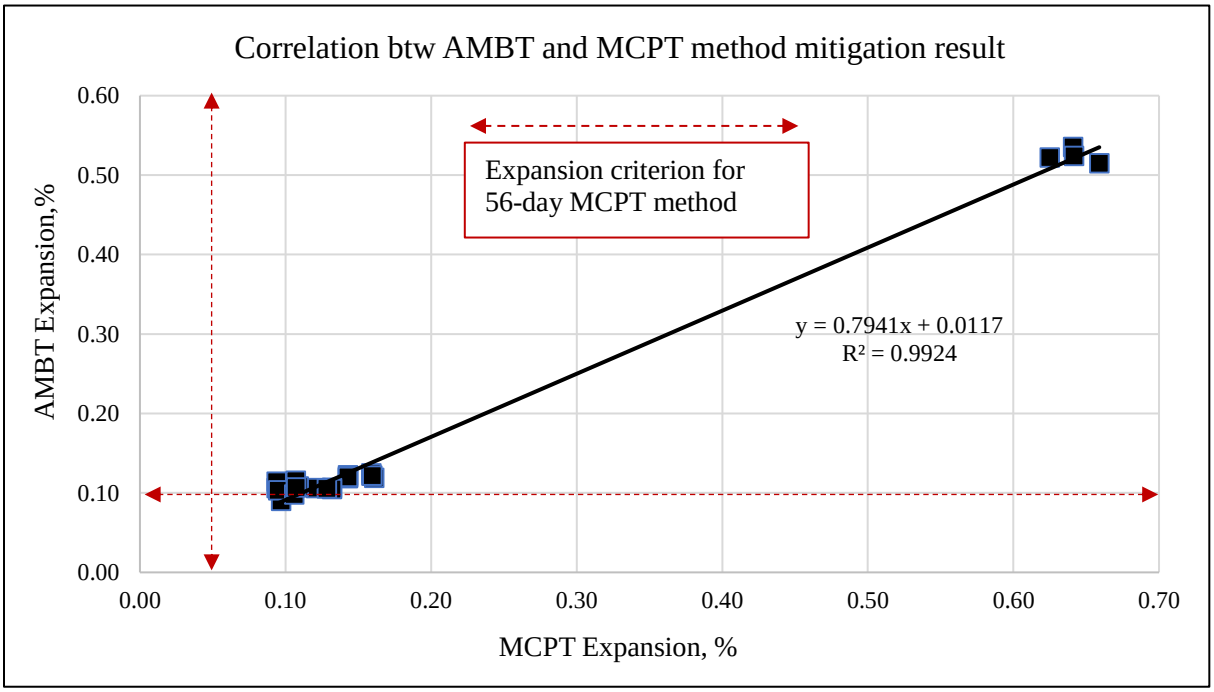

Figure 6.23: Correlation between 14-day AMBT and 56-day MCPT methods

CHAPTER SEVEN: MICROSTRUCTURAL ANALYSIS

7.1 Thermogravimetric Analysis (TGA)

The TGA was used in this study to examine the pozzolanic activity of binary and ternary blends of SCMs and glass powder. The weight loss corresponding with the calcium hydroxide decomposition (CH_{loss}) can be quantified to assess the pozzolanic activity. Such activity changes the concrete rate of reaction leading to improved properties including improved sulfate resistance, reduced chloride penetration, reduced freeze-thaw effects or acid resistance, improved strength and abrasion resistance (Sims and Massazza, 1998). Thus, pozzolanic reactivity of test samples conventional pozzolans (e.g., slag cement and silica fume) and waste glass powder was compared to the control mix prepared without SCMs after 14 and 28 days. Figure 7.1 shows a typical chart of weight loss during the TGA test. In this evaluation, the cement replacement was kept at 20% and 30% for both binary and ternary mixes to understand the effectiveness of cementitious materials on ASR mitigation. Table 5.7 provides the testing matrix for TGA and SEM testing.

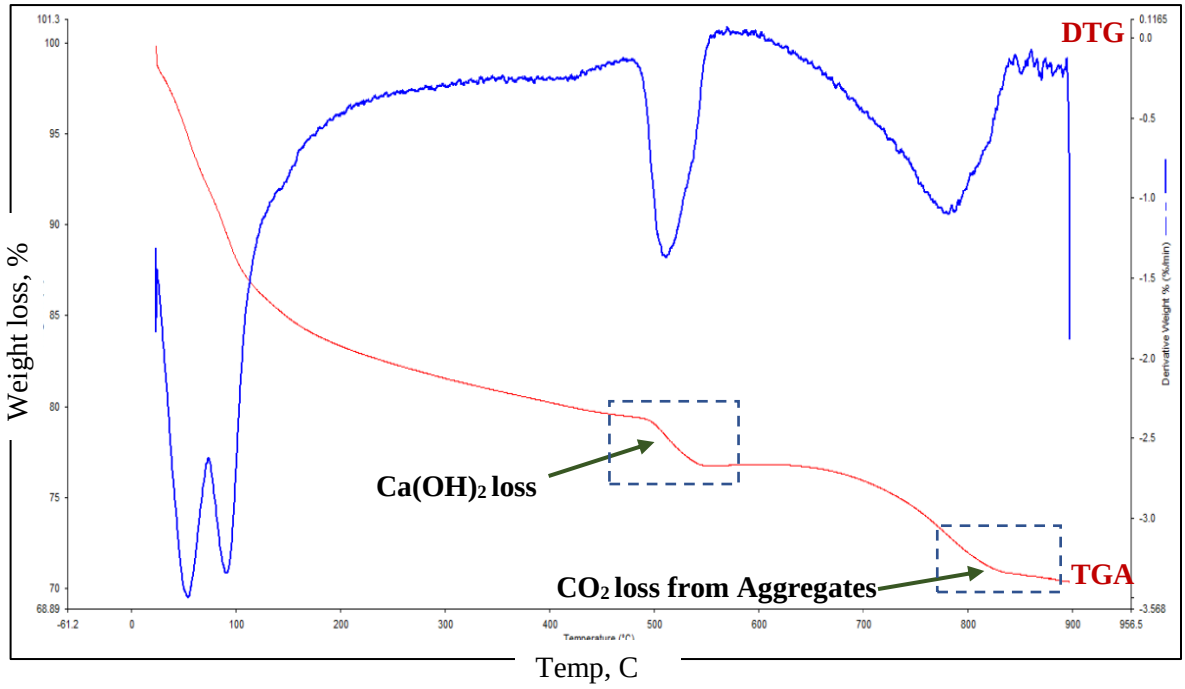

Figure 7.1: Change in percent weight with temperature using TGA

Figure 7.2 shows the plot of percentage weight loss with temperature from 440C to 520C for various test mixes. This chart illustrates the decomposition of calcium hydroxide content in the mix. As shown in Figure 7.2, the weight loss increased with the temperature. The control mixture had highest loss of 87% while the blend with 20% silica fume and 20% glass powder had the lowest loss (75%) at 440C. Ian and Brown (1998) indicated that mixtures with SCMs and waste glass (as tested in this study), provide low weight loss due to the contribution to hydration process which is consistent with the results of this study. The percent mass loss decreased with test temperature until 520C. Figure 7.3 shows calcium hydroxide content ($Ca(OH)_2$) (measured from 440C to 520C temperature) of cement paste after 14 days and 28 days for control mix and blends of 20% replacement. The CH_{loss} content as acquired from the TGA test is equivalent to the weight loss of hydrated cement paste. Appendix H includes the TGA analysis of all test specimens.

All test mixtures containing SCMs had lower calcium hydroxide content compared to the control mixture after 28 days, indicating that the use of SCM increases the pozzolanic activity in concrete unlike the base mix (Figure 7.3). Among all mixtures prepared with SCMs in this study, test mixtures containing silica fume (SF) (binary level) and silica fume with glass powder (ternary level) were found to have the lowest calcium hydroxide content. The use of silica fume increases the pozzolanic reaction more than the other SCMs at earlier stages. This high reactivity is due to the extreme fineness of the silica fume and the high amorphous silicon dioxide (SiO_2) content (Iqbal, 2007). Generally, calcium hydroxide content for mixtures with SCMs at 28 days were lower compared to 14 days, while it increased for the control mix (18% increase). These results are consistent with the SAI results presented in Figure 6.6. Test mixtures containing 20% glass powder reduced calcium hydroxide content by 35% while that of slag and silica fume reduced by 17% and 52%, respectively after 28 days. Better performance (in term of pozzolanic reactivity) was observed with mixtures containing glass powder compared to the ones with slag. The dilution effect of glass powder is the main source of the CH reduction according to Rashidian and Dezfoulia (2018).

All ternary mixtures followed similar trends to those of binary combinations at both 20% and 30% dosages.In which mixes containing SCM (at ternary level) having lower CH content

compare to control. The binary and ternary blends containing SCMs performed better in terms of the pozzolanic reactivity compared to the control mixture. This is consistent with reduction in ASR expansion as described in Section 6.3.1 and 6.3.2. Test mixtures with slag produce more calcium hydroxide content compared to other mixtures while test mixtures with silica fume produce lower calcium hydroxide content. These results are in good agreement with the strength measurements discussed in Section 6.3. Overall, the findings of this section agree with a study conducted by Afshinnia and Rangaraju (2015).

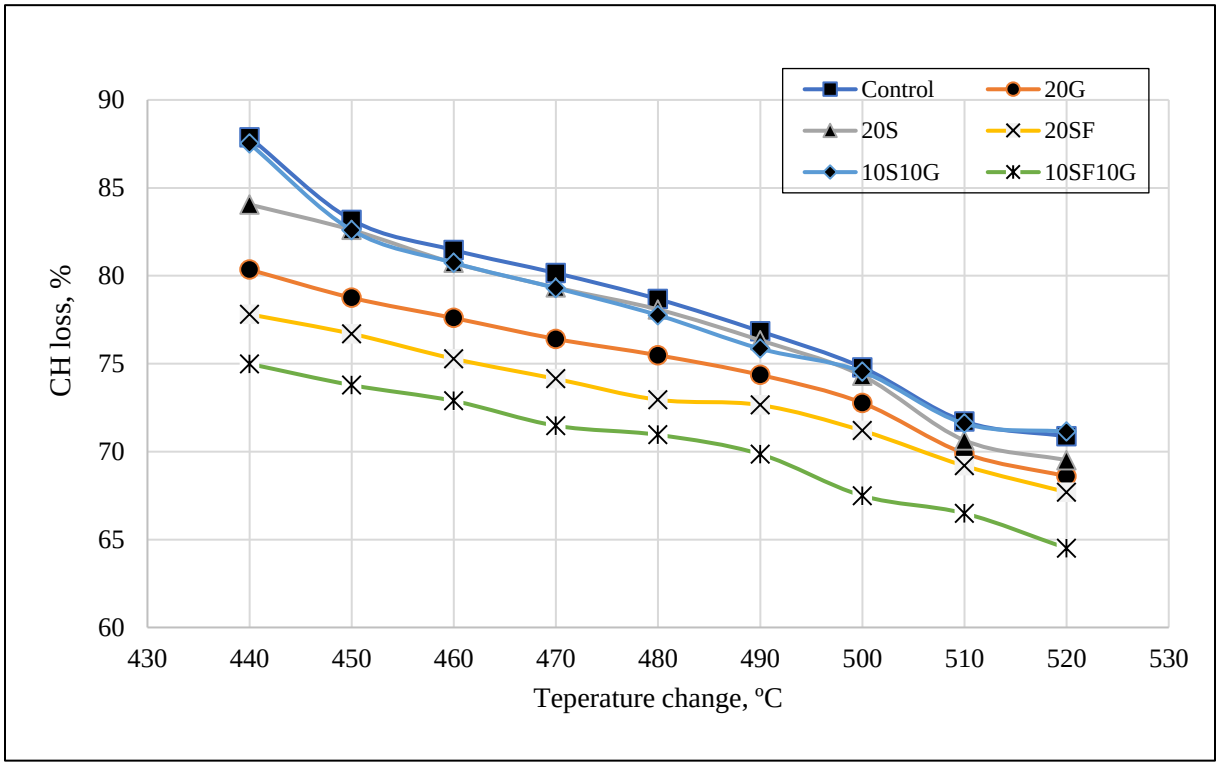

Figure 7.2: Percent weight loss with temperature for test mixtures

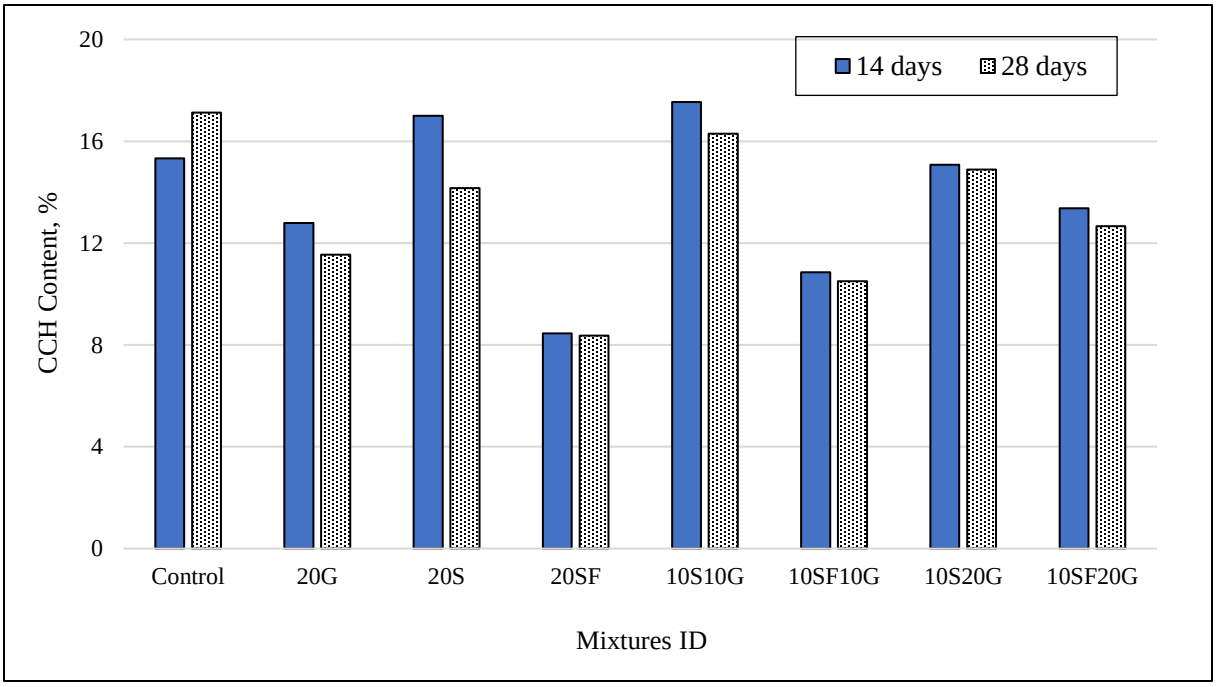

Figure 7.3: CH content (%) in specimens containing SCMs with or without glass at 14 and 28 days

7.2 Scanning Electrons Microscopy (SEM) and Energy Dispersive X-ray (EDX)

This study used SEM and EDX to study the surface microstructure and chemical composition of test samples prepared with SCMs and glass powder. The tests were conducted after 0, 14 and 28 days of curing. Figures 7.4 through 7.6 show the backscatter SEM images for (1) control mix, (2)10S10G mix that was found to adequately suppress ASR expansion, and (3) 30%GP which is prepared using 30% of glass powder replacement and was found to effectively mitigate ASR as discussed in Chapter 6. These AMBT mortar bars samples were scanned at zero, 14 and 28 days, soaked in 1N NaOH solution at 80C. Figure 7.4 shows the presence of cracks right after demolding (no curing yet). There was a presence of glass particles around the cement paste in mixtures containing glass. After 14 days of curing, there are cracks in the control mixtures (Figure 7.5a). As shown in Figure 7.5a, the ASR induced cracks appear on surface of the test section. These cracks are observed within the aggregate structures surrounded by ASR gel. This induced internal cracks within the aggregates could be associated to the presence of high percent of reactive silica content which opens up a path for alkaline pore solution coming from the cement and the NaOH solution. These results are

consistent with the expansion data obtained using the 14-day AMBT method (0.54%) which was above the threshold for even highly reactive aggregates.

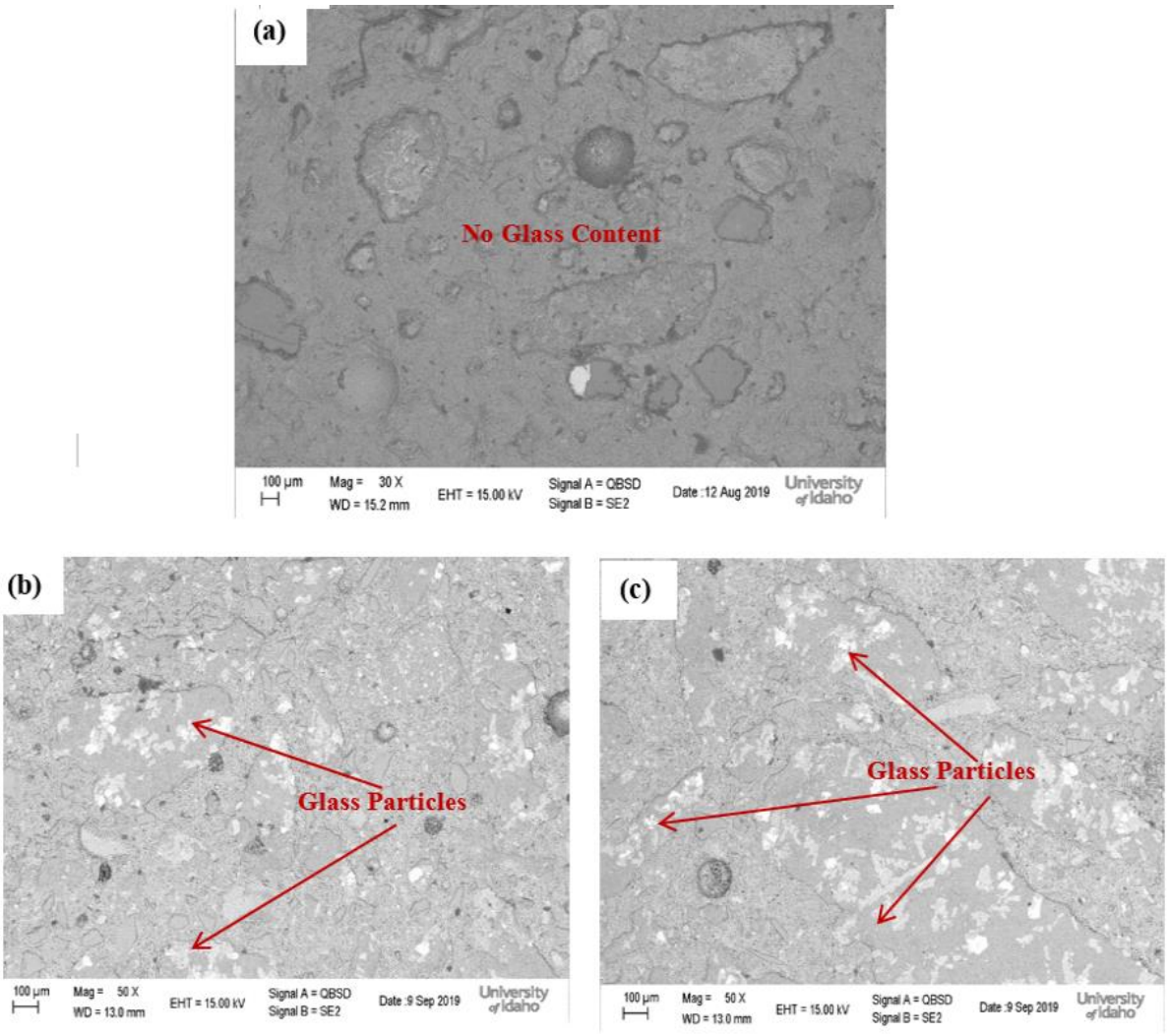

Figure 7.4: SEM images of mortar bar sections at initial stage (after casting) for a) control; b) 10S10G; and c) 30GP

The backscatter SEM images for the test samples after 14 days of curing are shown in Figure 7.5. Similar to the expansion data, small amount of cracks were observed in 30GP specimen (mixtures with 30% glass powder replacement) (Figure 7.5c). Meanwhile, the ternary blend of slag and glass powder showed some minor cracks around the surface (Figure 7.5b). At initial stages of chemical reaction, the mix containing slag cement displayed less pozzolanic activity causing high presence of alkalinity in pore solution hence leading to ASR gel. Likewise, the low viscosity made it possible to penetrate through pore structure without resulting in large expansive stresses (Afshinnia and Rangaraju, 2015). These results are

consistent with the 14 days AMBT measured expansion where mixtures containing 30% glass powder showed lower expansion values (0.04%) to that of 10% slag and 10% glass powder (0.10%) for the same reactive aggregates. In the control mixture, ASR gel-filled cracks were observed around aggregates; the sample made with slag and glass powder displayed minor cracks and little ASR gel (Figure 7.5).

Figure 7.6 shows the backscatter images after 28 days of curing. From this images, we can see that the rate of ASR expansion and induced cracks increased significantly especially for the control mix (containing no SCMs or glass powder). However, the mixes containing SCMs also show an increase in ASR induced cracks, but still less than the control mix. There was no formation of an ASR ring nor microcracks around aggregates particles of test specimens made with SCMs in contrast to the control mix without SCMs. The C-S-H gel of the control mix reacts rapidly with SiO2 resulting in ASR ring formation (Shuhua et al., 2015). Overall, the cracks increased with the increase of curing time. These results are in agreement with the expansion measurements as described in Table 6.3 where the control mix, 10S10G, and 30GP had an expansion of 0.77%, 0.28%, and 0.09% respectively, after 28 days. (Ranraraju et al., 2016) also obtained similar results.

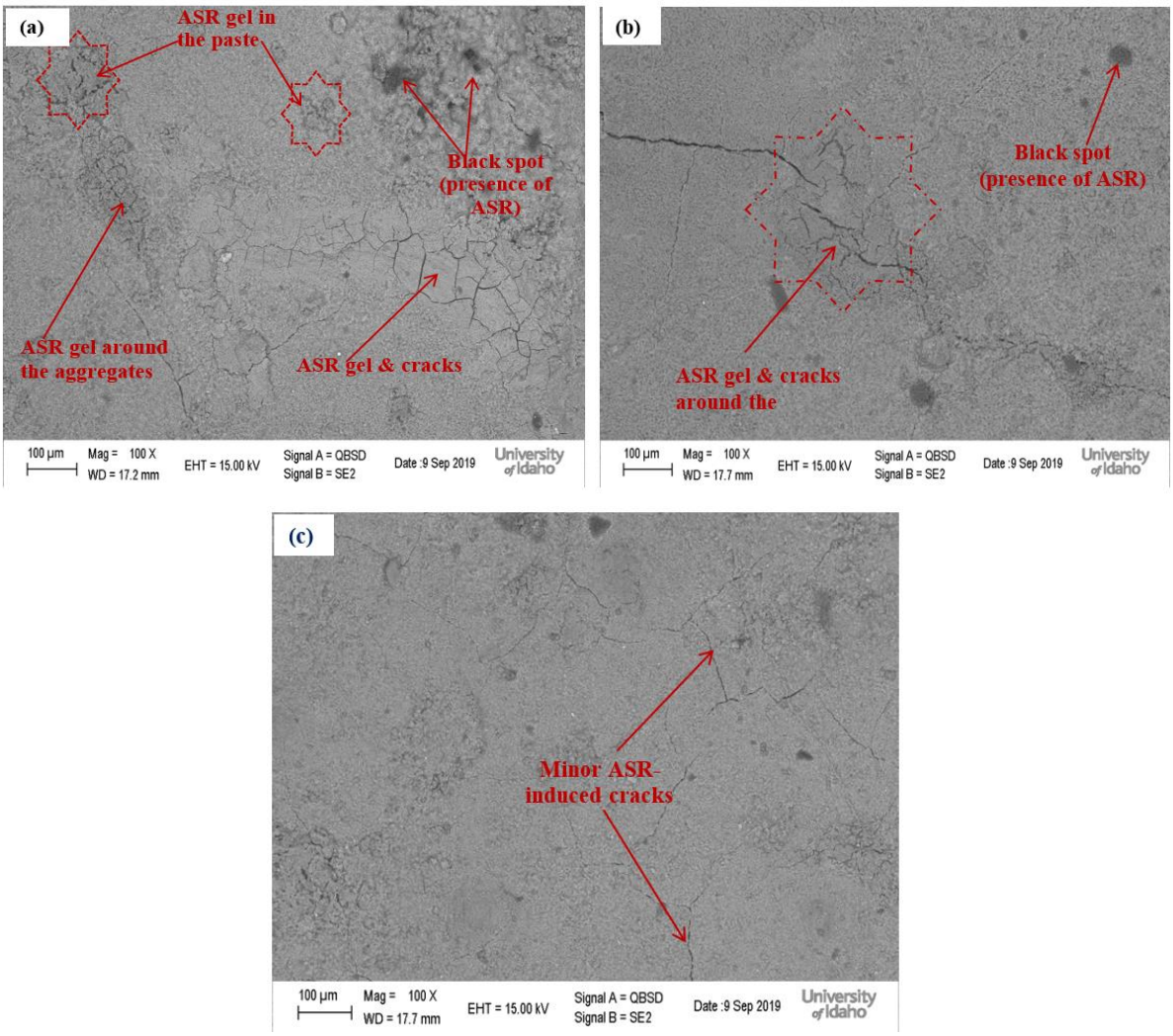

Figure 7.5: SEM images of mortar bar sections after 14 days for a) control; b) 10S10G, and c) 30GP

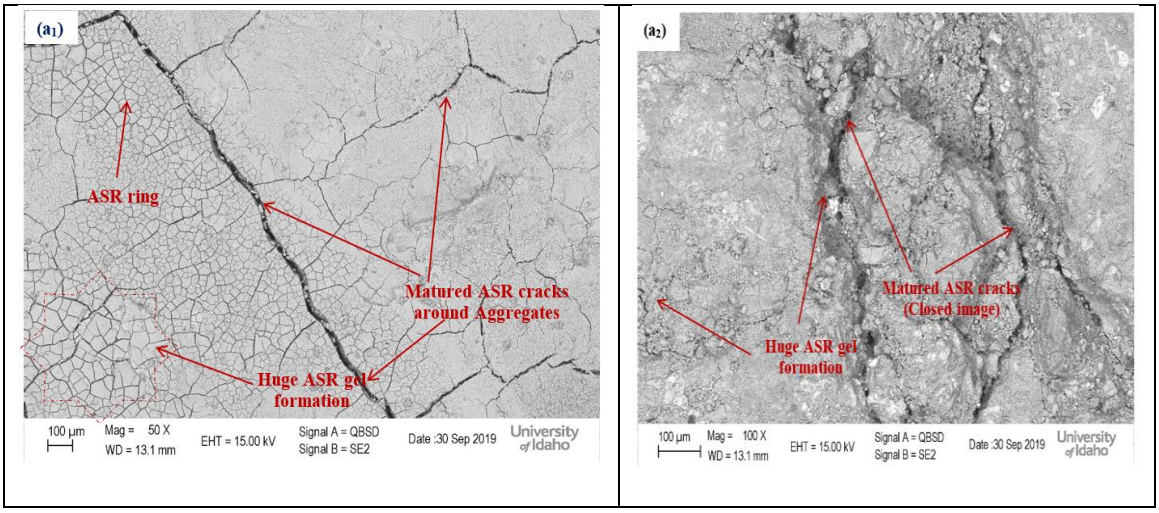
(a1)
ASR ring
Matured ASR cracks around Aggregates
Huge ASR gel formation
100 µm Mag = 50 X WD = 13.1 mm EHT = 15.00 kV Signal A = QBSD Signal B = SE2 Date :30 Sep 2019 University of Idaho
(a2)
Matured ASR cracks (Closed image)
Huge ASR gel formation
100 µm Mag = 100 X WD = 13.1 mm EHT = 15.00 kV Signal A = QBSD Signal B = SE2 Date :30 Sep 2019 University of Idaho

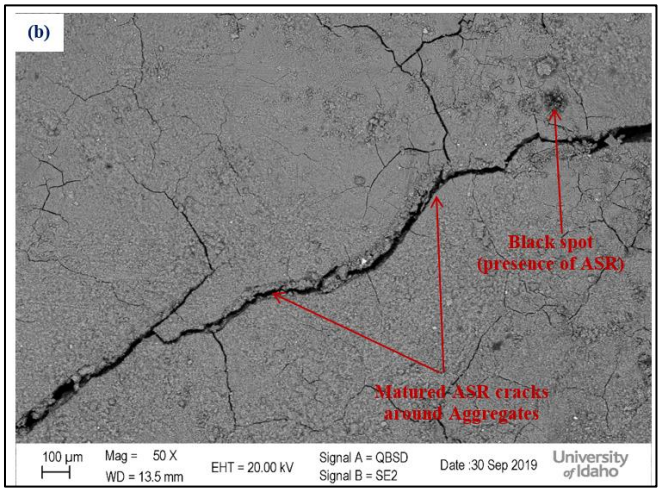
(b)
Black spot (presence of ASR)
Matured ASR cracks around Aggregates
100 µm Mag = 50 X WD = 13.5 mm EHT = 20.00 kV Signal A = QBSD Signal B = SE2 Date :30 Sep 2019 University of Idaho

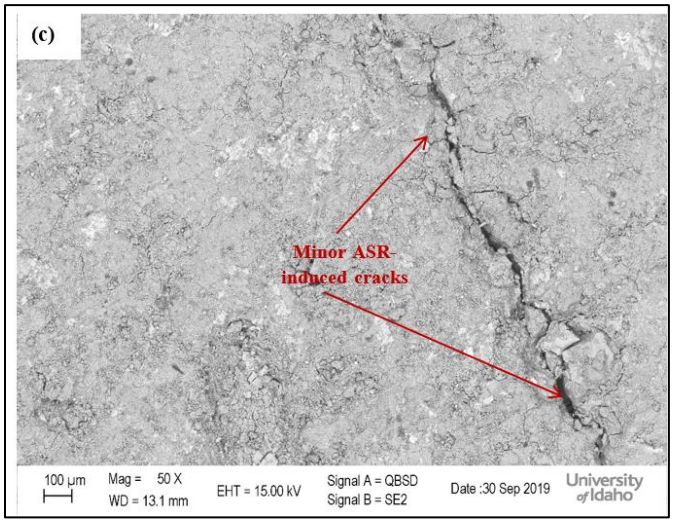
(c)
Minor ASR-induced cracks
100 µm Mag = 50 X WD = 13.1 mm EHT = 15.00 kV Signal A = QBSD Signal B = SE2 Date :30 Sep 2019 University of Idaho

Table 7.1 summarizes the EDX results for cement paste and ASR gel for the test samples. The chemical composition was analyzed at zero, 14, and 28 days of curing for cement paste. While the chemical composition of ASR gel was investigated after 14 and 28 days only since no gel occurs at initial age. From Table 7.1, there is a significant increase in sodium content from the 0 to 14 days for test mixtures. A rise from 4.4% to 21.6%, 4.9 % to 34.8%, and 3.5% to 30.9% was observed for control, 10S10G and 30G mix respectively just after 14 days. This rise is due to the curing process where the test samples were impressed in 1N NaOH solution after casting. However, the sodium content of mixtures containing SCMs was higher than of the control mix, despite the control mix had large cracks and higher porosity. Most of Na^+ present in the control mix is greatly utilized in the ASR pore solution, bonding with silica content from aggregates, hence producing higher expansion values (as seen in Figure 6.4). Likewise, a reduction in sodium content was observed after 14 days which is associated with further use of Na^+ in pore solution.

In contrast to Na^+ content, the potassium (K^+) content had an initial approximate value of 2.6% for all mixtures before curing. The percentage K^+ of the control mix is relatively lower than that of mixes made with SCMs as shown in Table 7.1. This rise of potassium content in paste made with SCMs is due to their binding capacity with hydration products (low Ca/Si ratio compared to the control mixture (Afshinnia and Rangaraju, 2015). Similarly, a high percentage of aluminum (Al^{3+}) was also recorded at before curing for both mixtures containing SCMs and control mixture (9%, 11.6%, and 11.7% for control, 10S10G and 30GP, respectively). The aluminum is utilized in the pozzolanic reaction which enhances the alkali bonding properties of cement paste through the production of Calcium Alumina-Silicate Hydrate (C-A-S-H gel). A higher percentage of aluminum content was recorded in the binary blend made with 30% glass powder resulting in low expansion. These results agree with the findings of Hong and Glasser (2002).

Table 7.1: Chemical Compositions of Cement Paste obtained from EDX

Location	Specimens	Age (days)	Average % Mass present					Average Mass Ratio		
			Na	Al	Si	K	Ca	Na/Si	Ca/Si	Na/K
CEMENT PASTE	CONTROL	0-day	4.9	9.0	43.3	2.2	40.4	0.11	0.93	2.23
		14-day	21.6	1.7	34.7	0.6	41.2	0.62	1.19	36.61
		28-day	18.8	1.9	35.2	0.9	43.2	0.53	1.23	19.85
	10S10G	0-day	4.4	11.6	47.3	2.6	34.1	0.09	0.72	1.72
		14-day	34.3	1.2	34.3	1.2	29.0	1.00	0.85	29.17
		28-day	21.4	2.5	34.9	1.2	40.1	0.61	1.15	17.75
	30G	0-day	3.5	11.7	40.0	2.6	42.2	0.09	1.06	1.32
		14-day	30.9	0.6	40.9	1.0	26.5	0.76	0.65	29.98
		28-day	17.3	6.0	36.6	2.6	37.6	0.47	1.03	6.64
ASR GEL	CONTROL	14-day	17.3	2.5	57.8	0.6	21.8	0.30	0.38	28.83
		28-day	13.7	2.4	60.1	0.8	23	0.23	0.38	17.13
	10S10G	14-day	15.7	1.5	59.8	0.7	22.3	0.26	0.37	22.43
		28-day	14.1	4.4	58.3	2.2	21	0.24	0.36	6.41
	30G	14-day	19.7	2.6	58.6	1.4	17.7	0.34	0.30	14.07
		28-day	18.6	5.5	54.2	2.6	19.1	0.34	0.35	7.15

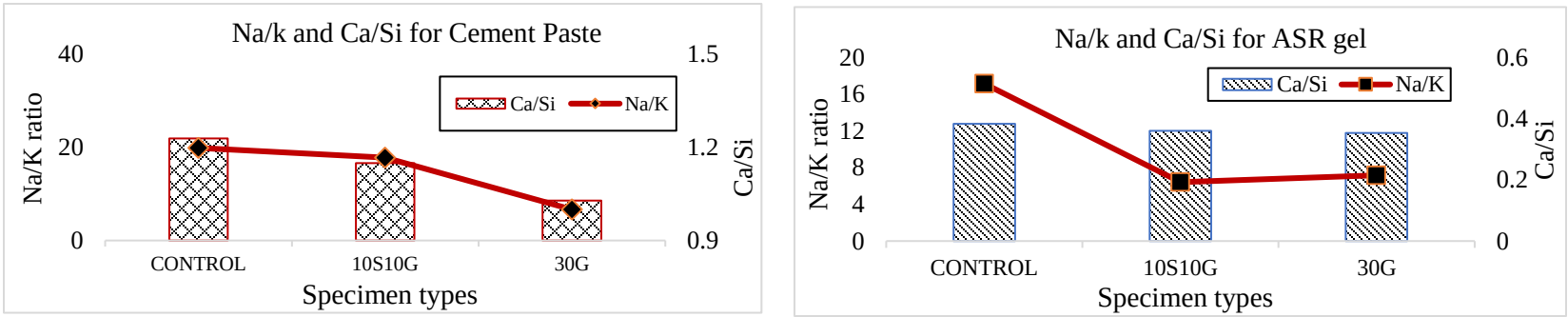

Figure 7.7: Chemical compositions a) Cement paste; b) ASR gel

Examining the chemical composition of the ASR gel, the sodium content of mixtures containing SCMs was also higher than of the control mix. In terms of curing age, mixes containing SCMs do not show significant differences after 14 or 28 days as compared to control mixture. Likewise, the potassium content for the ASR gel was similar to that of the cement paste results. Additionally, the control mix had higher Ca/Si ratio of C-S-H compared to the 30GP and 10S10G specimens as shown in Table 7.1. This C-S-H gel with low Ca/Si ratio attracts alkali and making the glass powder to react with $Ca(OH)_2$ leading to low ASR expansion (Shuhua et al., 2015).

The Na/K of the control mix was higher than the Na/K of mixes made with SCMs regardless of the location, whether in cement paste or ASR gel. These results produce good performance in potassium (alkali) bonding ability in samples made with SCMs compared to the control mix. However, for the sodium: silica (Na/Si) ratio result taking in both paste and ASR gel, there is no differences with samples made with or without SCMs (Figure 7.7). This inconsistency is due to the soaking solution which produces external sodium and the higher silica content in the aggregates tested. These results are consistent with of the findings by Afshinnia and Rangaraju (2015). In summary, the study of Ca/Si ratio in cement paste or ASR gel describes the pozzolanic activity in each mix while the examination of Na/K ratio indicates the source and level of alkali in the gel and the nature of its reaction.

CHAPTER EIGHT: CONCLUSIONS AND RECOMMENDATIONS

8.1 Findings and Conclusions

8.1.1 ASR Evaluation Using Various Test Methods

- Ten out of 11 aggregates tested were found reactive to ASR using the new MCPT method. Granite was the only nonreactive aggregate. Eight aggregates were found to be reactive using the 14-day AMBT method. Only three aggregates were nonreactive (e.g., granite, gabbro, and limestone).
- The expansion rate of MCPT method was highest between 7 to 21 days for fine aggregates. The average expansion rate for the reactive aggregates was 0.07% after 84 days, while non-reactive or moderately reactive aggregates had an expansion rate of 0.008%. Meanwhile, the coarse aggregates were found to have a slower expansion compared to the fine aggregates and the expansion of coarse aggregate was uniform over the testing period (84 days).
- The 14 day AMBT had an increased expansion rate over the testing period. Contrary to the ABMT and MCPT methods, an inconsistent expansion rate was recorded using CPT methods.
- Many of the test aggregates found to be reactive using the 14-day AMBT and CPT method were also found to be highly reactive using the new 56-day MCPT method. However, it is recommended to revise the MCPT expansion limit specified at 0.040% to account for slow reactive aggregates.
- The results of the new MCPT method (AASTHO TP 110) showed good correlation with both 14-day AMBT (ASTM 1260) and 1-year CPT (ASTM C 2393) expansion result with an R^2 value of 0.88 and 0.67, respectively. Furthermore, there was a good correlation between AMBT and CPT expansion results ($R^2 = 0.87$).
- The 6-month ACPT method showed similar results to the ones of the 1-year CPT method with high correlation between both methods ($R^2 = 0.94$). Hence, further research should be conducted to verify the correlation between the 6-month ACPT and the 1-year CPT method using additional aggregate sources.
- Pearson correlation analysis confirmed excellent correlation between the various test methods used in this study.

8.1.2 ASR Mitigation

- All mixtures containing pozzolans were found to suppress ASR. However, binary blends containing glass powder at 10%, 20%, and 30% cement replacement levels showed better performance compared to slag and silica fume at the corresponding replacement levels. Similarly, ternary mixtures containing slag and glass powder showed improved ASR mitigation compared to binary mixture with slag or ternary blend of silica fume and glass powder at corresponding replacement levels.
- Mixtures containing glass powder experienced much lower expansion after 14 days compared to the control mixture.
- The use of waste glass powder was found to reduce ASR expansion. This reduction is associated with the fineness of glass powder which enhances the pozzolanic activity.
- All binary blends containing glass powder or slag showed better flow behavior (workability) compared to silica fume. Among all the ternary blends containing glass powder, the combination of slag and glass powder showed the highest improvement in flowability compared to that of the other mixtures.
- The binary combinations at lower replacement percentages were able to achieve comparable strength to the control mixture. However, binary blends with greater percentages (e.g., higher than 20%) of silica fume and glass powder decreased the strength activity index. The ternary blend of slag and glass powder decreased the strength activity index but it was still above the 75% requirement. While ternary mixtures containing silica fume and glass powder decreased the strength activity index below the 75% requirement.
- The results showed that there was a solid relationship between concrete expansion due to ASR and strength. The higher the ASR expansion, the lower the strength over time.
- To validate the mitigation results using the AMBT method, the author also investigated using the new MCPT method. Similar to the correlation established between 14-day AMBT and 56-day MCPT (obtained in Section 4.4.1), there was also a strong correlation for the mitigation results of AMBT and MCPT ($R^2 = 0.99$). These results show that the 14-day test method can be adopted for evaluating various mitigation methods.

8.1.3 Microstructural Analysis

- The TGA results showed that binary and ternary mixtures containing SCMs performed better in term of the pozzolanic reactivity compared to control mixture. This is also consistent with reduction in ASR expansion data as described earlier in this study. Also, mixtures with slag produced higher CH content compared to other mixtures while the mixture with silica fume produced lower CH content. The addition of glass powder to other SCMs displayed little change in CH content.
- The microstructural examination of mixtures prepared with or without SCMs showed that the level of ASR-induce cracks and gel formation were consistent with the expansion results. Mixtures made with SCMs produced less cracks as compared to the control mix. Likewise, the chemical composition obtained from EDX supported these findings, where the level of alkalis (Na/K) utilized in ASR pore solution was higher in samples prepared without SCMs compared to mixtures with SCMs. Lastly, mixtures containing SCMs had low Ca/Si values resulting in low ASR expansion.

8.2 Recommendations

- Based on the number of aggregates tested and the correlation established, the new test method called AASTHO TP 110 (56-day MCPT) produced a similar result to both the ASTM C 1260 (14-day AMBT) method and the ASTM C1293 (1-year CPT) method. Therefore, Idaho should keep with the utilization of the 14-day test method for the classification of their aggregates. However, the expansion limit of 0.040% (very low) set to classify aggregates tested with MCPT method, should be modified as many aggregate considered to be low or moderately reactive with other method was seen to be highly reactive with this method.
- The use of SCM and waste glass powder mitigates ASR, producing a durable concrete. However, due to consideration of other properties of concrete, replacement up to 20% of Slag, GP or SF (either at binary or ternary) can be adopted for ASR Mitigation to any reactive aggregate. Replacement of these pozzolans up to 30% and beyond could be detrimental to other properties of concrete. The visual confirmation from microstructural examination back the expansion data gotten from the AMBT (mortar bar tests).

- Based on the results, the waste glass powder can be utilized as a potential replacement for cement which significantly reduced the ASR and solving the problem on being waste, dumbed into landfill causing an environmental problem.

8.3 Future Research

- This study examined 11 aggregates from different sources using the 14-day AMBT and 56-day MCPT methods, while six aggregates were evaluated using the 1-year CPT and 6-month ACPT methods. Therefore, a wide range aggregates should be considered and tested to validate the correlation between various test methods used in this study.
- The results of ASR mitigation showed a strong potential for reducing ASR using SCMs and glass powder, additional SCMs should be used along with waste glass at both binary and ternary levels to further validate the results of this study.

REFERENCE

AASTHO TP 110 (2014). Standard Method of Test for Potential Alkali Reactivity of Aggregates And Effectiveness of ASR Mitigation Measures (Miniature Concrete Prism Test, MCPT). American Association of State Highway and Transportation Officials, Washington, D.C.

ACI Committee 221 (1998). State-of-the-Art Report on Alkali-silca Reaction (ASR). ACI221.1R-98, American Concrete Institute, Farmington Hills, MI.

ACI 211-2, 2002. Standard practice for selecting proportions for structural lightweight concrete. American Concrete Institute, Farmington Hills, MI, USA.

ACI committee 234, (2012). Guide for the Use of Silica Fume in Concrete. American Concrete Institute, Farmington Hills, MI, USA.

Afshinnia K, Rangaraju P.R., (2015). Influence of fineness of ground recycled glass on mitigation Of alkali–silica reaction in mortars, Constr. Build. Mater. 81 257–267.

ASTM C 1260, (2008) Standard Method of Test for Accelerated Detection of Potentially Deleterious Expansion of Mortar Bars Due to AlkaliSilica Reaction, American Association Of State Highway and Transportation Officials, Washington, D.C.

ASTM C 1293, (2012) Standard Test Method for Determination of Length Change of Concrete Due to Alkali-Silica Reaction, American Society for Testing and Materials, West Conshohocken, PA, Annual Book of ASTM Standards (04.02): Concrete and Aggregates.

ASTM C (138) 2001. Standard test method for density (unit weight), yield, and air content (Gravimetric) of concrete. Annual Book of ASTM Standards, vol. 04.02.

AASTM C 1437(2001). Standard test method for flow of hydraulic cement mortar. Annual Book Of ASTM Standards, vol. 04.01.

ASTM C 192, (2002) Making and curing concrete test specimens in the Laboratory. Annual Book of ASTM Standards, vol. 04.02.

ASTM C295 (2003). Standard Practice for Petrographic Examination of Hardened Concrete, ASTM International, ASTM C856-02, Annual Book of ASTM Standards, Section Four, Vol. 04.02 Concrete and Aggregates, 434-450.

ASTM C311, (2013). Standard Test Methods for Sampling and Testing Fly Ash or Natural Pozzolans for use in Portland-Cement Concrete, ASTM Int'l, West Conshohocken, PA.

ASTM C 33, 2002. Standard specification for concrete aggregates. Annual Book of ASTM Standards, vol. 04.02.ASTM C 150, 2002. Standard specification for Portland cement. Annual Book of ASTM Standards, vol. 04.01.

ASTM C 39 (2003). Standard Test Method for Compressive Strength of Cylindrical Concrete Specimens. Annual Book of ASTM Standards, vol. 04.02.

ASTM C490/C 490M (2017). Standard Practice for Use of Apparatus for the determination of Length Change of Hardened cement Paste, Mortar and Concrete, ASTM International, ASTM C490-07, Annual Book of ASTM Standards, West Conshohocken, PA.

ASTM, C618, (2012). Standard Specification for Coal Fly Ash and Raw or Calcined Natural Pozzolan for Use in Concrete, ASTM International, West Conshohocken, PA, 2012.

Abo-ElEnein S., M. Daimon, S. Ohsawa, R. Kondo (1974). Hydration of low porosity slag-lime Pastes. Cem. Concr. Res., 4 pp. 299-312.

Aquino W., D.A. Lange, J. Olek, (2001). The influence of meta-kaolin and silica fume on the Chemistry of alkali–silica reaction products, Cem. Concr. Compos. 23 (6) 485–493.

Bach, F.; Thorsen, T.S.; Nielsen, M. P. Load-carrying capacity of structural members subjected to Alkali-silica reactions. Construct. Building Mater. 1993, 7(2), 109-115.

Bagheri A.R., H. Zanganeh, M.M. Moalemi, (2012). Mechanical and durability properties of Ternary concretes containing silica fume and low reactivity blast furnace slag. Cem. Concr. Compos. 34 (5) 663–670.

Baronio, B.; Montanaro, K.; Delmastro, B. (1987) Couplage d'action de certains parametres Physiques Sur le development de la reaction akxdis-granulate, Material Science to Construction Materials Engineering, 1st Int. Conf Versailles Vol. 3.

Bazant Z.P., A. Steffens, (2000). Mathematical model for kinetics of alkali–silica reaction in Concrete, Cem. Concr. Res. 30 (3) 419–428.

Beglarigale A., Yazici H., (2014) Mitigation of the Detrimental Effects of ASR in Cement Based Composites by Combination of Steel Micro-fibers and Ground granulated Blast-furnace Slag, J. Mater. Civ. Eng. 26 (12).

Berodier E., K. Scrivener, (2014). Understanding the filler effect on the nucleation and growth of C-S-H, J. Am. Ceram. Soc. 97 (12) 3764–3773.

Berube, M.A., and Fournier, B., (1993). "Canadian Experience with Testing for Alkali-Aggregate Reactivity in Concrete." Cement and Concrete Composites, Vol. 15, No. 1, pp. 27-47.

Bérubé, M. A., J. Duchesne, J.F. Dorion, and M. Rivest (2002). "Laboratory assessment of alkali contribution by aggregates to concrete and application to concrete structures affected by alkali– silica reactivity." Cem. Concr. Res., 32, p. 1215–1227.

Bleszynski, R.F. and Thomas, M.D.A. (1998). "Micro structural Studies of Alkali-Silica Reaction In Fly Ash Concrete Immersed in Alkaline Solutions." Advanced Cement Based Materials.

Boddy A.M., R.D. Hooton, M.D.A. Thomas, (2003). The effect of the silica content of silica fume On its ability to control alkali–silica reaction, Cem. Concr. Res. 33 (8) 1263–1268.

British Cement Association (BCA). (1992) "The Diagnosis of Alkali-Silica Reaction – Report of a Working Party." Wexham Springs, Slough, U.K. SL3 6PL, 44 p.

Broekmans, M.A.T.M. (2002). 'The alkali–silica reaction: mineralogical and geochemical aspects of some Dutch concretes and Norwegian mylonites.' PhD. Thesis, in, University of Utrecht, p.144.

C. Shi, R.L. Day (2000). Pozzolanic reaction in the presence of chemical activators: Part I. Reaction kinetic. Cem. Concr. Res., 30 (1) , pp. 51-58.

C. Shi, Z. Shi, X. Hu, R. Zhao, L. Chong, (2015) A review on alkali-aggregate reactions in Alkali-activated mortars/concretes made with alkali-reactive aggregates, Mater. Struct. 48 (3) 621–628.

Coats, A. W.; Redfern, J. P. (1963). Thermogravimetric Analysis A Review. Chemistry Department, Battersea College of Technology, London, S. W. 11 Vol. 88 (1053).

Danay,A., (1994) “Structural Mechanics Methodology in Diagnosing and Assessing Long-Term Effects of ASR in Reinforced Concrete Structures,” ACI Materials Journal, American Concrete Institute, Farmington Hills, Michigan, January–February, pages 54 to 62.

David S (1991). “The Handbook for the identification of ASR in Highway Structures. Construction Technology laboratory”, Inc, Skoke, Illonois.

De Schutter, G. (1999), Hydration and temperature development of concrete made with blast-Furnace slag Cem. Concr. Res., 29 (1) pp. 143-149.

DeGrosbois, M., Fontaine, E., (2000) Performance of the 60 °C-accelerated concrete prism test for the evaluation of potential alkali-reactivity of concrete aggregates, 11th International Conference on Alkali-Aggregate Reaction in Concrete, M.A. Bérubé, B. Fournier, B. Durand(Eds.), Québec City, QC, Canada, 277-286.

Dent-Glasser, L.S. and Kataoka, N. (1981b.). “The chemistry of alkali-aggregate reactions.” Cement and Concrete Research, 11: 1-9.

Diamond, S., (1981). "A Review of Alkali-Silica and Expansion Mechanisms: 2. Reactive Aggregate." Cement Concrete. Res., Vol. 6, No. 4, p. 549-560.

Diamond, S. (1992-2006). "Alkali aggregate reactions in concrete. “, Strategic Highway Research Program, National Research Council, Washington, DC.

Diamond, S. Alkali aggregate reactions in concrete: an annotated bibliography 1931-1991, Strategic Highway Research Program, National Research Council, Washington, DC, 1992.

Dron R., F. Brivot, (1993) Thermodynamic and kinetic approach to the alkali-silica reaction, Part 2: experiment, Cem. Concr. Res. 23 (1) 93–103.

Duyou Lu, Benoit Fournier, P. E. Grattan-Bellew ,Zhongzi Xu , Mingshu Tang (2008) Development of a universal accelerated test for alkali-silica and alkali-carbonate reactivity of concrete aggregates. Materials and Structures 41:235–246.

European Commission, (2010). Environmental Statistics and Accounts in Europe, Eurostat Statistical Books.

F.P. Glasser, (1992). Chemistry of the alkali aggregate reaction, in: R.N. Swamy (Ed.), The Alkali-Silica Reaction in Concrete, Blackie, Glasgow and London, and Van Nostrand-Reinhold, New York, pp. 30–53.

Farny, J. A.; Kosmatka, S. H. (1997) Diagnosis and control of alkali-aggregate reactions in Concrete, Concrete Information Series, No. IS413.01T, Portland cement Association. Skokie, IL, USA.

Farny, J. and Kerkhoff, B., (2007). "Diagnosis and Control of Alkali-Aggregate Reactions in Concrete." IS413, Portland Cement Association, Skokie, Illinois, USA, 26 pages.

Federal Highway Administration (2011). Alkali-Silica Reactivity – Selection, Implementation and Evaluation of Field Application and Demonstration Projects. Washington, DC: Federal Highway Administration. http://www.fhwa.dot.gov/pavement/concrete/asrfield.cfm

Fernández-Jiménez A., I. Garcia-Lodeiro, A. Palomo, (2007) Durability of alkaliactivated fly ash Cementitious materials, J. Mater. Sci. 42 (9) 3055– 3065.

Fertig Ryan, Angela Jones, Margaret Kimble, Darby Hacker, Saadet Toker, Jennifer Eisenhauer Tanner, (2013) Evaluation of ASR Potential in Wyoming Aggregates. WYDOT Research Center Wyoming Department of Transportation Cheyenne, WY 82009-3340

Figg,J. (1987)"ASR inside Phenomena and Outside Effects (Crack Origin and Pattern)," Concrete Alkali-Aggregate Reactions, Park Ridge, New Jersey, pages 152 to 156.

Folliard, K. J.; Ideker, J.; Thomas, M. D. A.; Fournier, B. (2005) Assessing aggregate reactivity Using the accelerated concrete prism test. Draft Report-Prepared for ICAR.

Folliard, K.J., Barborak, R., Drimalas, T., Du, L., Garber, S., Ideker, J., Ley, T., Williams, S., Juenger, M., Thomas, M.D.A., and Fournier, B., (2006). "Preventing ASR/DEF in New Concrete: Final Report," The University of Texas at Austin, Center for Transportation Research (CTR), CTR 4085-5.

Fournier, B.; Bilodeau, A.; Malhotra, V. M. (1994). "Effectiveness of high-volume fly concrete in controlling expansion due to Alkali-Silica Reaction." pp.721-756.

Fournier, B., Chevrier, R., DeGrosbois, M., Lisella, R., Folliard, K.J., Ideker, J., Shehatad, M., Thomas, M.D.A., Baxter, S., (2004) The accelerated concrete prism test (60 °C): variability of the test method and proposed expansion limits, 12th International Conference on Alkali-Aggregate Reaction in Concrete, Beijing, China, 314-323.

Frias M., J. Cabrera (2001). Influence of MK on the reaction kinetics in MK/lime and MK-blended Cement systems at 20 degree C. Cem. Concr. Res., 31 (4) pp. 519-527.

G. Villain, M. Thiery, G. Platret, (2007) Measurement methods of carbonation profiles in Concrete: thermogravimetry, chemical analysis and gammadensimetry, Cem. Concr. Res. 37 (8) (2007) 1182–1192.

Garcia-Diaz, E., D. Bulteel, Y. Monnin, P. Degrugilliers, and P. Fasseu (2010). ASR pessimum Behavior of siliceous limestone aggregates. Cem. Concr. Res., v 40, n 4, p. 546-549.

Gesog˘lu M., E. Güneyisi, E. Özbay, (2009). Properties of self-compacting concretes made with Binary, ternary, and quaternary cementitious blends of fly ash, blast furnace slag, and silica fume, Constr. Build. Mater. 23 (5) 1847– 1854.

Godart B., M. de Rooij, J.G.M. Wood, (2013). Guide to Diagnosis and Appraisal of AAR Damage to Concrete in Structures, Part 1 Diagnosis (AAR 6.1), RILEM State-ofthe-Art Reports, 12.

Grattan-Bellew, P. E.; Mitchell. (2002). Preventing concrete deterioration due to alkali-aggregate reaction, Institute for Research in Construction (IRC), Natural Research Council of Canada, Construction Technology Update No. 52.

Gruver M., In Cheyenne, glass pile shows recycling challenges (2009), Associated Press, Available: < http://www.komonews.com/news/business/62338547.html >, Retrieved on April 2014.

H. Du, K.H. Tan, (2013). Use of waste glass as sand in mortar. Part II. Alkali–silica reaction and Mitigation methods, Cement and Concrete Composites, 35 118–126.

Hamed Maraghechi, Seyed-Mohammad-Hadi Shafaatian, Gregor Fischer, and Farshad Rajabipour, (2012) “The role of residual cracks on alkali silica reactivity of recycled glass aggregates” Cement & Concrete Composites 34 41–47.

Han, S. and M. Tang. (1999) Alkali-aggregate reaction under high temperature, high pressure and high alkali content. Journal of Nanjing Institute of Chemical Technology, 2, p. 1–10.

Hassan Rashidian-Dezfouli1 and Prasada Rao Rangaraju, (2018). Evaluation of Selected Durability Properties of Portland cement Concretes Containing Ground Glass Fiber as a Pozzolan Transportation Research Record, Vol. 2672(27) 88–98.

Hester D., McNally C., Richardson M., (2005). A study of the influence of slag alkali level on the Alkali–silica reactivity of slag concrete, Constr. Build. Mater. 19 (9) 661–665.

Hobbs, W. D (1988). Alkali-silica reaction in concrete, Thomas Telford, London.

Hobbs, D.W. and W.A. Gutteridge. (1979), Particle size of aggregate and its influence upon the expansion caused by the alkali-silica reaction. Magazine of Concrete Research, 31 (109), p. 235– 242.

Hooton, R.D., (1991) New Aggregate Alkali-Reactivity Test Methods, Ontario Ministry of Transportation,

Sims Ian, F. Massazza, (1998). Lea's Chemistry of Cement and Concrete (Fourth Edition).

Ichikawa T., M. Miura, (2007). Modified model of alkali-silica reaction, Cem. Concr. Res. 37 (9) 1291–1297.

Ideker, J., East, B., Folliard, K.J., Thomas, M.D.A., Fournier, B., (2010) The current state of the Accelerated concrete prism test, Cement and Concrete Research, 40(4), 550-555.

Idir, R., M. Cyr, and A. Tagnit-Hamou. (2010). Use of Fine Glass as ASR Inhibitor in Glass Aggregate Mortars. Construction and Building Materials, Vol. 24, No. 7, pp. 1309–1312.

Iqbal Khan M. (2007) "Waste and Supplementary Cementitious Materials in Concrete; Characterization, Properties and Application" Woodhead publishing series in Civil and Structural Engineering.

Islam, M.S. (2010). Performance of Nevada's aggregates in alkali-aggregate reactivity of Portland cement concrete. Doctoral Dissertation, University of Nevada, Las Vegas, NV.

Jin, W. (1998) Alkali-Silica Reaction in Concrete with Glass Aggregate - a Chemo-Physico-Mechanical Approach. Ph.D. Dissertation, Columbia University, New York, NY.

Kaveh Afshinnia, Prasada Rangaraju (2015) "Efficiency of ternary blends containing fine glass Powder in mitigating alkali–silica reaction", Construction and Building Materials 100 234–24.

Kaveh Afshinnia and Prasada Rao Rangaraju (2015) "Mitigating Alkali–Silica Reaction in Concrete Effectiveness of Ground Glass Powder from Recycled Glass." Transportation Research Record: Journal of the Transportation Research Board, No. 2508, Transportation Research Board, Washington, D.C., 2015, pp. 65–72.

Khatib, J. M., E. M. Negim, H. S. Sohl, and N. Chileshe. (2012). Glass Powder Utilization in Concrete Production. European Journal of Applied Sciences, Vol. 4, No. 4, pp. 173–176.

Kuroda, T., S. Inoue, A. Yoshino, and S. Nishibayashi. (2004), Effects of particle size, grading and content of reactive aggregate on ASR expansion of mortars subjected to autoclave method, in: M. Tang, M. Deng (Eds.), 12th International Conference on Alkali-Aggregate Reaction in Concrete, International Academic Publishers, Beijing, China, p. 736–743.

Lane D.S., C. Ozyildirim, (1999). Preventive measures for alkali–silica reactions (binary and Ternary systems), Cem. Concr. Res. 29 (8) 1281–1288.

Langan, B.W, Wang, M.A. (2002). Ward Effects of silica fume and fly ash on heat of hydration Of Portland cement Cem. Concr. Res., 32 (7) pp. 1045-1051

Latifee E. R., Sunjida Akther and Karibul Hasnat A, (2015) "Critical Review of the Test Methods for Evaluating the ASR Potential of Aggregates Proceedings of 10th Global Engineering, Science and Technology Conference 2-3, BIAM Foundation, Dhaka, Bangladesh, ISBN: 978-1-922069-69-6.

Latifee E. R and Prasada Rao Rangaraju (2014) Miniature Concrete Prism Test: Rapid Test Method for Evaluating Alkali-Silica Reactivity of Aggregates Journal of Materials in Civil Engineering, 27(7): 04014215

Lee, G., T. C. Ling, Y. L. Wong, and C. S. Poon. (2011). Effects of Crushed Glass Cullet Sizes, Casting Methods and Pozzolanic Materials on ASR of Concrete Blocks. Construction and Building Materials, Vol. 25, No. 5, pp. 2611–2618.

Leger, P.; Cote, P.; Tinawi, R. (1996) “Finite element analysis of concrete swelling due to alkali-Aggregate Reactions in dams.” Computer Structure, 60(4), 601-611.

Liu, S.H.; Xie, G.S.; Wang, S. (2015) Effect of curing temperature on hydration properties of Waste glass powder in cement-based materials. J. Therm. Anal. Calorim. 119, 47–55.

Lu, D., Fournier, B., Grattan-Bellew, P.E., Xu, Z., Tang, M., (2008) Development of a universal Accelerated test for alkali-silica and alkali-carbonate reactivity of concrete aggregates, Materials and Structures, 41(2), 235-246.

M. Saito, M. Shukuya, (1996) Energy and material use in the production of insulating glass Windows, Solar Energy 58 247–252.

Malvar, J.; Lenke, L.R. (2006) Efficiency of fly ash in mitigating alkali-silica reaction based on

Chemical composition, Mater. J., 103(5), 319-326. [59] Mukhopadhyay, A. K.; Zollinger, D. G.; Shon,

Maraghechi, H., S. M. H. Shafaatian, G. Fischer, and F. Rajabipour. (2012). the Role of Residual Cracks on Alkali Silica Reactivity of Recycled Glass Aggregates. Cement and Concrete Composites, Vol. 34, No. 1, pp. 41–47.

Marsh B.K, R.L. (1988). Day Pozzolanic and cementitious reactions of fly ash in blended cement Pastes Cem. Concr. Res., 18 (2) pp. 301-310

Materials evaluation and engineering (MEE), inc (2014). A description of Techniques of Scanning Electron Microscopy (SEM), SEM Failure Analysis and SEM Material Analysis” Handbook of Analytical Methods for Materials Plymouth, MN, USA

Maraghechi H., G. Fischer, F. Rajabipour, (2012) “The role of residual cracks on alkali silica Reactivity of recycled glass aggregates, Cem. Concr. Compos. 34 (1) 41–47.

Mather, Katharine and Mather, Bryant, (1950) “Method of Petrographic Examination of Aggregates for Concrete,” Proceedings, ASTM, ASTEA, Vol. 50, pp. 1288-1312.

Mirzahosseini, M.R.; Riding, K.A. (2015). Influence of different particle sizes on reactivity of Finely ground glass as new supplementary cementitious material (SCM). Ceme. Concr. Compos. 56, 95–105.

Moisson, M., M. Cyr, E. Ringot, and A. Carles-Gibergues. (2004), Efficiency of reactive aggregate powder in controlling the expansion of concrete affected by alkali–silica reaction (ASR), in: M. Tang, M. Deng (Eds.), 12th International Conference on Alkali-Aggregate Reaction in Concrete, International Academic Publishers, Beijing, China, p. 617–624.

Monteiro, P. J. M.; Shomglin, K.(2001);, Wenk, H. R.; Hasparyk, N. P. Effect of Aggregate Deformation on the Alkali-Silica Reaction. Mater. J.; 179-183.

Moser R.D., A.R. Jayapalan, V.Y. Garas, K.E. Kurtis, (2010). Assessment of binary and ternary Blends of meta-kaolin and Class C fly ash for alkali–silica reaction mitigation in concrete, Cem. Concr. Res. 40 (12) 1664–1672.

Mostafa N.Y., S.A. El-Hemaly, E.I. Al-Wakeel, S.A. El-Korashy, P.W. Brown (2001). Characterization and evaluation of the pozzolanic activity of Egyptian industrial by-products: I. Silica fume and dealuminated kaolin Cem. Concr. Res., 31 (3) pp. 467-474.

Naik, T. R. (2008) "Sustainability of concrete Construction." ASCE J. [13(2), 1084.

Nassar R., Soroushian P., (2012) Strength and durability of recycled aggregate concrete containing Milled Glass as partial replacement for cement, Construction and Building Materials 29 368–377.

Neithalath, N., and N. Schwarz. (2009). Properties of Cast-In-Place Concrete and Precast Concrete Blocks Incorporating Waste Glass Powder. Open Construction and Building Technology Journal, Vol. 3, pp. 42–51

Nixon, P.; Sims, I. (1996) Testing aggregates for alkali-reactivity, Report of ILEM TC-106: alkali-aggregate reaction-accelerated tests. Mater. Struct. 29, 323-334.

Oberholster, R. E., and Davies, G., (1986) "An Accelerated Method for Testing the Potential Alkali Reactivity of Siliceous Aggregate." Cement Concrete Research, Vol. 16.

Pane I., W. Hansen (2005), Investigation of blended cement hydration by isothermal calorimetry And thermal analysis, Cem. Concr. Res. 35 (6) 1155–1164.

Park C., M. Noh, T. Park (2005) "Rheological properties of cementitious materials containing Mineral admixtures" Cem. Concr. Res., 35 (5), pp. 842-849.

Park, S. B., B. C. Lee, and J. H. Kim. (2004) Studies on Mechanical Properties of Concrete Containing Waste Glass Aggregate. Cement and Concrete Research, Vol. 34, No. 12, pp. 2181–2189.

Pedneault, A. (1996) Development of testing and analytical procedures for the evaluation of the residual potential of reaction, expansion and deterioration of concrete affected by ASR, M.Sc. Memoir, Laval University, Québec City, Canada.

Pettersson K., (1992). Effects of silica fume on alkali–silica expansion in mortar specimens, Cem. Concr. Res. 22 (1) 15–22.

Poole, A.B. (1992) Alkali-silica reactivity mechanisms of gel formation and expansion. Proceedings of the 9th ICAAR, In: Concr. Soc. Publ. CS104 1 (editor): London, England

Poon C.S., S.C. Kou, L. Lam (2006) 'Compressive strength, chloride diffusivity and pore structure Of high performance metakaolin and silica fume concrete', Construction and Building Materials, Volume 20, Issue 10, December 2006, Pages 858-865.

Q. Yu, K. Sawayama, S. Sugita, M. Shoya, Y. Isojima (1999). Reaction between rice husk ash and $Ca(OH)_2$ solution and the nature of its product Cem. Concr. Res., 29 (1) pp. 37-43

Radlinski M., J. Olek, (2012). Investigation into the synergistic effects in ternary cementitious Systems containing Portland cement, fly ash and silica fume, Cem. Concr. Compos. 34 (4) 451–459.

Rajabipour F, Maraghechi H, Fischer G. (2010). Investigating the alkali silica reaction of recycled Glass aggregates in concrete materials. ASCE J Mater Civ Eng 22(12):1201–8.

Ramamurthy, K., Nambiar, E.K.K., Ranjani, G.I.S. (2009). A classification of studies on properties Of foam concrete. Cement Concr. Compos. 31 (6), 388–396

Ranc, R., Debray, L., (1992) Reference test methods and a performance criterion for concrete Structures, Proceedings of the 9th International Conference on Alkali-Aggregate Reaction in Concrete (ICAAR), London, 110-116.

Rangaraju P.R, H. Rashidian-Dezfouli, G. Nameni and G. Q. Amekuedi (2016) Properties and Performance of Ground Glass Fiber as a Pozzolan in Portland cement, 2016 International Concrete Sustainability Conference.

Rivard, P., Bérubé, M.A., Ollivier, J.P., (2007) Decrease of pore solution alkalinity in concrete Tested for alkali-silica reaction, Materials and Structures, 40, 909-921.

Rivard, P., Bérubé, M.A., Ollivier, J.P., Ballivy, G., (2003) Alkali mass balance during the Accelerated concrete prism test for alkali aggregate reactivity, Cement and Concrete Research, 33, 1147-1153.

Ruth M., Dell'Anno P., (1997). An industrial ecology of the US glass industry, Resources Policy 23 109–124.

S. Kandasamy, M.H. Shehata, (2014). The capacity of ternary blends containing slag and high-Calcium fly ash to mitigate alkali silica reaction, Cem. Concr. Compos. 49 92–99.

Saccani, A., and M. C. Bignozzi. (2010). ASR Expansion Behavior of Recycled Glass Fine Aggregates in Concrete. Cement and Concrete Research, Vol. 40, No. 4, pp. 531–536.

Salwocki, Stephen Bray (2016) Novel Performance Tests for Evaluation of Alkali-silica Reaction. S Thesis, Pennsylvania State University.

Schmitz A., Kami_nski J., Scalet B, Maria, Soria A., (2011). Energy consumption and CO2 Emissions of the European glass industry, Energy Policy 39 142–155.

Schwarz, N., H. Cam, and N. Neithalath. (2008). Influence of a Fine Glass Powder on the Durability Characteristics of Concrete and Its Comparison to Fly Ash. Cement and Concrete Composites, Vol. 30, No. 6, pp. 486–496.

Shayan, A., A. Xu, H. Morris. (2008) Comparative study of the concrete prism test (CPT 60°C, 100% RH) and other accelerated tests, in: M.A.T.M. Broekmans, B.J. Wigum (Eds.), 13th International Conference on Alkali–Aggregate Reactions in Concrete, Trondheim, Norway, p. 391–400.

Shayan A., A. Xu, (2004) Value-added utilization of waste glass in concrete, Cem. Concr. Res. 34 (1) 81–89.

Shayan, A.; Xu, A.M. (2006). Performance of glass powder as a pozzolanic material in concrete: A field trial on concrete slabs. Cem. Concr. Res., 36, 457–468.

Shekarchi M., A. Bonakdar, M. Bakhshi, A. Mirdamadi, B. Mobasher, (2010). Transport Properties in meta-kaolin blended concrete, Constr. Build. Mater. 24 (11) 2217–2223.

Sekar, D., N. Ganesan, and D. Nampoothiri. (2011). Studies on Strength Characteristics on Utilization of Waste Materials as Coarse Aggregate in Concrete. International Journal of Engineering Science and Technology, Vol. 3, No. 7.

Serpa, D., A. S. Silva, J. de Brito, J. Pontes, and D. Soares. (2013). ASR of Mortars Containing Glass. Construction and Building Materials, Vol. 47, pp. 489–495.

Shao, Y., T. Lefort, S. Moras, and D. Rodriguez. (2000) Studies on concrete containing ground Waste glass. Cem. Concr. Res., 30 (1), p. 91–100.

Shayan A., (2002). Value-added utilization of waste glass in concrete, IABSE Symposium, Melbourne, pp. 1–11.

Shehata M.H., Thomas M.D. (2000). The effect of fly ash composition on the expansion of concrete due to alkali–silica reaction, Cem. Concr. Res. 30 (7) 1063–1072.

Shi, C., Y. Wu, C. Riefler, and H. Wang. (2005). Characteristics and Pozzolanic Reactivity of Glass Powders. Cement and Concrete Research, Vol. 35, No. 5, pp. 987–993

Stanton, T.E., (1941). "Expansion of Concrete through Reaction between Cement andAggregate." Proceedings of the American Society of Civil Engineers, v. 66, no. 10, p. 1781-1811.

Stark, D. and Depuy, G. “Alkali-Silica Reaction in Five Dams in Southwestern United States.” Proceedings of the Katherine and Bryant Mather International Conference on Concret Durability, Atlanta, Georgia (USA), ACI SP-100, 1759-1786, April 1987

Stark, D. (1991). “Handbook for the Identification of Alkali-Silica Reactivity in Highway Structures.” SHRP-C/FR-91-101, TRB National Research Council, 49p. 1991.

State U., (2012) Environmental Protection Agency report.

Stewart, M.G.; Wang, X.; Nguyen, M.; Syme, M.; Leitch, A. (2010). "Analysis of Climate Change Impacts on the Deterioration of Concrete Infrastructure" – Part 1: Mechanisms, Practices, Modelling and Simulations – A review. CSIRO, Canberra.

Swamy R.N. (2002), the Alkali-Silica Reaction in Concrete, CRC Press.

T.K. Erdem, Ö. Kırca, (2008). Use of binary and ternary blends in high strength concrete, Constr. Build. Mater. 22 (7) 1477–1483.

Taha B., Nounu G., (2008). Properties of concrete contains mixed colour waste recycled glass as Sand and cement replacement, Construction and Building Materials 22 713–720.

Tatematsu, H. and T. Sasaki. (1989). "Proposal of a New Index for a Modified Chemical Method." Proceedings, 8th International Conference on Alkali-Aggregate Reaction in Concrete, Kyoto, Japan, p. 333-338.

Thaulow N., U.H. Jakobsen, B. Clark, (1996) Composition of alkali silica gel and ettringite in Concrete railroad ties: SEM-EDX and X-ray diffraction analyses, Cem. Concr. Res. 26 (2) 309–318.

Thomas, M.D.A., Fournier, B., Folliard, K.J., Ideker, J.H., Shehata, M., (2006) Test methods for Evaluating preventative measures for controlling expansion due to alkali-silica reaction in concrete, Cement and Concrete Research, 36, 1842-1856.

Thomas, M. D. A.; Fournier, B.; Folliard, K.; Ideker, J.; Resendez, Y. (2007). The use of lithium to prevent or mitigate alkali-silica reaction in concrete pavements and structures. Publication no. FHWA-HRT-06-133. The Transtec Group Inc. Austin, TX.

Thomas, M. D. A., B. Fournier, and K. J. Folliard. (2008). "Selecting Measures to Deleterious Alkali-Silica Reaction in Concrete." Rationale for the AASHTO P65 Prescriptive Approach. Washington DC: Office of Pavement Technology, Federal Highway Administration.

Thomas, M.D.A.; Fournier, B.; and Folliard, K. J., (2012). "Report on Determining the Reactivity of Concrete Aggregates and Selecting Appropriate Measures for Preventing Deleterious Expansion in New Concrete Construction." FHWA-HIF-09-001, Federal Highway Administration, Washington, D.C., April 2008, 28 pages.

Touma, W. E.; Fowler, D. W.; Carrasquillo, R. L. (2001) Alkali-silica reaction in Portland cement Concrete: testing methods alternatives. International Center for Aggregates Research (ICAR), Research Report ICAR-301-1F.

Turgut, P., and E. S. Yahlizade. (2009). Research into Concrete Blocks with Waste Glass. International Journal of Env. Science and Engineering, Vol. 1, No. 4, pp. 202–208.

Vanjare, M. B., and S. H. Mahure. (2012). Experimental Investigation on Self Compacting Concrete Using Glass Powder. International Journal of Engineering Application and Research, Vol. 2, No. 3,, pp. 1488–1492.

Wang, X.; Nguyen, M.; Stewart, M.G.; Syme, M.; Leitch, A. Analysis of Climate Change Impacts on the Deterioration of Concrete Infrastructure – Part 1: Mechanisms, Practices, Modelling and Simulations – A review. CSIRO, Canberra, 2010.

Wenk, H.R., P.J. Monteiro, and K. Shomglin. (2008). "Relationship between aggregate microstructure and mortar expansion." A case study of deformed granitic rocks from the Santa Rosa mylonite zone, J. Mater. Sci. 43, p. 1278–1285.

Woods, H. (1968) Durability of Concrete Construction. Monograph, vol. 4, American Concrete Institute, Detroit, Michigan.

U.S. Committee on Large Dams, Second International Conference on “Alkali Aggregate Reactions in Hydroelectric Plants and Dams,” U. S. Committee on Large Dams, Denver, Colorado, 1995.

Venkatanarayanan H.K., P.R. Rangaraju, (2011). Effect of blended fly ashes in mitigating alkali–Silica reaction, Transp. Res. Rec. 2240 (1) 80–88.

Venkatanarayanan H.K., P.R. Rangaraju, (2013). Decoupling the effects of chemical composition And fineness of fly ash in mitigating ASR, Cem. Concr. Compos. 43 54–68.

Xiong, Q. (2006). The Testing Method and Suppressing Measure of Alkali Aggregate Reaction. Master's Thesis, Southwest Jiaotong University, Chengdu, China.

Y. Zhang, W. Sun, S. Lin. (2002), Study of the heat of hydration of binder paste in high Performance concrete Cem. Concr. Res., 32 (9) pp. 1483-1488.

Zhang, C., A. Wang, M. Tang, B. Wu, and N. Zhang. (1999). Influence of aggregate size and aggregate size grading on ASR expansion. Cem. Concr. Res. 29. P. 1393–1396.

Zheng K., (2016). Pozzolanic reaction of glass powder and its role in controlling alkali-silica Reaction, Cem. Concr. Compos. 67 30–38.

Appendix A

A1 Details on the ASR Test Methods

For the ASTM C1260 – Accelerated Mortar Bar Test (AMBT) method, a 1in. x 1in. x 11.25in are used to evaluate the reactivity of fine aggregates. While for the ASTM C 1293 – Concrete Prism Test (CPT), a 3in. x 3in. x 11.25in prism is used for aggregate evaluation.

For the new AASTHO TP 110- Miniature Concrete Prism Test (MCPT), a 2in. x 2in. x 11.25in prism is used to evaluate the reactivity for both coarse and fine aggregates. These steel molds are from the Humboldt Company for each test procedure. An example of the sample prism molds with the concrete prisms is displayed below:

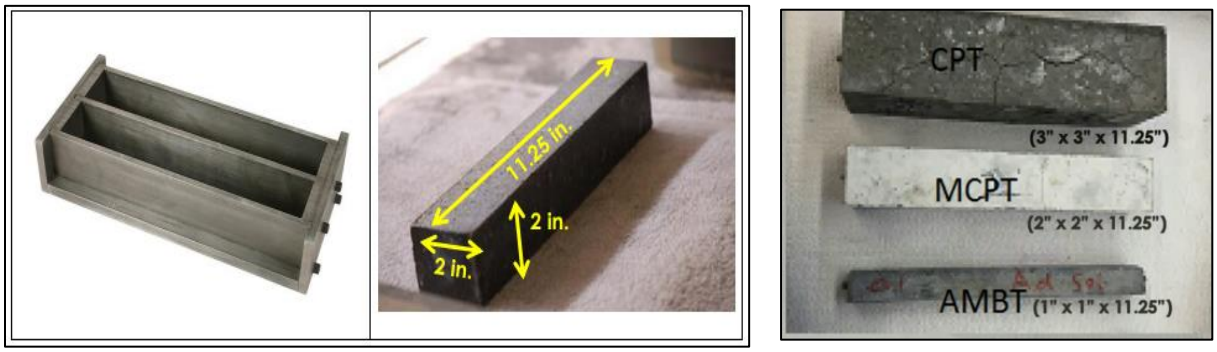

Figure A1: steel mold and the specimen concrete prism

A2 Mixture Design (AASTHO TP 110)

The mix design for the new MCPT method employed for each aggregate tested is illustrated below:

ASHTO TP-110 (MCPT): 1. Specimen

Specimen Size: 2in x2inx11.50 in
Volume of 3 specimens = 0.0838 ft3
Weight of 3 specimens = 5.7173kg or 5717g
ASHTO TP-110 (MCPT): 1. Water Content
W/C ratio: 0.45 (TP-110)
Cement content = 420 kg/m3
Cement required for 3 Specimens = 0.997 kg or 997 g
Specific gravity of non-air-entrained type 1 cement = 3.15
Density of water = 1000 kg/m^3
Volume of Cement = 0.000317 m^3
Water required for 3 Specimens: 0.449 kg or 449 g
Volume of water 0.000449 m^3

ASHTO TP-110 (MCPT): 1. Air Content
Maximum Aggregate Size: 9.5mm or 0.374in
Allowable Slump: 75mm or 3in
From ACI mix design for non-air-entrained concrete,
Air content = 3% or 0.00251ft^3 or 7.12345E-05m^3
Volume of 3 specimens w/out air content = 0.081339 ft^3 or 0.0023 m^3
Weight of 3 specimens w/out air content = 5.5458 kg or 5546 g

ASHTO TP-110 (MCPT): Coarse Aggregates

Volume of Coarse aggregate per unit volume of concrete: 0.65 (TP-110)
Volume of CA required for 3 samples: 0.001497111 m^3

Sieve passing	Seive Retained	Mass %
12.5mm (1/2 in.)	9.5 mm (3/8 in.)	57.5
9.5 mm (3/8 in.)	4.75 mm (No. 4)	42.5

Normal weight aggregate approximate bulk density 1520-1680 kg/m^3
For 9.5 mm aggregate bulk density (tested in our lab) = 1520
For 3 sample required 9.5mm coarse aggregate: = 1.308 kg or 1308 g
For 4.75 mm aggregate bulk density (tested in our lab) = 1590
For 3 sample required 4.75 mm coarse aggregate: = 1.012kg or 1012g

ASHTO TP-110 (MCPT): Fine Aggregate: ASTM C 33 gradation
Fine Aggregate required for 3 specimens 1780g

Seive Size	**Individual weight %**	**Individual weight (g)**	**Percent of individual fraction retained, by mass**	**Cumulative Percent of retained by mass**
2.36-mm (No. 8)	10	178	10	10
1.18-mm (No. 16)	25	445	25	35
600-µm (No. 30)	25	445	25	60
300-µm (No. 50)	25	445	25	85
150-µm (No. 100)	15	267	15	100

NaOH required for Concrete: Cement-Only Mixtures

1.898 kg/m3, NaOH required to achieve a total alkali content of 1.25 percent of Na2O in 1 m3 of concrete
So, NaOH required for 3 MCPT specimens = 0.00437kg or 4.37g
NaOH required for soak the specimen
1L solution: 900ml water+ 40g NaOH + additional distilled water to obtain 1L solution (AASHTO TP - 110)
For soaking 3 MCPT specimens solution required = 4.5L
So, NaOH required to soak 3 specimens = 180g
Water required to soak 3 specimens = 4050ml
Distilled water required to soak 3 specimens = 270ml.

As illustrated above for the mix design calculations using the MCPT, similar procedure was follow for the 14-day AMBT using 1:2.25 and 1-year CPT Method. In summary, the mix design of every test method use to characterize aggregates is presented in table below

Sieve Analysis	**MIX DESIGN**					
	AMBT		**MCPT**		**CPT**	
	1in x 1in x 11.25in		**2in x 2in x 11.25in**		**3in x 3in x 11.25in**	
FA	**Percentage**	**Mass (g)**	**Percentage**	**Mass (g)**	**Percentage**	**Mass (g)**
No 8	0.1	132	0.1	178	0.1	360
No 16	0.25	330	0.25	445	0.25	901
No 30	0.25	330	0.25	445	0.25	901
No 50	0.25	330	0.25	445	0.25	901
No 100	0.15	198	0.15	267	0.15	540
CA	**Percentage**	**Mass (g)**	**Percentage**	**Mass (g)**	**Percentage**	**Mass (g)**
1/2in					0.33	2377
3/8 in			0.575	1308	0.33	2377
No 4			0.425	1012	0.33	2377
Mass of cement		587		997		2672
Mass of Water		276		449		1072
Mass of NaOH in water				4.4		7.2

A3 Aggregate Bulk Density Test (ASTM C 29/29M)

For nominal maximum size of aggregate equal to or less than 12.5mm (1/2 in.)

Bulk Density – Calculate the bulk density for the rodding, jigging or shoveling procedure as follows

$$\mathbf{M} = \frac{(\mathbf{G} - \mathbf{T})}{\mathbf{V}}$$

OR

$$\mathbf{M} = (\mathbf{G} - \mathbf{T})\mathbf{F}$$

where:

M = Bulk density of the aggregates, Ib/ft3 (kg/m3)

G = Mass of the aggregates plus the measures, Ib (kg)

T = mass of the measured, Ib (kg)

V = Volume of the measure, ft^3 (m^3)

F = Factor for the measure, ft^{-3} (m^{-3})

Mass of the measures, T = 1.5799kg

Volume of the measure, V = 0.0028 m^3

Appendix B

MCPT Expansion Data (Results)

MCPT Coarse Aggregates (CA)

Table B.1: expansion for El-116c

Age, days	Avg Exp, %	Std. Dev	CV
control	0	0	0
1-day	0.0500	0.0008	1.63
3-day	0.0543	0.0021	3.78
7-day	0.0613	0.0031	5.04
14-day	0.0687	0.0041	5.98
21-day	0.0877	0.0024	2.69
28-day	0.0967	0.0057	5.93
42-day	0.1097	0.0076	6.92
56-day	0.1167	0.0076	6.50
70-day	0.1263	0.0056	4.40
84-day	0.1357	0.0063	4.67

Table B.2: Expansion for ORE-8c (CA)

Age, days	Avg Exp, %	Std. Dev	CV
control	0	0	0
1-day	0.0503	0.0039	7.67
3-day	0.0600	0.0022	3.60
7-day	0.0800	0.0014	1.77
14-day	0.1107	0.0005	0.43
21-day	0.1410	0.0042	3.01
28-day	0.1620	0.0041	2.52
42-day	0.1857	0.0070	3.79
56-day	0.2073	0.0058	2.79
70-day	0.2313	0.0031	1.34
84-day	0.2530	0.0088	3.49

Table B.3: Expansion for Md-45c (CA)

Age, days	Avg Exp, %	Std. Dev	CV
control	0	0	0
1-day	0.0610	0.0036	5.83
3-day	0.0663	0.0021	3.10
7-day	0.0610	0.0016	2.68
14-day	0.0883	0.0017	1.92
21-day	0.0990	0.0022	2.18
28-day	0.1040	0.0054	5.15
42-day	0.1200	0.0082	6.80
56-day	0.1367	0.0090	6.61
70-day	0.1450	0.0078	5.37
84-day	0.1683	0.0085	5.05

Table B.4: Expansion for Pw-84c (CA)

Age, days	Avg Exp, %	Std. Dev	CV
control	0	0	0
1-day (Na)	0.0567	0.0017	3.00
3-day	0.0653	0.0017	2.60
7-day	0.0747	0.0017	2.28
14-day	0.0937	0.0021	2.19
21-day	0.1100	0.0037	3.40
28-day	0.1243	0.0037	2.96
42-day	0.1293	0.0045	3.48
56-day	0.1413	0.0063	4.49
70-day	0.1613	0.0054	3.37
84-day	0.1710	0.0050	2.90

Table B.5: Expansion for Ma-22c (CA)

Age, days	Avg Exp, %	Std. Dev	CV
control	0	0	0
1-day	0.0460	0.0008	1.77
3-day	0.0430	0.0008	1.90
7-day	0.0433	0.0005	1.09
14-day	0.0510	0.0016	3.20
21-day	0.0600	0.0022	3.60
28-day	0.0613	0.0031	5.04
42-day	0.0657	0.0034	5.18
56-day	0.0810	0.0071	8.79
70-day	0.0943	0.0100	10.58
84-day	0.1207	0.0148	12.28

Table B.6: Expansion for Basalt (CA)

Age, days	Avg Exp, %	Std. Dev	CV
control	0	0	0
1-day	0.0453	0.0021	4.53
3-day	0.0467	0.0012	2.67
7-day	0.0497	0.0012	2.51
14-day	0.0517	0.0009	1.82
21-day	0.0573	0.0012	2.18
28-day	0.0583	0.0012	2.14
42-day	0.0687	0.0017	2.48
56-day	0.0800	0.0008	1.02
70-day	0.0887	0.0009	1.06
84-day	0.1003	0.0012	1.24

Table B.7: Expansion for L.stone (CA)

Age, days	Avg Exp, %	Std. Dev	CV
control	0	0	0
1-day	0.0510	0.0014	2.77
3-day	0.0440	0.0014	3.21
7-day	0.0500	0.0014	2.83
14-day	0.0523	0.0019	3.60
21-day	0.0523	0.0019	3.60
28-day	0.0530	0.0014	2.67
42-day	0.0593	0.0005	0.79
56-day	0.0660	0.0000	0.00
70-day	0.0697	0.0005	0.68
84-day	0.0757	0.0005	0.62

Table B.8: Expansion for Wn-56c (CA)

Age, days	Avg Exp, %	Std. Dev	CV
control	0	0	0
1-day	0.0480	0.0050	10.39
3-day	0.0580	0.0062	10.75
7-day	0.0630	0.0057	9.10
14-day	0.0693	0.0058	8.35
21-day	0.0710	0.0065	9.20
28-day	0.0833	0.0065	7.86
42-day	0.0887	0.0070	7.94
56-day	0.0972	0.0087	8.98
70-day	0.1002	0.0070	7.03
84-day	0.1034	0.0087	8.44

Table B.9: Expansion for Granite (CA)

Age, days	Avg Exp, %	Std. Dev	CV
control	0	0	0
1-day	0.0236	0.0005	2.19
3-day	0.0113	0.0005	4.40
7-day	0.0023	0.0005	21.59
14-day	0.0103	0.0010	9.61
21-day	0.0133	0.0005	3.73
28-day	0.0233	0.0005	2.13
42-day	0.0280	0.0009	3.07
56-day	0.0253	0.0009	3.39
70-day	0.0253	0.0005	1.96
84-day	0.0253	0.0005	1.96

MCPT Fine Aggregates (FA)

Table B.10: Expansion for El-116c (FA)

Age, days	Avg Exp, %	Std. Dev	CV
control	0	0	0
1-day	0.0610	0.00294	4.83
3-day	0.0897	0.00205	2.29
7-day	0.2630	0.03001	11.41
14-day	0.3780	0.00891	2.36
21-day	0.5447	0.01021	1.87
28-day	0.6100	0.01283	2.10
42-day	0.7023	0.01342	1.91
56-day	0.7710	0.01772	2.30
70-day	0.8237	0.01658	2.01
84-day	0.8717	0.01808	2.07

Table B.11: Expansion for ORE-8c (FA)

Age, days	Avg Exp, %	Std. Dev	CV
control	0	0	0
1-day	0.1300	0.00497	3.82
3-day	0.2987	0.00309	1.04
7-day	0.4897	0.00981	2.00
14-day	0.6540	0.01283	1.96
21-day	0.7513	0.01167	1.55
28-day	0.8203	0.01520	1.85
42-day	0.9190	0.01899	2.07
56-day	0.9897	0.02210	2.23
70-day	1.0493	0.01797	1.71
84-day	1.0967	0.02451	2.24

Table B.12: Expansion for Md-45c (FA)

Age, days	Avg Exp, %	Std. Dev	CV
control	0	0	0
1-day (Na)	0.0853	0.00754	8.84
3-day	0.1387	0.00943	6.80
7-day	0.3127	0.01406	4.50
14-day	0.5110	0.02031	3.98
21-day	0.6057	0.02001	3.30
28-day	0.6617	0.02001	3.02
42-day	0.7380	0.02368	3.21
56-day	0.8100	0.02223	2.74
70-day	0.8670	0.02220	2.56
84-day	0.9227	0.02210	2.39

Table B.13: Expansion for Pw-84c (FA)

Age, days	Avg Exp, %	Std. Dev	CV
control	0	0	0
1-day	0.0693	0.00309	4.46
3-day	0.0807	0.00249	3.09
7-day	0.1270	0.00163	1.29
14-day	0.2733	0.00704	2.58
21-day	0.3527	0.00776	2.20
28-day	0.3993	0.00736	1.84
42-day	0.4693	0.00939	2.00
56-day	0.5343	0.00953	1.78
70-day	0.5803	0.01087	1.87
84-day	0.6070	0.01178	1.94

Table B.14: Expansion for Ma-22c (FA)

Age, days	Avg Exp, %	Std. Dev	CV
control	0	0	0
1-day	0.0670	0.00356	5.31
3-day	0.0763	0.00525	6.88
7-day	0.1190	0.00424	3.57
14-day	0.2290	0.00455	1.99
21-day	0.3040	0.00141	0.47
28-day	0.3559	0.00290	0.82
42-day	0.4550	0.00356	0.78
56-day	0.5497	0.00929	1.69
70-day	0.6147	0.01066	1.73
84-day	0.6787	0.00899	1.33

Table B.15: Expansion for Basalt (FA)

Age, days	Avg Exp, %	Std. Dev	CV
control	0	0	0
1-day	0.0497	0.00340	6.84
3-day	0.0503	0.00309	6.14
7-day	0.0523	0.00309	5.91
14-day	0.0730	0.00294	4.03
21-day	0.0933	0.00368	3.94
28-day	0.1220	0.00779	6.38
42-day	0.1677	0.01228	7.33
56-day	0.2177	0.01297	5.96
70-day	0.2347	0.01226	5.22
84-day	0.2570	0.01203	4.68

Table B.16: Expansion for M. sand (FA)

Age, days	Avg Exp, %	Std. Dev	CV
control	0	0	0
1-day	0.0523	0.00499	9.53
3-day	0.0583	0.00624	10.69
7-day	0.0643	0.00573	8.91
14-day	0.0647	0.00579	8.96
21-day	0.0740	0.00653	8.83
28-day	0.0763	0.00655	8.58
42-day	0.0863	0.00704	8.15
56-day	0.1117	0.00873	7.82
70-day	0.1117	0.00873	7.82
84-day	0.1293	0.00946	7.32

Table B.17: Expansion for Gabbro (FA)

Age, days	Avg Exp, %	Std. Dev	CV
control	0	0	0
1-day	0.0507	0.00519	10.23
3-day	0.0570	0.00455	7.98
7-day	0.0623	0.00368	5.91
14-day	0.0620	0.00432	6.97
21-day	0.0697	0.00386	5.54
28-day	0.0700	0.00408	5.83
42-day	0.0843	0.00929	11.01
56-day	0.1003	0.01034	10.30
70-day	0.1010	0.01027	10.17
84-day	0.1173	0.00984	8.39

Table B.18: Expansion for L. stone (FA)

Age, days	Avg Exp, %	Std. Dev	CV
control	0	0	0
1-day	0.0420	0.01424	33.90
3-day	0.0517	0.01533	29.66
7-day	0.1103	0.01443	13.08
14-day	0.1980	0.01236	6.24
21-day	0.3083	0.01190	3.86
28-day	0.3943	0.01066	2.70
42-day	0.5153	0.01464	2.84
56-day	0.6417	0.01389	2.16
70-day	0.7003	0.01190	1.70
84-day	0.7833	0.02104	2.69

Table B.19: Expansion for Wn-56c (FA)

Age, days	Avg Exp, %	Std. Dev	CV
control	0	0	0
1-day	0.0527	0.01424	27.03
3-day	0.0547	0.01533	28.04
7-day	0.0643	0.01443	22.43
14-day	0.0743	0.01236	16.62
21-day	0.0793	0.01190	15.00
28-day	0.0880	0.01066	12.11
42-day	0.1013	0.01464	14.44
56-day	0.1153	0.01389	12.04
70-day	0.1193	0.00170	1.42
84-day	0.1293	0.00309	2.39

Table B.20: Expansion for Granite (FA)

Age, days	Avg Exp, %	Std. Dev	CV
control	0	0	0
1-day (Na)	0.0236	0.00052	2.19
3-day	0.0113	0.00050	4.40
7-day	0.0023	0.00050	21.59
14-day	0.0303	0.00099	3.27
21-day	0.0133	0.00050	3.73
28-day	0.0233	0.00050	2.13
42-day	0.0280	0.00086	3.07
56-day	0.0253	0.00086	3.39
70-day	0.0253	0.00050	1.96
84-day	0.0253	0.00050	1.96

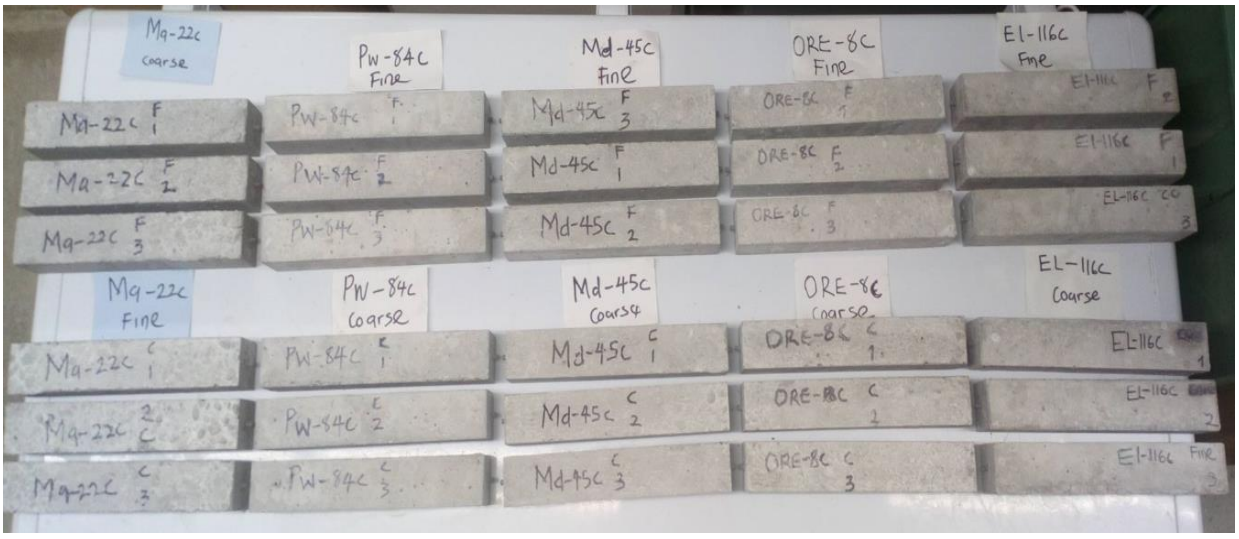

Appendix C

14-Day AMBT Expansion Data (Results)

Table C.1: Expansion for El-116c (FA)

Age, days	Avg Exp, %	Std. Dev	CV
control	0	0	0
1-day	0.147	0.0000	0.000
3-day	0.279	0.0025	0.896
7-day	0.316	0.0030	0.951
10-day	0.434	0.0075	1.728
14-day	0.593	0.0600	10.118

Table C.2: Expansion for ORE-8c (FA)

Age, days	Avg Exp, %	Std. Dev	CV
control	0	0	0
1-day	0.266	0.0000	0.000
3-day	0.465	0.0010	0.215
7-day	0.537	0.0005	0.093
10-day	0.646	0.0005	0.077
14-day	0.755	0.0100	1.325

Table C.3: Expansion for Md-45c (FA)

Age, days	Avg Exp, %	Std. Dev	CV
control	0	0	0
1-day	0.177	0.0005	0.283
3-day	0.289	0.0025	0.867
7-day	0.330	0.0050	1.515
10-day	0.423	0.0055	1.302
14-day	0.535	0.0035	0.655

Table C.4: Expansion for Pw-84c (FA)

Age, days	Avg Exp, %	Std. Dev	CV
control	0	0	0
1-day	0.048	0.0005	1.031
3-day	0.146	0.0000	0.000
7-day	0.183	0.0005	0.274
10-day	0.228	0.0005	0.220
14-day	0.312	0.0010	0.321

Table C.5: Expansion for Ma-22c (FA)

Age, days	Avg Exp, %	Std. Dev	CV
control	0	0	0
1-day	0.026	0.0005	1.887
3-day	0.103	0.0020	1.942
7-day	0.145	0.0015	1.038
10-day	0.266	0.0005	0.188
14-day	0.402	0.0010	0.249

Table C.6: Expansion for Basalt (FA)

Age, days	Avg Exp, %	Std. Dev	CV
control	0	0	0
1-day	0.023	0.00049	2.130
3-day	0.063	0.00591	9.426
7-day	0.147	0.00572	3.888
10-day	0.245	0.00406	1.657
14-day	0.375	0.01327	3.537

Table C.7: Expansion for M. sand (FA)

Age, days	Avg Exp, %	Std. Dev	CV
control	0	0	0
1-day	0.005	0.00009	2.020
3-day	0.023	0.00125	5.502
7-day	0.076	0.00698	9.179
10-day	0.145	0.00688	4.746
14-day	0.223	0.00873	3.909

Table C.8: Expansion for Gabbro (FA)

Age, days	Avg Exp, %	Std. Dev	CV
control	0	0	0
1-day	0.012	0.00082	6.804
3-day	0.024	0.00249	10.251
7-day	0.031	0.00309	9.866
10-day	0.059	0.00450	7.665
14-day	0.070	0.00411	5.843

Table C.9: Expansion for L. stone (FA)

Age, days	Avg Exp, %	Std. Dev	CV
control	0	0	0
1-day	0.008	0.00025	3.254
3-day	0.034	0.00082	2.401
7-day	0.035	0.00291	8.226
10-day	0.041	0.00367	9.031
14-day	0.049	0.00287	5.812

Table C.10: Expansion for Wn-56c (FA)

Age, days	Avg Exp, %	Std. Dev	CV
control	0	0	0
1-day	0.118	0.01085	9.235
3-day	0.148	0.00692	4.669
7-day	0.213	0.01296	6.100
10-day	0.336	0.01810	5.393
14-day	0.518	0.00846	1.633

Table C.11: Expansion for Granite (FA)

Age, days	Avg Exp, %	Std. Dev	CV
control	0	0	0
1-day	0.001	0.00005	3.536
3-day	0.002	0.00012	5.345
7-day	0.006	0.00024	4.082
10-day	0.007	0.00026	3.579
14-day	0.009	0.00022	2.400

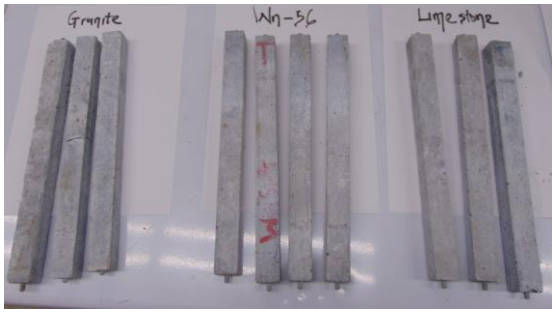

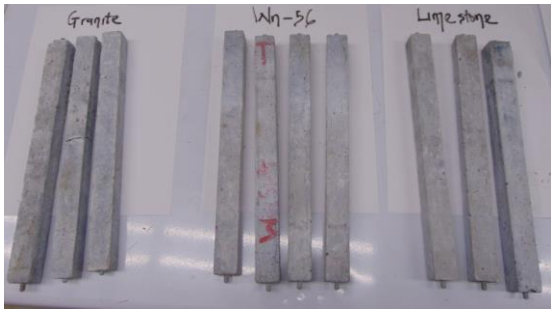

Appendix D

6-month CPT Expansion Data (Results)

Table D.1: Aggregate expansion for M. sand

Age, days	Avg Exp, %	Std. Dev	CV
control	0	0	0
1-day	0.0733	0.00179	2.437
3-day	0.0738	0.00238	3.234
7-day	0.0533	0.00109	2.046
14-day	0.0545	0.00229	4.204
28-day	0.0590	0.00187	3.171
56-day	0.0648	0.00148	2.284
84-day	0.0655	0.00112	1.707
112-day	0.0678	0.00130	1.917
140-day	0.0683	0.00164	2.402
168-day	0.0723	0.00109	1.508

Table D.2: Aggregate expansion for Basalt

Age, days	Avg Exp, %	Std. Dev	CV
control	0	0	0
1-day	0.0645	0.00150	2.326
3-day	0.0655	0.00150	2.290
7-day	0.0538	0.00377	7.008
14-day	0.0550	0.00212	3.857
28-day	0.0608	0.00356	5.863
56-day	0.0680	0.00339	4.987
84-day	0.0688	0.00356	5.181
112-day	0.0625	0.00384	6.145
140-day	0.0690	0.00394	5.706
168-day	0.0710	0.00332	4.671

Table D.3: Aggregate expansion for Wn-56c

Age, days	Avg Exp, %	Std. Dev	CV
control	0	0	0
1-day	0.0757	0.00957	10.252
3-day	0.0777	0.00998	12.847
7-day	0.0877	0.00834	9.513
14-day	0.0780	0.00883	11.323
28-day	0.0877	0.00772	8.803
56-day	0.0937	0.00713	7.616
84-day	0.0950	0.00712	7.493
112-day	0.0880	0.00942	10.700
140-day	0.0967	0.00834	8.628
168-day	0.1003	0.00881	8.777

Table D.4: Aggregate expansion for L. stone

Age, days	Avg Exp, %	Std. Dev	CV
control	0	0	0
1-day	0.0223	0.00262	11.752
3-day	0.0283	0.00125	4.402
7-day	0.0293	0.00170	5.794
14-day	0.0300	0.00163	5.443
28-day	0.0303	0.00047	1.554
56-day	0.0343	0.00047	1.373
84-day	0.0370	0.00082	2.207
112-day	0.0387	0.00818	21.151
140-day	0.0423	0.00125	2.946
168-day	0.0423	0.00094	1.992

Table D.5: Aggregate expansion for Gabbro

Age, days	Avg Exp, %	Std. Dev	CV
control	0	0	0
1-day	0.0690	0.00374	2.326
3-day	0.0640	0.00432	2.290
7-day	0.0640	0.00432	7.008
14-day	0.0573	0.00450	3.857
28-day	0.0510	0.01203	5.863
56-day	0.0607	0.01087	4.987
84-day	0.0630	0.01042	5.181
112-day	0.0653	0.01053	6.145
140-day	0.0647	0.01034	5.706
168-day	0.0660	0.01071	4.671

Table D.6: Aggregate expansion for Granite

Age, days	Avg Exp, %	Std. Dev	CV
control	0	0	0
1-day	0.0077	0.00205	26.802
3-day	0.0097	0.00189	19.506
7-day	0.0183	0.00330	17.999
14-day	0.0123	0.00249	20.225
28-day	0.0190	0.00294	15.494
56-day	0.0177	0.00189	10.673
84-day	0.0233	0.00189	8.081
112-day	0.0240	0.00408	17.010
140-day	0.0273	0.00368	13.470
168-day	0.0293	0.00450	15.330

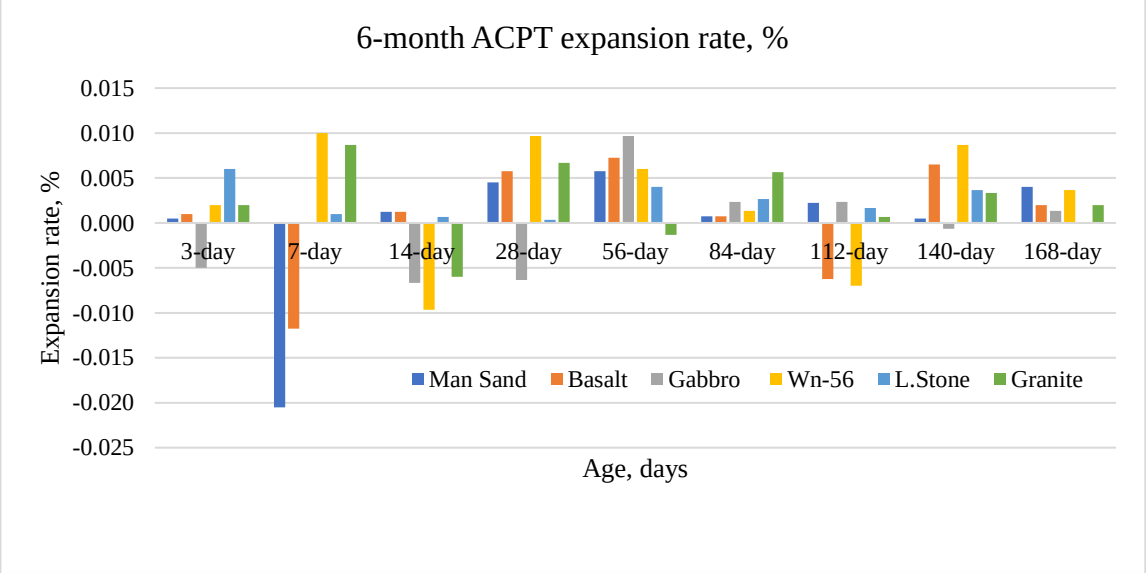

Figure D1: The 6-month ACPT expansion rate, %.

Appendix E:

1-Year CPT Expansion Data (Results)

Table E.1: Aggregate expansion for M. sand

Age, days	Avg Exp, %	Std. Dev	CV
control	0	0	0
1-day	0.0565	0.00111	1.96
3-day	0.0705	0.00269	3.82
7-day	0.0715	0.00260	3.63
14-day	0.0635	0.00166	2.61
28-day	0.0708	0.00476	6.73
56-day	0.0790	0.01107	14.01
84-day	0.0847	0.01117	13.18
112-day	0.0815	0.01128	13.84
140-day	0.0875	0.01069	12.22
168-day	0.0840	0.00292	3.47
196-day	0.0850	0.00334	3.94
252-day	0.0858	0.00311	3.63
308-day	0.0858	0.00311	3.63
365-day	0.0858	0.00311	3.63

Table E.2: Aggregate expansion for Basalt

Age, days	Avg Exp, %	Std. Dev	CV
control	0	0	0
1-day	0.0390	0.00101	2.60
3-day	0.0467	0.00112	2.40
7-day	0.0730	0.00418	5.73
14-day	0.0710	0.00245	3.45
28-day	0.0690	0.00187	2.71
56-day	0.0747	0.00268	3.59
84-day	0.0762	0.00286	3.75
112-day	0.0760	0.00187	2.46
140-day	0.0785	0.00229	2.92
168-day	0.0820	0.00212	2.59
196-day	0.0823	0.00192	2.33
252-day	0.0837	0.00217	2.59
308-day	0.0823	0.00192	2.33
365-day	0.0837	0.00217	2.59

Table E.3: Aggregate expansion for Wn-56c

Age, days	Avg Exp, %	Std. Dev	CV
control	0	0	0
1-day	0.0500	0.00170	3.40
3-day	0.0663	0.00759	11.44
7-day	0.0707	0.00750	10.60
14-day	0.0820	0.00726	8.85
28-day	0.0867	0.00694	8.01
56-day	0.0853	0.00806	9.44
84-day	0.0928	0.00619	6.67
112-day	0.1060	0.00638	6.02
140-day	0.1100	0.00707	6.43
168-day	0.1100	0.00685	6.23
196-day	0.1117	0.00712	6.37
252-day	0.1137	0.00330	2.90
308-day	0.1137	0.00330	2.90
365-day	0.1150	0.00356	3.09

Table E.4: Aggregate expansion for L. stone

Age, days	Avg Exp, %	Std. Dev	CV
control	0	0	0
1-day	0.0157	0.00094	6.02
3-day	0.0303	0.00125	4.11
7-day	0.0323	0.00047	1.46
14-day	0.0197	0.00094	4.79
28-day	0.0357	0.00170	4.77
56-day	0.0337	0.00236	7.00
84-day	0.0407	0.00094	2.32
112-day	0.0393	0.00205	5.22
140-day	0.0457	0.00170	3.72
168-day	0.0477	0.00170	3.57
196-day	0.0490	0.00141	2.89
252-day	0.0490	0.00141	2.89
308-day	0.0490	0.00141	2.89
365-day	0.0490	0.00141	2.89

Table E.5: Aggregate expansion for Gabbro

Age, days	Avg Exp, %	Std. Dev	CV
control	0	0	0
1-day	0.0310	0.00510	16.45
3-day	0.0413	0.00411	9.94
7-day	0.0417	0.00450	10.79
14-day	0.0330	0.00356	10.78
28-day	0.0450	0.00216	4.80
56-day	0.0433	0.00236	5.44
84-day	0.0480	0.00356	7.41
112-day	0.0483	0.00386	7.98
140-day	0.0533	0.00450	8.43
168-day	0.0537	0.00478	8.91
196-day	0.0543	0.00464	8.55
252-day	0.0543	0.00464	8.55
308-day	0.0557	0.00419	7.53
365-day	0.0557	0.00419	7.53

Table E.6: Aggregate expansion for Granite

Age, days	Avg Exp, %	Std. Dev	CV
control	0	0	0
1-day	0.0011	0.0026	2.61
3-day	0.0037	0.0012	34.02
7-day	0.0049	0.0017	34.90
14-day	0.0057	0.0016	28.82
28-day	0.0077	0.0005	6.15
56-day	0.0183	0.0026	14.32
84-day	0.0123	0.0012	10.11
112-day	0.0190	0.0017	8.95
140-day	0.0177	0.0016	9.24
168-day	0.0233	0.0005	2.02
196-day	0.0240	0.0005	1.96
252-day	0.0243	0.0016	6.78
308-day	0.0246	0.0014	5.74
365-day	0.0239	0.0001	0.52

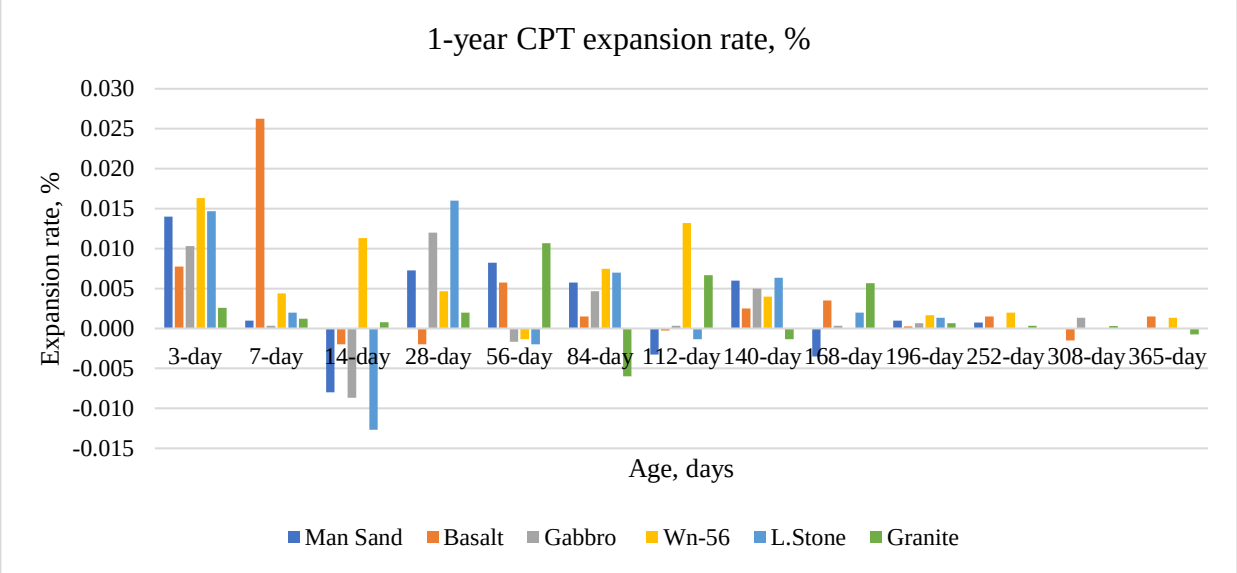

Figure E1: The 1-year CPT expansion rate, %.

Appendix F

Wn-56 Mitigation Data (Results)

Table F.1: Wn-56 expansion data without SCMs

Age, days	Avg Exp, %	Std. Dev	CV
Control	0	0	0
1-day	0.0679	0.0017	2.57
3-day	0.1782	0.0130	7.27
7-day	0.3509	0.0181	5.16
14-day	0.5242	0.0085	1.61
21-day	0.6459	0.0276	4.27
28-day	0.7746	0.0276	3.56

Table F.2: Mitigation result using 10GP

Age, days	Avg Exp, %	Std. Dev	CV
Control	0	0	0
1-day	0.01	0.0004	2.39
3-day	0.06	0.0039	6.90
7-day	0.14	0.0147	10.26
14-day	0.33	0.0101	3.07
21-day	0.49	0.0273	5.63
28-day	0.56	0.0020	0.36

Table F.3: Mitigation result using 20GP

Age, days	Avg Exp, %	Std. Dev	CV
Control	0	0	0
1-day	0.06	0.0015	2.31
3-day	0.09	0.0016	1.91
7-day	0.10	0.0096	9.72
14-day	0.12	0.0016	1.31
21-day	0.14	0.0026	1.87
28-day	0.16	0.0049	3.14

Table F.4: Mitigation result using 30GP

Age, days	Avg Exp, %	Std. Dev	CV
Control	0	0	0
1-day	0.02	0.0008	4.33
3-day	0.03	0.0009	3.41
7-day	0.04	0.0023	5.40
14-day	0.05	0.0006	1.35
21-day	0.07	0.0038	5.41
28-day	0.09	0.0047	5.31

Table F.5: Mitigation result using 10S

Age, days	Avg Exp, %	Std. Dev	CV
Control	0	0	0
1-day	0.04	0.0073	16.92
3-day	0.05	0.0015	3.36
7-day	0.12	0.0009	0.71
14-day	0.33	0.0122	3.70
21-day	0.49	0.0271	5.50
28-day	0.63	0.0343	5.42

Table F.6: Mitigation result using 20S

Age, days	Avg Exp, %	Std. Dev	CV
Control	0	0	0
1-day	0.02	0.0008	3.94
3-day	0.03	0.0008	2.96
7-day	0.07	0.0061	8.23
14-day	0.21	0.0132	6.33
21-day	0.38	0.0114	3.05
28-day	0.50	0.0144	2.87

Table F.7: Mitigation result using 30S

Age, days	Avg Exp, %	Std. Dev	CV
Control	0	0	0
1-day	0.002	0.0001	7.20
3-day	0.03	0.0024	7.54
7-day	0.07	0.0095	14.41
14-day	0.10	0.0030	2.91
21-day	0.17	0.0080	4.61
28-day	0.25	0.0101	4.11

Table F.8: Mitigation result using 10SF

Age, days	Avg Exp, %	Std. Dev	CV
Control	0	0	0
1-day	0.06	0.0021	3.55
3-day	0.17	0.0139	8.00
7-day	0.34	0.0044	1.29
14-day	0.47	0.0096	2.05
21-day	0.53	0.0256	4.78
28-day	0.60	0.0319	5.34

Table F.9: Mitigation result using 20SF

Age, days	Avg Exp, %	Std. Dev	CV
Control	0	0	0
1-day	0.02	0.0005	3.38
3-day	0.09	0.0243	26.64
7-day	0.22	0.0344	15.45
14-day	0.28	0.0231	8.26
21-day	0.31	0.0184	5.87
28-day	0.37	0.0198	5.31

Table F.10: Mitigation result using 30SF

Age, days	Avg Exp, %	Std. Dev	CV
Control	0	0	0
1-day	0.03	0.0018	6.03
3-day	0.09	0.0067	7.23
7-day	0.17	0.0045	2.71
14-day	0.21	0.0025	1.17
21-day	0.23	0.0133	5.89
28-day	0.24	0.0120	5.06

Table F.11: Mitigation result using 10S10G

Age, days	Avg Exp, %	Std. Dev	CV
Control	0	0	0
1-day	0.01	0.0007	11.73
3-day	0.02	0.0013	5.84
7-day	0.07	0.0045	6.53
14-day	0.11	0.0005	0.48
21-day	0.17	0.0144	8.45
28-day	0.22	0.0116	5.25

Table F.12: Mitigation result using 10SF10G

Age, days	Avg Exp, %	Std. Dev	CV
Control	0	0	0
1-day	0.03	0.0017	4.83
3-day	0.04	0.0023	5.33
7-day	0.09	0.0197	21.68
14-day	0.12	0.0023	1.87
21-day	0.20	0.0012	0.62
28-day	0.26	0.0029	1.11

Table F.13: Mitigation result using 10S20G

Age, days	Avg Exp, %	Std. Dev	CV
Control	0	0	0
1-day	0.01	0.0008	10.62
3-day	0.03	0.0066	19.45
7-day	0.07	0.0096	13.92
14-day	0.10	0.0099	9.60
21-day	0.16	0.0244	15.44
28-day	0.20	0.0291	14.51

Table F.14: Mitigation result using 10SF20G

Age, days	Avg Exp, %	Std. Dev	CV
Control	0	0	0
1-day	0.09	0.0057	6.47
3-day	0.13	0.0163	12.65
7-day	0.18	0.0046	2.59
14-day	0.19	0.0011	0.58
21-day	0.23	0.0144	6.32
28-day	0.28	0.0176	6.41

Table F.13: Mitigation result using 15S15G

Age, days	Avg Exp, %	Std. Dev	CV
Control	0	0	0
1-day	0.03	0.0039	12.26
3-day	0.04	0.0043	11.67
7-day	0.08	0.0048	6.01
14-day	0.11	0.0071	6.61
21-day	0.18	0.0095	5.37
28-day	0.22	0.0137	6.21

Table F.14: Mitigation result using 15SF15G

Age, days	Avg Exp, %	Std. Dev	CV
Control	0	0	0
1-day	0.04	0.0012	2.77
3-day	0.08	0.0096	11.49
7-day	0.14	0.0107	7.41
14-day	0.16	0.0045	2.80
21-day	0.20	0.0081	4.00
28-day	0.25	0.0115	4.62

Appendix G

SEM Images of Pozzolans

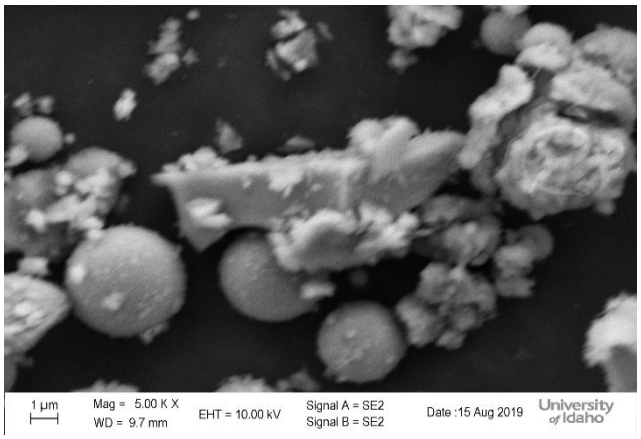

Figure G.1: SEMs of Slag Cement

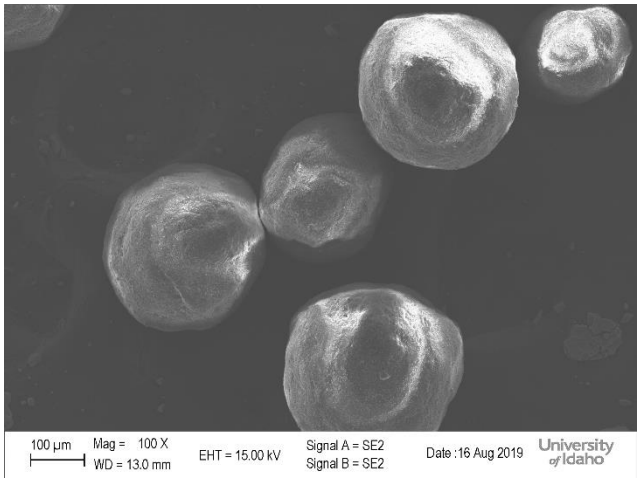

Figure G.2: SEMs of Silica Fume

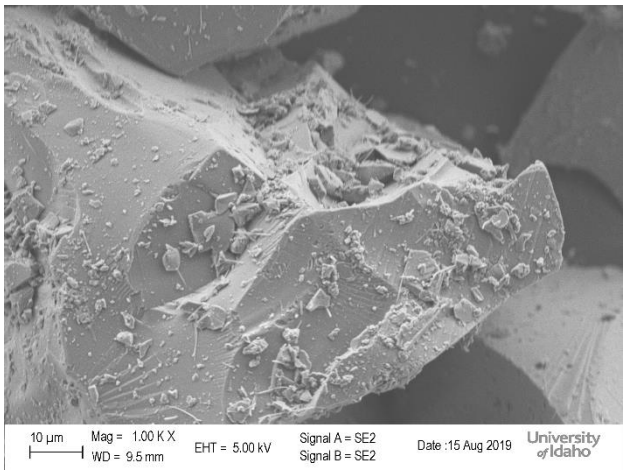

Figure G.3: SEMs of Glass Powder

Appendix H

Thermogravimetric Analysis, TGA (Results)

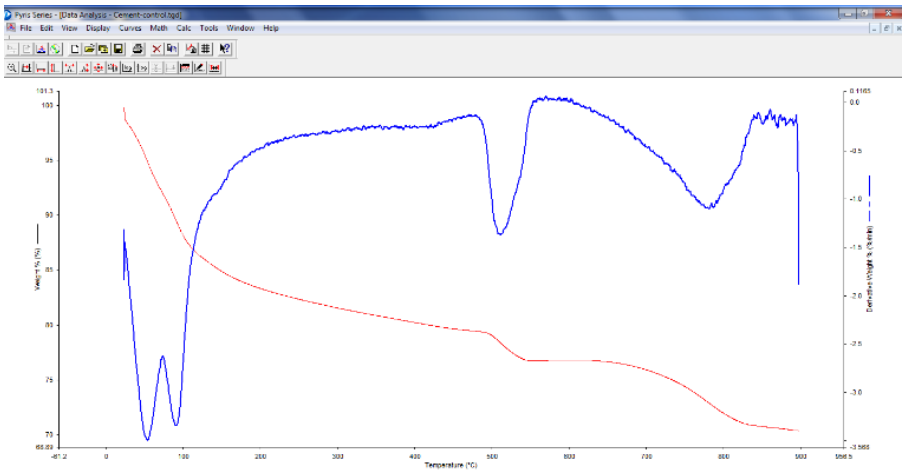

Figure H.1: TGA result for mix without SCMs

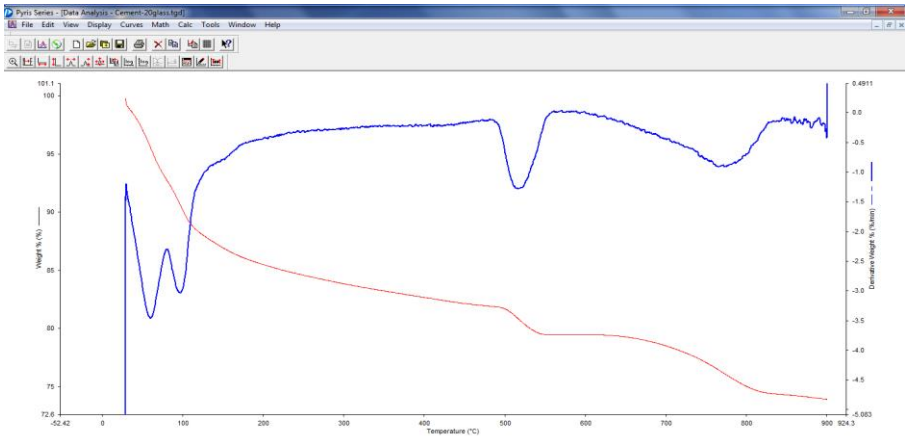

Figure H.2: TGA result for mix with 20GP

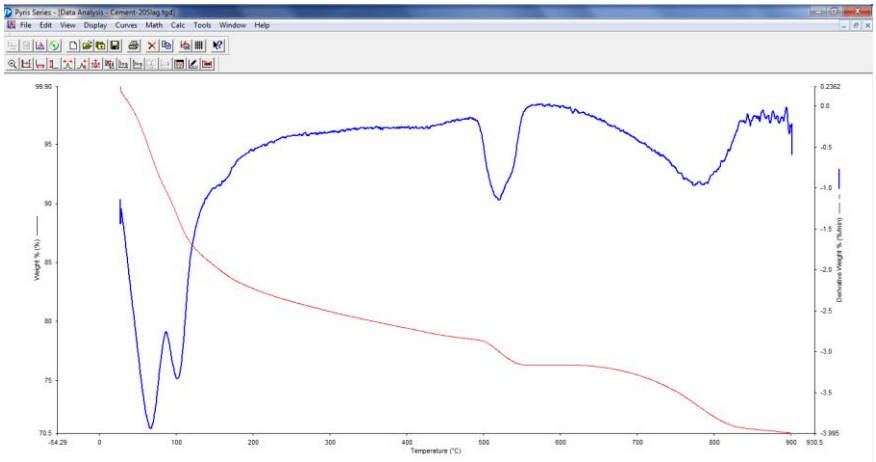

Figure H.3: TGA result for mix with 20S

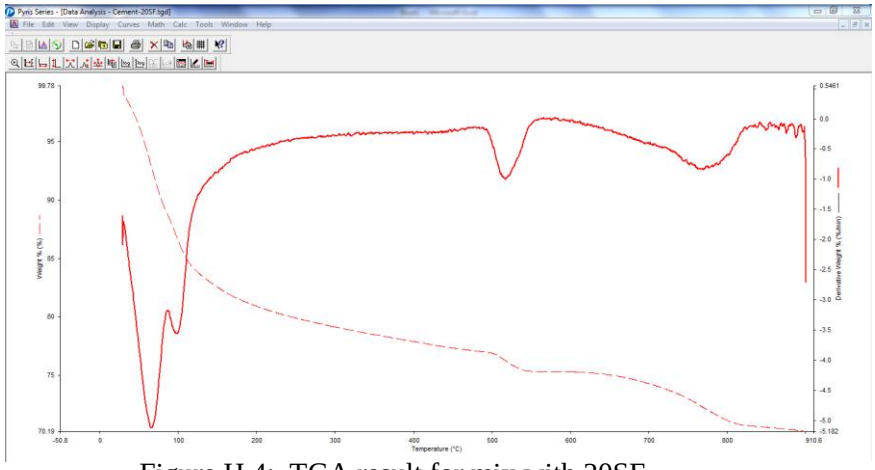

Figure H.4: TGA result for mix with 20SF

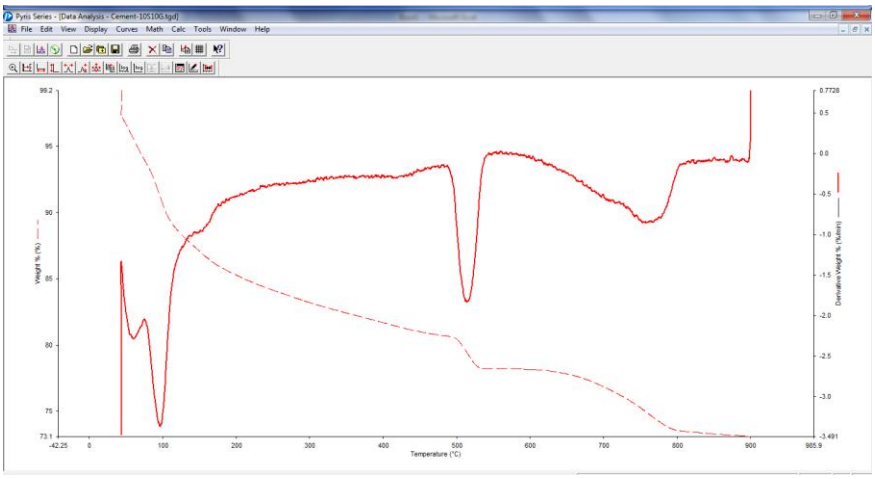

Figure H.5: TGA result for mix with 10S10G

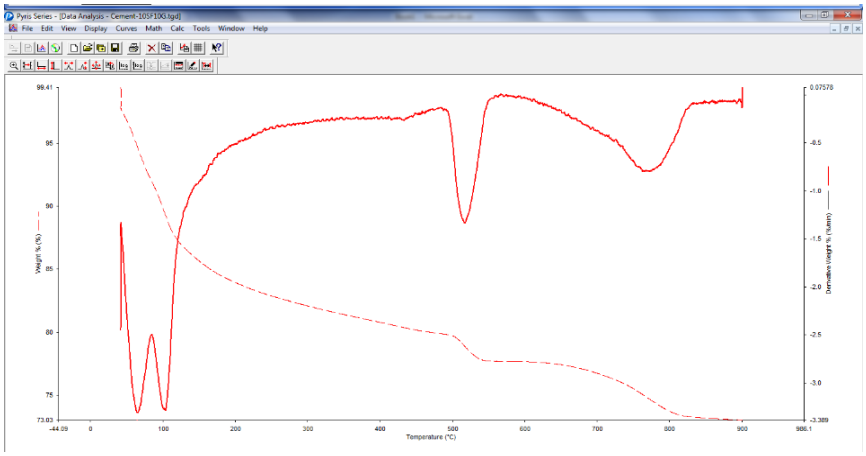

Figure H.6: TGA result for mix with 10SF10G

Appendix H

EDS (Results)